FABRICATION OF COBALT-IRON THIN FILM FOR MAGNETIC RECORDING HEAD CORE BY ELECTRODEPOSITION AND HEAT TREATMENT

Mr. Thanakrit Chotibhawaris

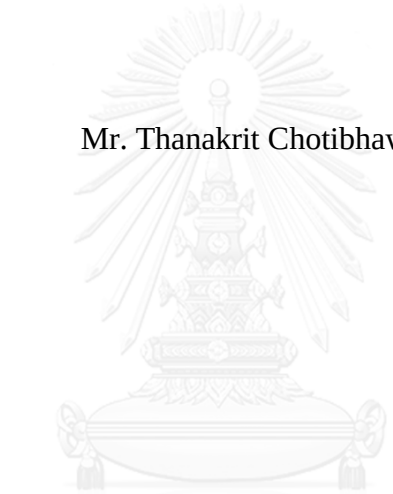

จุฬาลงกรณ์มหาวิทยาลัย
Chulalongkorn University

บทคัดย่อและแฟ้มข้อมูลฉบับเต็มของวิทยานิพนธ์ตั้งแต่ปีการศึกษา 2554 ที่ให้บริการในคลังปัญญาจุฬาฯ (CUIR)
เป็นแฟ้มข้อมูลของนิสิตเจ้าของวิทยานิพนธ์ ที่ส่งผ่านทางบัณฑิตวิทยาลัย
The abstract and full text of theses from the academic year 2011 in Chulalongkorn University Intellectual Repository (CUIR)
are the thesis authors' files submitted through the University Graduate School.

A Dissertation Submitted in Partial Fulfillment of the Requirements
for the Degree of Doctor of Philosophy Program in Nanoscience and Technology
(Interdisciplinary Program)
Graduate School
Chulalongkorn University
Academic Year 2015
Copyright of Chulalongkorn University

การสร้างแผ่นฟิล์มบางโคบอลท์-เหล็ก สำหรับแกนหัวบันทึกแม่เหล็ก โดยการชุบเคลือบด้วยไฟฟ้าและการอบชุบความร้อน

นายธนกฤต โชติภาวิศ

จุฬาลงกรณ์มหาวิทยาลัย
Chulalongkorn University

วิทยานิพนธ์นี้เป็นส่วนหนึ่งของการศึกษาตามหลักสูตรปริญญาวิทยาศาสตรดุษฎีบัณฑิต
สาขาวิชาวิทยาศาสตร์นาโนและเทคโนโลยี (สหสาขาวิชา)
บัณฑิตวิทยาลัย จุฬาลงกรณ์มหาวิทยาลัย
ปีการศึกษา 2558
ลิขสิทธิ์ของจุฬาลงกรณ์มหาวิทยาลัย

Thesis Title	FABRICATION OF COBALT-IRON THIN FILM FOR MAGNETIC RECORDING HEAD CORE BY ELECTRODEPOSITION AND HEAT TREATMENT
By	Mr. Thanakrit Chotibhawaris
Field of Study	Nanoscience and Technology
Thesis Advisor	Associate Professor Yuttanant Boonyongmaneerat, Ph.D.
Thesis Co-Advisor	Associate Professor Tachai Luangvaranunt, Ph.D.

Accepted by the Graduate School, Chulalongkorn University in Partial Fulfillment of the Requirements for the Doctoral Degree

.....Dean of the Graduate School
(Associate Professor Sunait Chutintaranond, Ph.D.)

THESIS COMMITTEE

.....Chairman
(Associate Professor Vudhichai Parasuk, Ph.D.)
.....Thesis Advisor
(Associate Professor Yuttanant Boonyongmaneerat, Ph.D.)
.....Thesis Co-Advisor
(Associate Professor Tachai Luangvaranunt, Ph.D.)
.....Examiner
(Assistant Professor Sukkaneste Tungasmita, Ph.D.)
.....Examiner
(Ratthapol Rangkupan, Ph.D.)
.....External Examiner
(Assistant Professor Pongsakorn Jantaratana, Ph.D.)

ธนกฤต โชติภาวริศ : การสร้างแผ่นฟิล์มบางโคบอลท์-เหล็ก สำหรับแกนหัวบันทึกแม่เหล็ก โดยการชุบเคลือบด้วยไฟฟ้าและการอบชุบความร้อน (FABRICATION OF COBALT-IRON THIN FILM FOR MAGNETIC RECORDING HEAD CORE BY ELECTRODEPOSITION AND HEAT TREATMENT) อ.ที่ปรึกษาวิทยานิพนธ์หลัก: รศ. ดร. ยุทธนันท์ บุญยงมณีรัตน์, อ.ที่ปรึกษาวิทยานิพนธ์ร่วม: รศ. ดร. ธาชาย เหลืองวรานันท์, หน้า.

เนื่องด้วยคุณสมบัติที่โดดเด่นด้านความเป็นแม่เหล็ก ทำให้โลหะผสมโคบอลท์เหล็กเป็นวัสดุที่มีศักยภาพสูงในการใช้สร้างเป็นฟิล์มแม่เหล็กอ่อนสำหรับการประยุกต์ใช้งานด้านชิ้นส่วนอุปกรณ์ไฟฟ้าและอิเลคทรอนิคส์ โดยเฉพาะอย่างยิ่งหัวเขียนข้อมูลของฮาร์ดดิสก์ไดร์ฟ อย่างไรก็ตาม ความรู้และการศึกษาอย่างเป็นระบบสำหรับการพัฒนาคุณสมบัติแม่เหล็กอ่อนของวัสดุดังกล่าวยังจำกัด ดังนั้นงานวิจัยนี้จึงได้ทำการศึกษาปัจจัยต่างๆที่เกี่ยวข้องกับคุณสมบัติความเป็นแม่เหล็กอ่อนของวัสดุนี้อย่างเป็นระบบ โดยใช้วิธีการผลิตด้วยการชุบเคลือบด้วยไฟฟ้าร่วมกับการอบชุบความร้อน ทั้งนี้ปัจจัยด้านการผลิต ได้แก่ ส่วนประกอบทางเคมี ความหนา อุณหภูมิการอบชุบความร้อน รวมถึงอิทธิพลของสนามแม่เหล็กที่เหนี่ยวนำขนานกับพื้นผิวชิ้นงานขณะทำการชุบเคลือบด้วยไฟฟ้าที่อุณหภูมิห้องและที่อุณหภูมิต่ำ ซึ่งพิจารณาร่วมกับองค์ประกอบต่างๆของโครงสร้างฟิล์มดังกล่าว ได้แก่ ขนาดของเกรน ความหยาบผิว สัณฐานผลึก โดเมนแม่เหล็ก ความเค้น โดยการวิจัยนี้แบ่งออกเป็นสามส่วน ส่วนแรกทำการศึกษาผลกระทบของส่วนผสมทางเคมีกับความหนาที่แตกต่างกันของฟิล์มโลหะผสมโคบอลท์เหล็ก พบว่าความหนาช่วยกำจัดความบกพร่องในฟิล์มได้ ส่งผลให้ค่าความเป็นแม่เหล็กอ่อนดีขึ้น อีกทั้งปริมาณส่วนผสมของเหล็กน้อยจะมีค่าสัมประสิทธิ์พื้นผิว (Texture coefficient) ของระนาบ (110) สูง ส่งผลโดยตรงต่อค่าการเหนี่ยวนำแม่เหล็กอิ่มตัว (Saturation magnetization) สูงขึ้นตามไปด้วย นอกจากนี้ขนาดของเกรนเป็นปัจจัยสำคัญที่มีผลต่อสภาพบังคับ (Coercivity) ของฟิล์ม โดยฟิล์มที่มีสภาพบังคับต่ำจะมีโครงสร้างโดเมนเป็นแบบวงกลม (Bubble-liked pattern) ส่วนที่สองศึกษาฟิล์มโลหะผสมโคบอลท์เหล็กที่ผ่านการอบด้วยความร้อนเพื่อพิจารณาผลกระทบของความเค้น พบว่าความเค้นมีแนวโน้มลดลงแต่ไม่ได้ทำให้ค่าสภาพบังคับของฟิล์มลดลง เนื่องจากค่าความแข็งแรงของโดเมนในทิศทางเดียว (Uniaxial anisotropy constant) ที่เพิ่มขึ้นจากการอบดังกล่าว แต่การอบด้วยความร้อนไม่มีผลอย่างชัดเจนต่อค่าการเหนี่ยวนาแม่เหล็กอิ่มตัว (Saturation magnetization) ที่ยังคงแปรผันตามกับค่าสัมประสิทธิ์พื้นผิว (Texture coefficient) ของระนาบ (110) ส่วนที่สามศึกษาผลกระทบจากสนามแม่เหล็กที่เหนี่ยวนำขณะทำการชุบเคลือบด้วยไฟฟ้าที่อุณหภูมิห้องและอุณหภูมิต่ำ พบว่าทิศทางบนระนาบฟิล์ม (In-plane direction) ของค่าความแข็งแรงของโดเมนในทิศทางเดียวที่เกิดจากการเหนี่ยวนำของสนามแม่เหล็กทำให้ค่าสภาพบังคับลดต่ำลงและยังคงผันแปรตามขนาดของเกรน ในขณะที่ค่าการเหนี่ยวนำแม่เหล็กอิ่มตัวแปรผันตามค่าความแข็งแรงของโดเมนในทิศทางเดียว ทั้งนี้อุณหภูมิต่ำยังส่งผลให้ค่าความแข็งแรงของโดเมนดังกล่าวและค่าการเหนี่ยวนำแม่เหล็กอิ่มตัวเพิ่มขึ้นด้วย

สาขาวิชา วิทยาศาสตร์นาโนและเทคโนโลยี ลายมือชื่อนิสิต .....

ปีการศึกษา 2558 ลายมือชื่อ อ.ที่ปรึกษาหลัก .....

ลายมือชื่อ อ.ที่ปรึกษาร่วม .....

5387864020 : MAJOR NANOSCIENCE AND TECHNOLOGY
KEYWORDS: ELECTRODEPOSITION, / ANNEALING / SOFT MAGNETIC / ANISOTROPY

THANAKRIT CHOTIBHAWARIS: FABRICATION OF COBALT-IRON THIN FILM FOR MAGNETIC RECORDING HEAD CORE BY ELECTRODEPOSITION AND HEAT TREATMENT. ADVISOR: ASSOC. PROF. YUTTANANT BOONYONGMANEERAT, Ph.D., CO-ADVISOR: ASSOC. PROF. TACHAI LUANGVARANUNT, Ph.D., pp.

According to the dominant soft magnetic properties of CoFe alloy, it has a high potential as soft magnetic films for applications in electrical and electronics industries, especially the writing head core of hard disk drive. However, the knowledge and systematic study to improve the soft magnetic properties of such materials is limited. This research investigates the factors associated with soft magnetic properties of the material produced by electrodeposition and post annealing techniques. The factors of the fabrication include chemical composition, thickness, annealing temperature. These factors are considered with the film's structural elements, namely grain size, roughness, crystallographic orientation, magnetic domain, stress and the applied magnetic field both at room and low temperature. The research is divided into three parts. In Part I, the effects of the chemical composition on the thickness of the electrodeposited CoFe films were studied. It was found that high thickness improves the homogeneity and suppresses defects in the films providing good soft magnetic properties. When the Fe content is low, the texture coefficient at plane (110) and the saturation magnetization is high. Moreover, the grain size is the factor controlling the coercivity of the film. The film with low coercivity contains 'bubble-liked' domain pattern. In Part II, the effect of the stress on the annealed CoFe films were considered. It is found that annealing reduces stress but does not decrease the coercivity due to the increase in uniaxial anisotropy constant. The saturation magnetization varies directly with the texture coefficient of (110) plane. In Part III, the effects of applied magnetic field both at room and low temperature were observed. The in-plane direction of the uniaxial anisotropy reduces the coercivity and varies directly with the grain size while the saturation magnetization depends on the uniaxial anisotropy. Furthermore, the low temperature increases the uniaxial anisotropy constant and the magnetic induction saturation.

Field of Study: Nanoscience and Technology
Academic Year: 2015

Student's Signature .....
Advisor's Signature .....
Co-Advisor's Signature .....

ACKNOWLEDGEMENTS

First of all, I would like to express my deepest gratitude to my advisor and co-advisor, Assoc. Prof. Dr. Yuttanant Boonyongmaneerat and Assoc. Prof. Dr. Tachai Luangvaranant, for the continuous support with their expertise, understanding, motivation, enthusiasm, patience and kindness. I appreciate their vast knowledge and skill in many areas and their assistance in writing thesis report and articles. Their guidance helped me throughout my research. I am so particularly appreciated in Assoc. Prof. Dr. Yuttanant Boonyongmaneerat. He is not only my advisor, but also my Bodhisattva. He always endures a lot of my mistakes by his kindness and forgiveness, again and again. I am very lucky and so proud that he is my advisor. I cannot imagine having a better advisor than him in my life.

I feel profoundly grateful to the chairman, Assoc. Prof. Dr. Vudhichai Parasuk, for his moral support, encouragement and insightful comments. I am also sincerely appreciated the committees, Asst. Prof. Dr. Sukkaneste Tungasmita and Dr. Ratthapol Rangkupan, for the valuable advices and comments. Appreciation also goes out to Asst. Prof. Dr. Pongsakorn Jantaratana, not only with his valuable guidance as an external examiner, but also with his assistance for supporting the service of VSM apparatus and important basic knowledge of magnetism.

I am extremely thankful and indebted to all lecturers, in the Department of Nanoscience and Technology and other departments. Not only for their sharing expertise and worth knowledge in the field of material science, metallurgy, physics and other fields related to my dissertation, but also for their moral supports with a full sense of being Ajarn.

I am so especially thankful to Mr.Narin Jantaping. It seems to me that he is as a god of XRD analysis and also my third advisor. He became a Ph.D. candidate of the department during I was suffering the difficult trouble of XRD measurement. I could solve the hard problem because of his specialism and very kind assistance.

I wish to express my very special thanks to my all friends in PORETEGE research unit, Metallurgy and Materials Science Research Institute, Chulalongkorn University which I am so appreciated. I cannot mention them all here for sacrificing their valuable time to support a lot of helps for everything they could complete my dissertation. Moreover, they give me kindness, companionship including vivid memories of great experiences.

Also, I recognize that this research would not be possible without financial assistance from The 72nd Anniversary of His Majesty King Bhumibol Adulyadej and The 90th Anniversary of Chulalongkorn University Fund (Ratchadaphiseksomphot Endowment Fund).

I sincerely thank all friends (from the past to the present), which I cannot mention them all here, for their assistance in all aspects since the beginning to the end of this study. Also thank all faculty members in the Department of Nanoscience and Technology for their help and support. I also place on record, my sense of appreciation to one and all, which directly or indirectly, have given their hands in this venture.

I take this opportunity to express gratitude to my parents, Mr.Wasu Chotibhawaris and Mrs.Jira Chotibhawaris, for giving birth to me, supporting and comforting me throughout my life. I am also grateful for my partner, Ms.Thanida Sunarak, for the unceasing encouragement, support and attention through this venture.

Lastly, I am duteous to the Buddha and Holy spirits for the good health and well-being that were necessary to achieve this doctorate degree.

CONTENTS

Page

THAI ABSTRACT iv

ENGLISH ABSTRACT v

ACKNOWLEDGEMENTS vi

CONTENTS vii

LIST OF TABLES x

LIST OF FIGURES xi

CHAPTER I INTRODUCTION 1

1.1 Motivation 1

1.2 Objective of Research 5

1.3 Scope of Research 5

1.3.1 Magnetic Properties of Electrodeposited CoFe Films 6

1.3.2 Magnetic Properties of Annealed CoFe Films 6

1.3.3 Magnetic Properties of CoFe Films Fabricated by Electrodeposition with Magnetic Field 6

1.4 Benefits of Research 6

CHAPTER II THEORETICAL ASPECTS AND LITERATURE SURVEY 8

2.1 Soft Magnetic Properties of Ferromagnetic Alloys 8

2.1.1 Magnetization Process 8

2.1.2 Magnetic Anisotropy 10

2.2 Magnetic Thin Film for Recording Head Core of Hard Disk Drive 18

2.3 Electrodeposition of CoFe Based Magnetic Thin Films 20

2.3.1 Effect of Additive 22

2.3.2 Current Density 26

2.3.3 pH 26

2.3.4 Temperature 28

2.3.5 Magnetic Field 29

2.4 Thermal Annealing 31

2.5 Electroplated CoFe Based Alloy Films and Their Soft Magnetic Properties 32

Page

CHAPTER III EXPERIMENTAL PROCEDURE 36
3.1 Part I – Effects of Composition and Thickness 37
3.1.1 Electrodeposition 37
3.1.2 Characterization 39
3.2 Part II – Effects of Annealing 41
3.2.1 Thermal Annealing 42
3.2.2 Characterization 42
3.3 Part III – Effects of Magnetic Field and Low Temperature 43
3.3.1 Electrodeposition with Magnetic Field and Low Temperature 44
3.3.2 Characterization 45
CHAPTER IV EXPERIMENTAL RESULTS 46
4.1 Part I – Effects of Composition and Thickness 46
4.1.1 Plating Films and Compositions 46
4.1.2 Magnetic Properties 48
4.1.3 Films' Characteristics 51
4.1.4 Magnetic Domain Structure 57
4.2 Part II – Effects of Annealing 58
4.2.1 Magnetic Properties 58
4.2.2 Films' Characteristics 61
4.3 Part III – Effects of Magnetic Field and Low Temperature 67
4.3.1 Plating Films' Compositions 67
4.3.2 Magnetic Properties 68
4.3.3 Films' Characteristics 71
CHAPTER V DISCUSSION 78
5.1 Part I – Effects of Composition and Thickness 78
5.1.1 Coercivity 78
5.1.2 Saturation Magnetization 82
5.2 Part II – Effects of Annealing 84
5.2.1 Coercivity 84

จุฬาลงกรณ์มหาวิทยาลัย
CHULALONGKORN UNIVERSITY

Page

5.2.2 Saturation Magnetization 94
5.3 Part III – Effects of Magnetic Field and Low Temperature 94
5.3.1 Coercivity 94
5.3.2 Saturation Magnetization 100
5.4 Contribution of Microstructure and Magnetic Domain for Magnetic Properties of CoFe Films 103
5.5 Comparison of CoFe Alloyed Films' Soft Magnetic Properties 106
CHAPTER VI CONCLUSION 107
REFERENCES 109
APPENDICES 115
APPENDIX A AFM Images of The Surface of The CoFe Deposits 116
APPENDIX B Crystallographic and Structural Data of The CoFe Deposits 122
APPENDIX C Magnetic Data of The CoFe Deposits 128
VITA 130

จุฬาลงกรณ์มหาวิทยาลัย
Chulalongkorn University

LIST OF TABLES

Table 2.1 The samples of CoFe based magnetic thin films produced by electroplating process within the past decade. 22

Table 3.1 Composition of the plating bath for Co-Fe electrodeposition.....38

Table 5.1 Lattice constant of the CoFe films with 57.3 wt.% Fe and 80 wt.% Fe from XRD analysis.....92

จุฬาลงกรณ์มหาวิทยาลัย
Chulalongkorn University

LIST OF FIGURES

Fig. 2.1 Magnetic dipole moments' ordering in magnetic materials: (a) paramagnetic, (b) antiferromagnetic, (c) ferromagnetic and (d) ferrimagnetic materials [33]. 8

Fig. 2.2 Hysteresis loop of magnetization process of ferromagnetic material [2]. 10

Fig. 2.3 Magnetization curves of Fe single crystal [27]. 12

Fig. 2.4 Schematic illustration of random anisotropy pattern [36]. 13

Fig. 2.5 Relation of grain size and coercivity of ferromagnetic materials [40]. 13

Fig. 2.6 Magnetization curve of Ni-Fe alloy with and without tensile stress [27]. 14

Fig. 2.7 Magnetization curve of Ni alloy with and without tensile stress [27]. 15

Fig. 2.8 Directional order of like-atom pairs in magnetic material as a result of induced anisotropy processes [2]. 16

Fig. 2.9 Recording geometry of writing head core [5]. 18

Fig. 2.10 Thin film components in recording head core [3]. 18

Fig. 2.11 CoNiFe ternary diagram with saturation magnetization of each area [5]. 19

Fig. 2.12 Schematic feature of electrodeposition apparatus for metal coating from aqueous electrolyte and metal salt, MA [52]. 21

Fig. 2.13 Coercivity and sulfur inclusion of electrodeposited CoNiFe thin films deposited from the sulfur-containing additive (SCA) baths; (a) saccharin bath; (b) thiourea bath [6]. 23

Fig. 2.14 The dependence of Co and Fe contents in the films on pH value [61]. 28

Fig. 2.15 Hydrodynamic flow system of Lorentz force as a result of current density and magnetic flux density [28]. 29

Fig. 2.16 Schematic illustration of magnetohydrodynamic (MHD) effect interplaying with micro-magnetic convection (MMC) in diffusion zone of electroplating process [65]. 30

Fig. 2.17 TEM images of CoFe deposits: (a) and (b) cross sections of the deposits without and with magnetic field perpendicular to electrode surface respectively [32]. 31

Fig. 2.18 In-plane hysteresis loops from VSM measurements of layers deposited without, with magnetic field parallel and perpendicular to electrode surface of CoFe films [32]. 31

Fig. 3.1 The relation of plating factors, film characteristic and magnetic properties. 36

Fig. 3.2 Schematic illustration of the set-up of electrodeposition for CoFe deposits production. 38

Fig. 3.3 XPF measurement points on each CoFe sample. 40

Fig. 3.4 Schematic illustration of the set-up of magnetic-field electrodeposition for CoFe deposits production. 45

Fig. 4.1 The Fe content in the deposits as a function of Fe^{2+} /(Co^{2+} + Fe^{2+}) ratio in the plating baths with 0.5-hour and 4-hour plating durations. 47

Fig. 4.2 The optical micrographs of surface morphology of (a) 0.5-hour plating and (b) 4-hour plating films from the bath of electrolyte with 85 % Fe^{2+}. ..47

Fig. 4.3 XRF results of the films' thickness. 48

Fig. 4.4 The VSM measurement of in-plane magnetic hysteresis loop of the as-deposited CoFe films with (a) low Fe content; 55.1 and 57.3 wt.% Fe from 0.5-hour and 4-hour plating, and (b) high Fe content; 80.9 and 80.0 wt.% Fe, from 0.5-hour and 4-hour plating, respectively. 49

Fig. 4.5 The in-plane magnetic properties of the 0.5-hour and 4-hour plated CoFe films as measured by VSM: (a) saturation magnetization, and (b) coercivity. 50

Fig. 4.6 The XRD profiles of the CoFe deposits electroplated for (a) 0.5 hour and (b) 4 hours. 53

Fig. 4.7 Texture coefficient of bcc (110) plane of the CoFe deposits as determined from XRD analysis. 54

Fig. 4.8 AFM images of the surface of the deposits with (a) 55.1 wt.% Fe and (b) 80.9 wt.% Fe of the 0.5-hour plated CoFe films, and the deposits with (c) 57.3 wt.% Fe and (d) 80.0 wt.% Fe of the 4-hour plated CoFe films. 55

Fig. 4.9 (a) Roughness and cluster size, and (b) XRD grain size of the CoFe films electroplated for 0.5 hour and 4 hours. 56

Fig. 4.10 MFM images of the magnetic domain structure: (a) 55.1, (b) 80.9 wt.% Fe of 0.5-hour plated CoFe films and (c) 57.3, (d) 80.0 wt.% Fe of 4-hour plated CoFe films. 57

Fig. 4.11 The VSM measurement of in-plane magnetic hysteresis loop of the as-deposited, 200°C annealed and 300°C annealed CoFe films with: (a) 57.3 wt.% Fe, and (b) 80.0 wt.% Fe. 59

Fig. 4.12 The in-plane magnetic properties of the as-deposited, 200°C and 300°C annealed CoFe films as measured by VSM: (a) saturation magnetization, and (b) coercivity. 60

Fig. 4.13 The AFM images of the surface of CoFe deposits with 57.3 wt.% Fe; (a) as-deposited, (b) 200°C annealed, (c) 300°C annealed, and the films with 80.0 wt.% Fe; (d) as-deposited, (e) 200°C annealed, (f) 300°C annealed. 61

Fig. 4.14 Measurement of the films' thickness by XRF. 62

Fig. 4.15 Thickness measurement by optical microscope of the selective specimen; (a) as-deposited and (b) 300°C annealed CoFe film with 80.0 wt.% Fe. 63

Fig. 4.16 XRD analysis of the CoFe deposits of: (a) 57.3 wt.% Fe, and (b) 80.0 wt.% Fe. 65

Fig. 4.17 Estimated grain size of the films by XRD. 65

Fig. 4.18 AFM measurement of the films' roughness. 66

Fig. 4.19 Texture coefficient of bcc(110) plane of the films by XRD analysis. 66

Fig. 4.20 The Fe content in the deposits as a function of $Fe^{2+}/(Co^{2+} + Fe^{2+})$ ratio in the plating baths with and without 6 kG magnetic field at room temperature and with 6 kG magnetic field at -2°C. 67

Fig. 4.21 The VSM measurement of in-plane magnetic hysteresis loops of (a) high Fe content, and (b) low Fe content of the CoFe films from plating: without magnetic field, with 6 kG magnetic field at room temperature and the field at -2°C. 69

Fig. 4.22 The in-plane magnetic properties: (a) saturation magnetization, and (b) coercivity measured by VSM of the CoFe films from plating: without magnetic field, with 6 kG magnetic field at room temperature and the field at -2°C. 70

Fig. 4.23 The AFM images of the surface of CoFe deposits with; (a) 57.3 wt.% Fe as-deposited, (b) 57.8 wt.% Fe with magnetic field at room temperature, (c) 64.4 wt.% Fe with magnetic field at -2°C , and the films with; (d) 80.0 wt.% Fe as-deposited, (e) 82.0 wt.% Fe with magnetic field at room temperature, (f) 89.1 wt.% Fe with magnetic field at -2°C. 71

Fig. 4.24 The XRD profiles of the CoFe deposits electroplated with magnetic field at (a) room temperature and (b) -2°C. 73

Fig. 4.25 Texture coefficient of bcc: (a) (110), (b) (200) and (c) (211) planes of the CoFe films by XRD analysis. 75

Fig. 4.26 Estimated grain size of the CoFe films by XRD. 76

Fig. 4.27 AFM measurement of the films' roughness. 76

Fig. 4.28 XRF measurement of the films' thickness. 77

Fig. 5.1 Coercivity as a function of the XRD grain size of the CoFe deposits..... 79

Fig. 5.2 Uniaxial anisotropy constant as a function of Fe content in CoFe films. 80

Fig. 5.3 The coercivity of the CoFe films as a function of uniaxial anisotropy constant..... 81

Fig. 5.4 The relation of coercivity and the ratio of estimated grain size (d) to exchange length (L_{ex}) of the CoFe films. 82

Fig. 5.5 Demagnetization of defects in the CoFe thin film, (a) porous defects in CoFe thin film (extended from Fig. 4.2) and (b) schematic view of demagnetizing field generated inside the pores. 83

Fig. 5.6 Plots of coercivity and roughness of the CoFe films..... 84

Fig. 5.7 Plots of coercvity and thickness of the CoFe films. 85

Fig. 5.8 In-plane uniaxial anisotropy constant of the CoFe films. 86

Fig. 5.9 Plots of coercivity and uniaxial anisotropy constant of the CoFe films..... 87

Fig. 5.10 The comparisons between coercivity and ratio of estimated grain size (d) to exchange length (L_{ex}) of the CoFe films. 88

Fig. 5.11 The coercivity of the CoFe films as a function of grain size. 88

Fig. 5.12 Linear dependence of lattice spacing (d) versus $\sin^2\psi$ of the CoFe films with (a) 57.3 and (b) 80.0 wt.% Fe. 90

Fig. 5.13 Residual stress and coercivity of 57.3 and 80.0 wt.% Fe films..... 91

Fig. 5.14 The relation of coercivity and uniaxial anisotropy constant of the CoFe films with 57.3 and 80.0 wt.% Fe..... 93

Fig. 5.15 Relation between coercivity and the CoFe films' roughness. 95

Fig. 5.16 Plots of coercivity and thickness of the CoFe films. 95

Fig. 5.17 The determination of anisotropy field (H_k) estimated from hysteresis loop of hard direction of 64.4 wt.% Fe film from magnetic-field plating at -2°C, easy and hard directions of specimen are the direction along

and perpendicular to the magnetic field direction during plating respectively. 96

Fig. 5.18 In-plane uniaxial anisotropy constant of the CoFe films. 98

Fig. 5.19 Plots of coercivity and uniaxial anisotropy constant of the CoFe films. 98

Fig. 5.20 The comparisons between coercivity and ratio of estimated grain size (d) to exchange length (L_{ex}) of the CoFe films. 99

Fig. 5.21 The coercivity of the CoFe films as a function of estimated grain size. 100

Fig. 5.22 The relation between saturation magnetization and texture coefficient of (a) (110), (b) (200) and (c) (211). 102

Fig. 5.23 The relation between saturation magnetization and uniaxial anisotropy constant. 103

Fig. 5.24 The soft magnetic properties of CoFe alloyed films from previous researches compared to the results of this thesis. 106

จุฬาลงกรณ์มหาวิทยาลัย
Chulalongkorn University

CHAPTER I
INTRODUCTION

1.1 Motivation

Magnetic thin film plays an important role in various electronic industries, such as micro and nano-electromechanical systems (MEMS, NEMS), hard disk drive and electronic sensors. Soft magnetic properties are needed for the film of these practices including magnetic recording head core in magnetic data storage [1]. High saturation magnetization of the head core helps to record data bits in narrow tracks of media with high coercivity giving rise a high storage density. Furthermore, its low coercivity supports easy reversing magnetic direction during writing process. The properties accomplish high performance hard disk drive in both of higher capacity and swifter working rate [2].

In recent decades, many researches have explored and improved soft magnetic materials, involving NiFe and CoFe-based alloys [3]. For examples, Qin et al. fabricated NiFe alloyed film with 11 kG of saturation magnetization and 100 Oe of coercivity by sputtering method [4]. Osaka et al. used electroless-plating to generate NiFeB film with 10 kG of saturation magnetization and 40 Oe of coercivity [3]. Recently, CoFe alloyed film is found as the most potential material for recording head core of hard disk drive [5, 6]. High saturation magnetization with 24.5 kG and low coercivity with 6.5 Oe can be generated [7].

Furthermore, many researches reveal that the composition proportion of Co and Fe also influences on CoFe films' saturation magnetization. For instances, Miyake et al. and Yokoshima et al. investigated CoFe films' saturation magnetization reaches optimum point at around 65 at.% of Fe content [8, 9]. Kim et al. found that the saturation magnetization increases with of Fe content in CoFe [10]. In addition, the coercivity of the film has been also found to depend on the Fe content. For examples, Yokoshima et al. reported that the highest coercivity of CoFe film is attained with 55 at.% of Fe content, while Miyake et al. found that the coercivity of CoFe film reduce with Fe content in the film [8, 9] and Kim et al. informed that the coercivity of CoFe film varies with Fe content increment [10]. It appears therefore

that good soft magnetic properties of CoFe could be achieved with Fe content above 55 wt.%.

In addition, thickness is found to affect soft magnetic properties. The thickness effect of CoFe film from sputtering has been studied. The research exhibits that the saturation magnetization and coercivity of the sputtered CoFe films decreases and increases with increasing of the film thickness, respectively [11]. Electrodeposited NiFe alloys have also been investigated and it was found that magnetization behavior and anisotropy degree depends on the film thickness. Isotropic behavior was observed in a thick NiFe film deposited on a plated polycrystalline copper substrate [12]. Furthermore, thickness of NiFe film deposited on polycrystalline copper wire also alters easy direction of anisotropy from a wire-axis orientation to a hard direction [13]. It is possible that the the film thickness may play some role controlling the magnetic properties of electroplated CoFe films.

Although the previous papers study the connection between the chemical compositions and the magnetic outputs of the deposit, it is still inconclusive that how the films' microstructure and domain structure are systematically affected by its composition, which contributes the magnetic properties. The indefinite knowledge of this matter is still limited for CoFe alloyed film.

According to several processes can be performed to produce CoFe deposit, for instance, sputtering, melt-spun ribbon method, electroless plating and electrodeposition [6, 14-16]. However, electroplating is considerable and advantageous manufacturing in practical mass production, owing to low cost, simply process and accurately control films layer [17]. Various parameters of the method including electrolyte concentration, current density, plating duration and additive type affect the film characteristics which contribute to the film's magnetic properties.

Previous researches have confirmed that the plating variables of electrodeposition process influence on films' composition and then result in the soft magnetic properties. For examples, high current density increases Fe content and low plating temperature induce coercivity decrement for CoFe film [18]. Plating additive type and content in turn the deposit morphology, which significantly lead to saturation magnetization and coercivity change [18, 19].

Moreover, the additional process, post heat treatment applied to the soft magnetic deposit also alters the characters of the soft magnetic alloy. So, the electrodeposition followed by heat treatment technique for CoFe and other soft magnetic materials are potential to develop both magnetic properties and manufacturing of CoFe thin film [3, 7]. Prior studies exhibit that the film's microstructure and crystallographic orientation can be variously changed by varying the temperature and soaking duration of the method, which inevitably result in the soft magnetic properties. In addition, internal stress of the film is able to be released that it also effects on the magnetic responses [20]. For instances, annealing at around 400°C can enlarge grain size and affect texture change as the principle factors, then promotes high coercivity of $Co_{50}Fe_{50}$ and $Co_{60}Fe_{20}Ni_{20}$ deposits [21, 22]. In contrast to $Co_{50}Fe_{50}$ alloyed film, post thermal treatment at 700 – 850°C extends grain size, but induces low coercivity [23]. The coercivity of $Co_{68}Fe_{32}$ film can be reduced by annealing at the temperature in approximate range of 1,000 – 1,200°C because of residual stress relief from quenching process [24]. Furthermore, low temperature annealing around 200°C can also lead to low coercivity of CoFe films, as what have been observed in electroplated $Co_{40}Fe_{60}$ and $Co_{19}Fe_{52}Ni_{29}$ films developed by Zong et al. and Liu et al. respectively [7, 25]. Since the low temperature annealing requires low energy and short heating duration, it is an attractive heat treatment process. However, as the justification, the systematic research of low temperature annealing effects on the CoFe films with various compositions is still limited especially in the range of 200 – 300°C.

The optional techniques for electrodeposition process, applying magnetic field during plating of magnetic film, can assist to modify films' crystallographic plane, nucleation, grain size and roughness leading to change of film's magnetic responses [26, 27]. For example, Koza et al. reported that a constant magnetic field of 1 T applied in the plating process of CoFe alloys induces more homogeneous and smoother surface of their CoFe films resulting in low coercivity of 4.15 – 7.63 Oe [28]. Zielinski presented the effects of magnetic field during plating of Co alloy films, and showed that it helps altering the films' structure, improving density and reducing internal stress of the films due to crack annihilation [29]. Matsushima et al. found that magnetic field applied in parallel to an electrode surface affect

crystallographic structure, preferred orientation, and thickness of electroplated Fe films [30]. In addition, high concentration of magnetic field during pulse plating process is able to raise saturation magnetization and reduce coercivity of magnetic film by inducing phase change and smaller grain size with smoother surface. For instant, Yundan et al. showed that magnetic field of 1 T introduced in plating of Co magnetic films can enhance the intensity of (002) peak and induce small grain size of around 32 – 72 nm and smooth films' surface, leading to high saturation magnetization and low coercivity [31]. Furthermore, the direction of magnetic field also affects the electroplated film's microstructure and magnetic properties. For example, Koza et al. exhibited that electrodeposition of CoFe films with magnetic field parallel to an electrode surface promotes smooth layer, small grain size and low internal stress of the film owing to a low coercivity. On the other hand, a perpendicular field renders opposite results, and magnetic field has no significant effect on saturation magnetization [32]. Zong et al. applied 280 Oe magnetic field parallel to an electrode surface during plating, resulting in high saturation magnetization and low coercivity [7]. This suggests that the parallel direction of magnetic field is able to improve softer magnetic properties of CoFe alloyed film.

It is well known that magnetic field induces anisotropy energy which attributes magnetic domain and grain orientation. The anisotropy energy has to be larger than the thermal energy which is a function of the temperature of film preparation process. Due to vibration created from the thermal energy can interrupt the orientation, high temperature leads to randomizing influence resulting in less directional order of like-pair atoms [26, 27]. Hence, it is possible that the orientation may be induced well and more easily aligns by the magnetic field when the effect of thermal energy is decreased by reducing the temperature of plating bath, because low temperature means low thermal energy. Thus, by this method, the magnetic properties of film should be improved. However the comprehension extracted from the investigation of magnetic field under low temperature affecting the relations of microstructure, and magnetic properties of plated CoFe film with various compositions is still very limited and no systematic study. Furthermore, there is still no report about low temperature effect on CoFe film's electrodeposition especially at below 0°C. The prior work by Du et al. shows that, under a high magnetic field of 6

T in a thermal evaporation system. Fe films that are deposited on Si substrates exhibit higher soft magnetic characteristics (saturation magnetization of 1.42×10^6 A/m and coercivity of 0.47×10^3 A/m) when deposited at the room temperature, as compared to a higher temperature above 400^oC [26].

Electrodeposition followed by annealing process is therefore a potential manufacturing method that provides qualitative control of the film's structure. This study will thus aim to shed the lights on the development of electrodeposited CoFe alloys, providing mechanistic views of the relationship between magnetic properties, chemical composition, and microstructure. In addition, the knowledge would be applicable and implementable for industrial manufacturing process, especially electronic and data storage sectors.

1.2 Objective of Research

This dissertation would aim to systematically study the influences of chemical composition of CoFe thin films fabricated by electrodeposition, thermal annealing applied to the films and magnetic field applied during electrodeposition process with different plating temperature which are performed with a wide range of the films' composition. The analysis would be done through the crystallography, microstructure transformation and internal stress of the alloys corresponding magnetic characteristics. The process variables-structure-properties correlations are determined.

จุฬาลงกรณ์มหาวิทยาลัย
Chulalongkorn University

1.3 Scope of Research

In this work, soft magnetic properties of the CoFe deposits would be investigated including characterization and analysis for relation and mechanism of chemical composition and film's structure features, such as roughness, grain size, domain structure, internal stress and crystalline orientation controlling by electrodeposition and annealing process variables. The study is planned and separated into three parts as the following:

1.3.1 Magnetic Properties of Electrodeposited CoFe Films

As by far discussion, it is known that alloy composition plays an important role on microstructure, grain size, phase and finally including magnetic response. For CoFe film, previous researches confirmed that the Fe content in CoFe film from around 55 – 80 wt.% induces outstanding soft magnetic properties [5, 10]. The composition range should be considered. The film's composition will be controlled mainly by electrolyte concentration in plating bath and the film's thickness will be controlled by plating duration. The magnetic properties of the films will be investigated depending on chemical composition in the films, grain size, roughness, domain feature, thickness and crystallographic plane.

1.3.2 Magnetic Properties of Annealed CoFe Films

The plated CoFe films with various compositions will be annealed in different temperatures to modify the films' structure which affects their magnetic properties. The films' changes of crystallographic plane, grain size, roughness and internal stress would be investigated and cooperated with magnetic properties analysis.

1.3.3 Magnetic Properties of CoFe Films Fabricated by Electrodeposition with Magnetic Field

In this section, the research aim to elucidate the influence of magnetic field applied during plating process. The constant magnetic field generated from a pair of magnets is put in the plating bath with different temperature of electrolyte. The insight gained from this experiment will extract the mechanistic view into the ascendency of magnetic field on the CoFe plating approach.

1.4 Benefits of Research

There are benefits from this work: (i) the knowledge of magnetic properties of CoFe films from electrodeposition with and without magnetic field including annealing treatment will be provided correlating with microstructure, morphology, internal stress and crystallographic plane of the films in various chemical compositions, the controlling factors of the process are investigated, (ii) the insight of the influences of the additional process, annealing, and the optional function for

electrodeposition, magnetic field, will be obtained to attain the comprehension of these effects shining the light on fundamentals of magnetic materials including practical application for industrial production of CoFe alloys. Furthermore, the knowledge can assist to develop the fabrication process of CoFe magnetic film with its improved potential.

จุฬาลงกรณ์มหาวิทยาลัย
Chulalongkorn University

CHAPTER II
THEORETICAL ASPECTS AND LITERATURE SURVEY

2.1 Soft Magnetic Properties of Ferromagnetic Alloys

The ferromagnetic alloys are the metals containing the magnetic moments align parallel to each other that is the ferromagnetism phenomenon which produces a huge magnetization, while other magnetic materials have difference of magnetic dipole moments' ordering as shown in Fig. 2.1. The dipole moments' directions in paramagnet are randomly. Antiferromagnetic material has dipole moments align antiparallel to each other obtaining zero net magnetization. The dipole moments' orientation in ferrimagnetic material is like that of antiferromagnet but some of the dipole moments are greater than others then creating net magnetization [33]. The ferromagnetic alloys can be fabricated from Fe, Co and Ni without/with another element or other elements to enhance high magnetization. The writing head core needs ferromagnetic film with soft magnetic properties that high saturation magnetization and low coercivity are required.

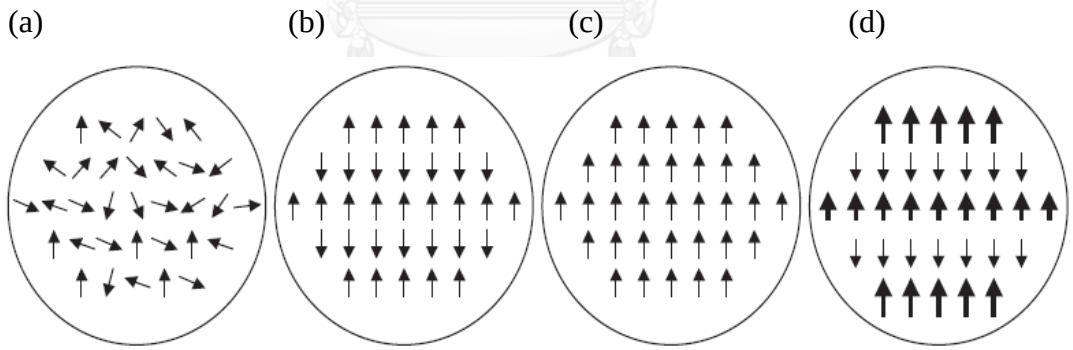

Fig. 2.1 Magnetic dipole moments' ordering in magnetic materials: (a) paramagnetic, (b) antiferromagnetic, (c) ferromagnetic and (d) ferrimagnetic materials [33].

2.1.1 Magnetization Process

A material exerted by a magnetic field (H), the unit is Oe (Oersted), generates the response called the magnetic flux density or the induction (B), the unit is G (Gauss). The equation of the relationship between these variables in the terms of centimeter-gram-second (cgs) units is

$$B = H + 4\pi M \tag{2-1}$$

where, M is the intensity of magnetization (emu/cm^3) as determined by the equation

$$M = \sigma\rho \tag{2-2}$$

Here, σ is specific magnetization (emu/g), and ρ is density of material (g/cm^3). The intensity of magnetization depends on magnetic dipole moments of ions or atoms and the interaction of the moments with each other.

The magnetization is generated from a ferromagnet by applying a magnetic field, but it is not zero when the field is reduced. The magnetization of the magnet is still remained. The plot which represents the relationship between the magnetic induction (intensity of magnetization) and the magnetic field is called a hysteresis loop as shown in Fig. 2.2. When the field is increased, the magnetic induction continues to increase and then reaches the constant value called the saturation induction of saturation magnetization (B_s). When the field is decreased to zero, the induction reduces from saturation level to residual induction or retentivity (B_r). The amount of the reverse field is applied to deplete the induction into zero, the field is called coercivity (H_c). For soft magnetic metals, the coercivity is very small attributing easily magnetized and demagnetized comparing to hard magnetic materials. The ratio of B/H is permeability (μ) which is the slope of the hysteresis loop.

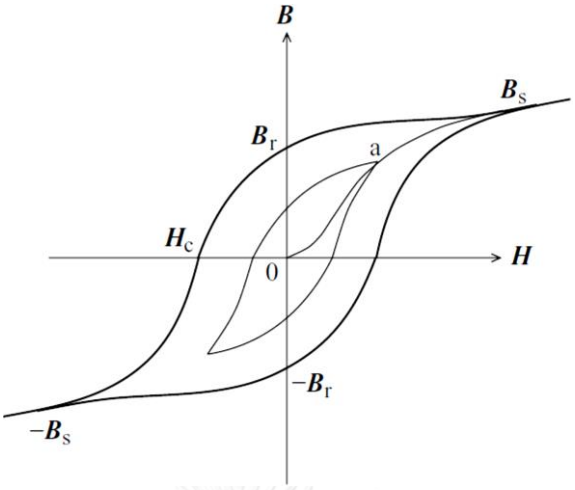

Fig. 2.2 Hysteresis loop of magnetization process of ferromagnetic material [2].

2.1.2 Magnetic Anisotropy

A material expresses anisotropic property when its magnetic property depends on measured directions in the specimen. The magnetization appearance which differs as a result of fixed directions in the specimen is called magnetic anisotropy. The anisotropy is the axis of a ferromagnetic or antiferromagnetic specimen lying along a particular direction. When the material is magnetized from zero to saturation state with lowest magnetic field or magnetic energy along some direction, the direction is easy direction or easy axis of magnetization. In contrast, magnetization in hard direction requires largest energy to reach saturation level, because anisotropy force tries to hold magnetization of any domain along its easy direction.

The anisotropy affects magnetization curve and hysteresis loop shape of magnetic materials that can depict its coercivity. The strong anisotropy leads to the difficulty or needs high energy for magnetization change in domain contributing strongly to the coercivity field.

The anisotropy can be not only a function of intrinsic characteristic of the material, such as crystal structure, but also extrinsic property, such as stress and shape, or induced by magnetic field and plastic deformation [27, 34]. The good soft magnetic response is retained in magnetic material with effectively low

magnetocrystalline anisotropy [35, 36]. The essential anisotropies relevant to the research and playing an important role on soft magnetic material are:

1. Magnetocrystalline anisotropy or crystal anisotropy,
2. Magnetoelastic anisotropy or stress anisotropy,
3. Induced anisotropy.

2.1.2.1 Magnetocrystalline Anisotropy

When magnetization process of a single crystal is various when magnetic field applied along different crystallographic directions, the crystal exhibits magnetocrystalline anisotropy. The easy direction of magnetization in crystal means the crystallographic direction of the spontaneous magnetization inside domain in demagnetized state. The magnetization in easy direction is driven with low energy of small magnetic field to reach saturation state. In contrast, when the magnetization is tried to change its direction to others, higher energy is required to perform by larger magnetic field because the anisotropy resists the rotation of magnetization to other directions. For example, the easy direction of Fe is <100> as shown in Fig. 2.3. This direction, the saturation state is reached easier than other crystallographic directions. The different energy between the hard and easy oriented magnetization is magnetocrystalline anisotropy energy [27, 37].

The original source of magnetocrystalline anisotropy is the interaction of spin, orbit and lattice. The orbit-lattice coupling plays an important role on the magnetocrystalline anisotropy because high strength of the orbit-lattice coupling fixes the orientation of the orbit strictly to the lattice, so the large magnetic field cannot differentiate the orientation. The coupling also resists the spin rotation. The energy required for spin rotation away from the easy direction is called the anisotropy energy.

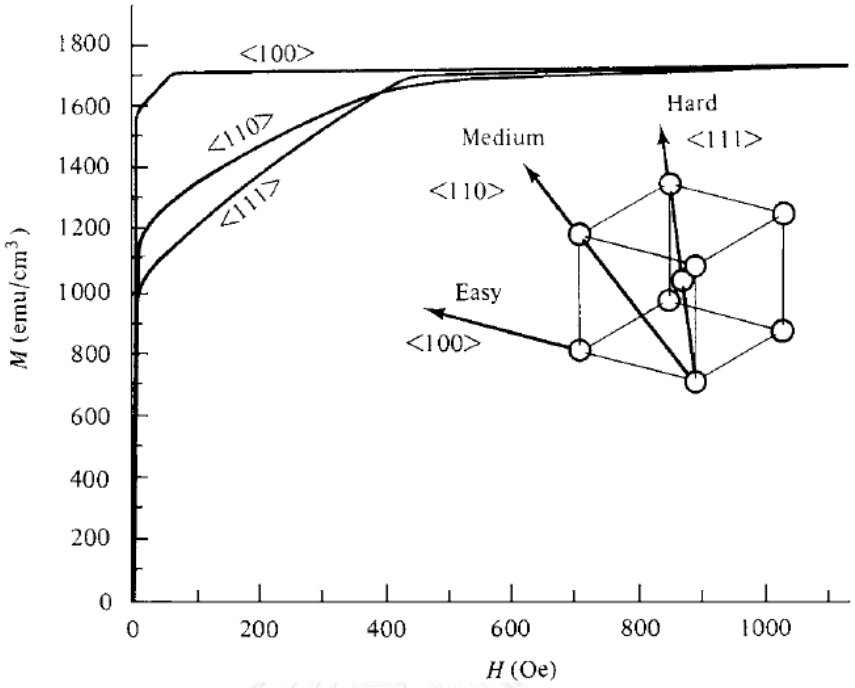

Fig. 2.3 Magnetization curves of Fe single crystal [27].

The magnetocrystalline anisotropy closely relates to grain size of ferromagnetic material. Many domains are able to be contained in a large grain which holds net high magnetocrystalline anisotropy energy because of the long-ranged anisotropy and the mechanism of grain boundary obstructing domain wall movement [36, 37]. In contrast, when the grain size is smaller than the ferromagnetic exchange length of the material, the magnetocrystalline anisotropy decreases as the grain size reduction and becomes random anisotropy which low energy of magnetization as shown in Fig. 2.4. This results in small coercivity. The relationship between coercivity and grain size is as Herzer's plot shown in Fig. 2.5 [37-39].

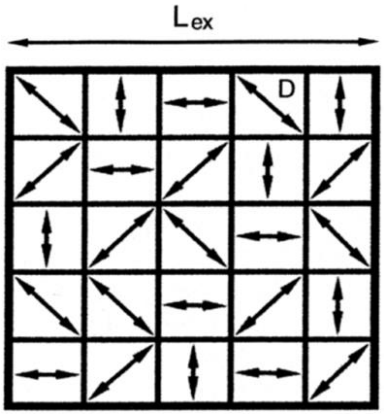

Fig. 2.4 Schematic illustration of random anisotropy pattern [36].

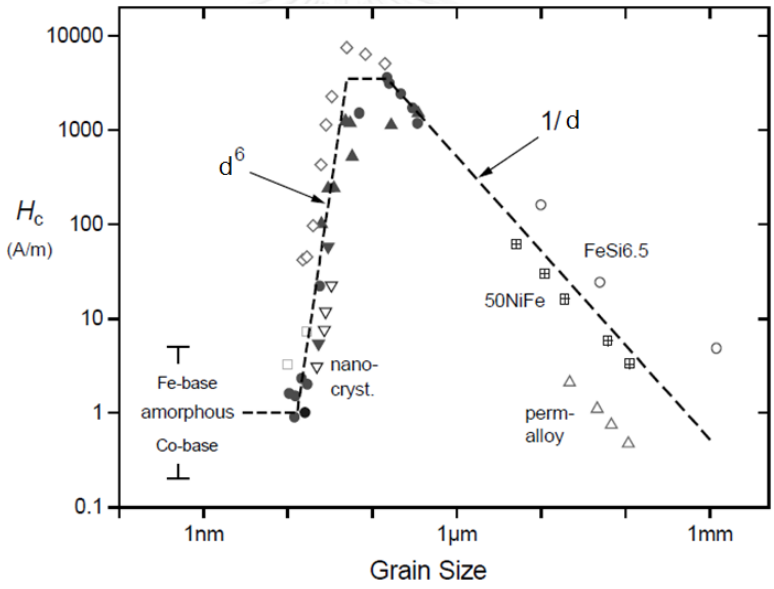

Fig. 2.5 Relation of grain size and coercivity of ferromagnetic materials [40].

In general, the influence of grain size (d) on coercivity depends on the size of the grain with respect to exchange length (L_{ex}) and domain wall width (δ). In particular, for grain size smaller than exchange length, it follows that $H_c \, \alpha \, d^6$ due to the presence of random anisotropy [36]. On the other hand, if grain size is larger than domain wall width, the coercivity is reversely related to grain size by the relation of $H_c \, \alpha \, d^{-1}$, owing to domain wall pinning by grain boundaries [4, 21, 41].

2.1.2.2 Magnetoelastic Anisotropy

The stress applied on magnetic materials can create anisotropy. It means that the mechanical stress modifies the magnetic dipole moments' orientation in the materials, then the magnetic behaviors of the materials are altered. The results of stress on magnetic properties are differently responded in various materials. For instance, applied tensile stress on Ni-Fe alloy leads to permeability improvement, the phenomenon is called positive magnetostriction, while negative magnetostriction is induced in Ni, as shown in Fig. 2.6 and Fig. 2.7 respectively. Both tensile and compressive stress creates an easy axis of magnetization in magnetic material. The change in anisotropy finally attributes to softness of magnetic material, such as coercivity and permeability [27, 42].

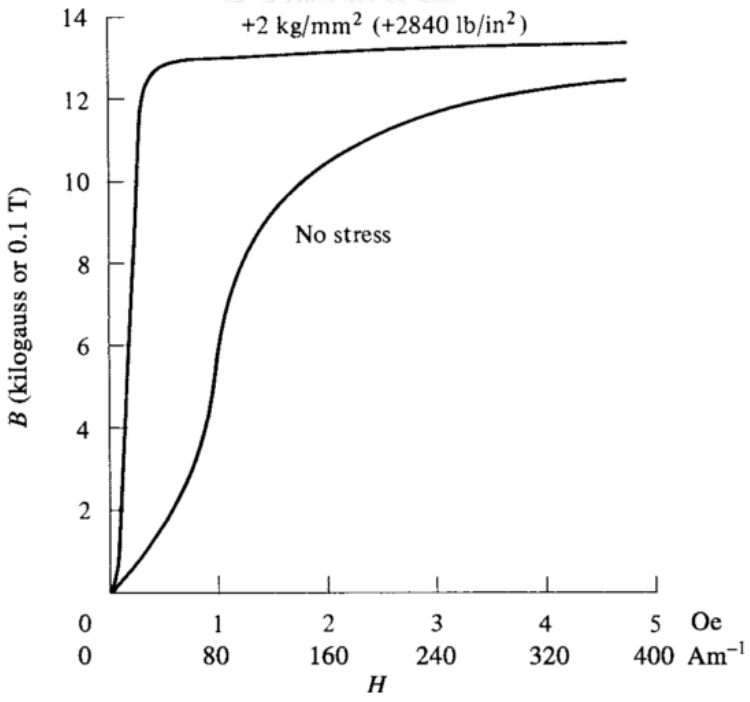

Fig. 2.6 Magnetization curve of Ni-Fe alloy with and without tensile stress [27].

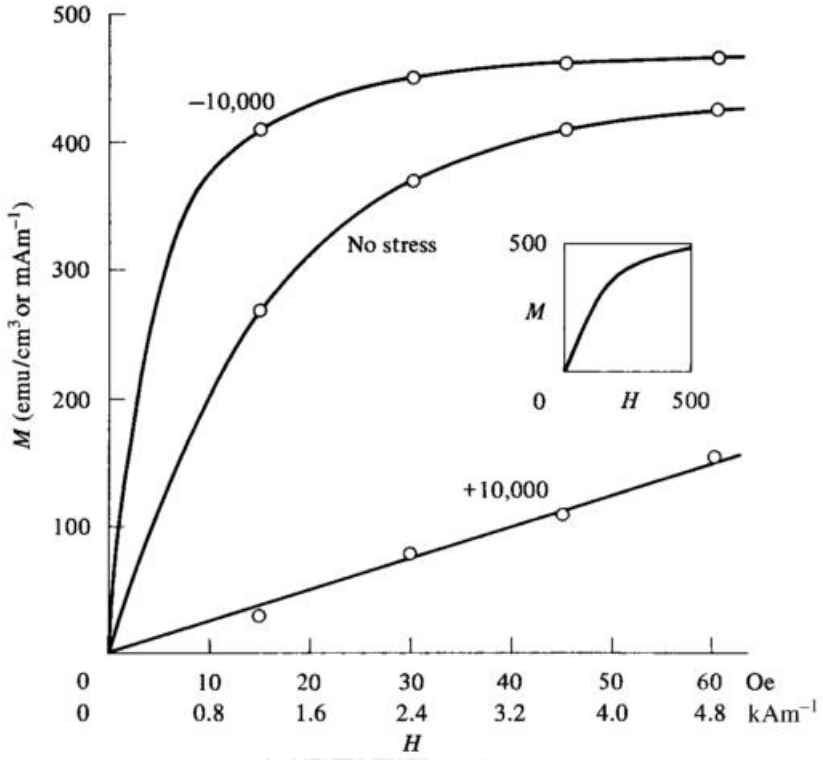

Fig. 2.7 Magnetization curve of Ni alloy with and without tensile stress [27].

2.1.2.3 Induced Anisotropy

The anisotropy can be generated due to directional ordering of like-atom pairs created in magnetic materials by the processes of magnetic field annealing, stress annealing or plastic deformation. The processes can control the like-atom pair orientation over the strength and direction of the easy direction along the direction of applied field, stress and rolling in the magnetic field annealing, stress annealing and plastic deformation respectively, as shown in Fig. 2.8. The like-atom pair orientation is induced by diffusion in annealing process or during plating, but by slip in the plastic deformation treatment [27, 43].

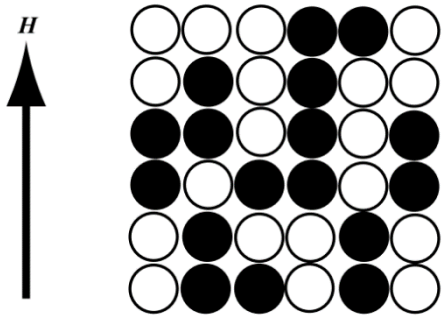

Fig. 2.8 Directional order of like-atom pairs in magnetic material as a result of induced anisotropy processes [2].

The strength or energy of the induced anisotropy is uniaxial anisotropy constant, K_u which can be determined and relates to exchange length and domain wall width as expressed by [27]

$$L_{ex} = \sqrt{\frac{A}{K_u}} \tag{2-3}$$

where K_u is uniaxial anisotropy constant determined by the equation [27]

$$K_u = \frac{M_s H_k}{2} \tag{2-4}$$

here, H_k is anisotropy field and M_s is saturation magnetization measured from hysteresis loop [27, 41]. A is exchange stiffness which is estimated by the formula [4]:

$$A = \frac{nJS^2}{a} \tag{2-5}$$

Chulalongkorn University

here, n is the number of atoms in unit cell, S is total spin of electron assumed 1 for CoFe, a is the lattice constant determined from XRD analysis, J is exchange integral, for CoFe it is estimated by the relation [44]:

$$J = 0.15kT_c \tag{2-6}$$

where, k is Boltzmann's constant and T_c is Curie temperature [44]. The domain wall width δ is related to the exchange length by [27, 41]

$$\delta = \pi L_{ex} \tag{2-7}$$

The anisotropy is able to provide by proper post treatments or additional potential methods during specimen preparation processes. The a few potential techniques for creating induced anisotropy of magnetic film, such as magnetic annealing and magnetic-field plating [34, 45].

2.1.2.3.1 Magnetic Annealing

This method depends on heating and gradually cooling steps underneath a magnetic field. The easy axis of magnetization is created parallel to the field contributing to uniaxial anisotropy. The temperature of magnetic material is heated to below its Curie temperature. Then, the material loses its anisotropies and the magnetic dipoles are easy to alter their directions to align parallel to the applied magnetic field. After that, the material is cooled down to room temperature among the field [27, 46].

2.1.2.3.2 Magnetic-Field Plating

Magnetic field applied during plating, magnetic force exerts on ions, atoms, grains and layers in nucleation including growth of deposit, and then the field finally influences on surface morphology and its magnetic properties. The plating processes for magnetic thin films, electrodeposition or thermal evaporation, can be implemented with magnetic field. The field produces magnetohydrodynamic convection during

plating contributing to atomic orientation in grains, there will be induced anisotropy in plated deposit [26, 45, 47].

2.2 Magnetic Thin Film for Recording Head Core of Hard Disk Drive

HDD recording density has been increasing tremendously with high rate, from 10^{-2} Mbit/in^2 in 1960 to around 10^6 Mbit/in^2 in 2017 [5, 48]. This high rate of area density increment was achieved by improvement of magnetic recording head core as a key component. The principle of recording head operation is shown in Fig. 2.9. A recording head core floating above moving a magnetic layer of medium creates magnetic field through the gap between the head core and the medium. The material of the medium underneath the magnetic field is magnetized in a pattern reproducing information recorded in the medium [27].

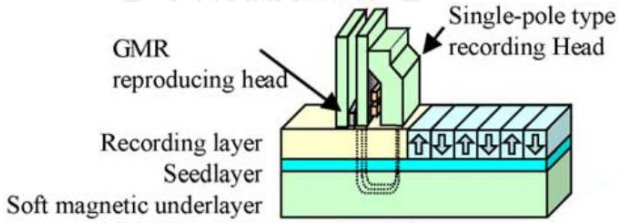

Fig. 2.9 Recording geometry of writing head core [5].

จุฬาลงกรณ์มหาวิทยาลัย
Chulalongkorn University

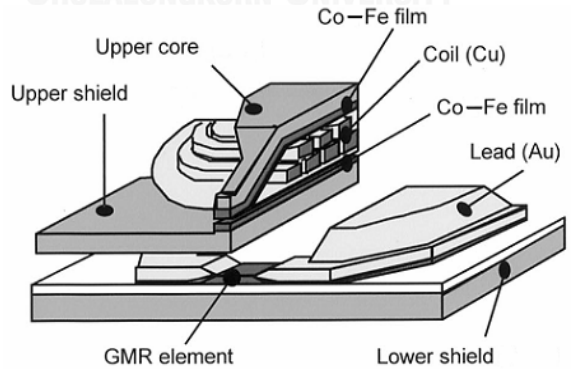

Fig. 2.10 Thin film components in recording head core [3].

The device needed soft magnetic material film which composes of ferromagnetic metals: Co, Fe and Ni (with saturation magnetization 17.6, 21.5 and 6.0

kG respectively [18]) used for fabrication as a core component as shown in Fig. 2.10. The soft magnetic film requires the properties as followed: the first, high saturation magnetization and the second, low coercivity. The magnetic writing head core with high saturation magnetization can induce concentrate magnetic field and record data in high coercivity media at narrow track widths, so that bit length is able to be decreased and more bits can be contained in a track. While low coercivity facilitates the head core to attain swift reverse of magnetization direction during writing data on medium. The two magnetic properties of the recording head core contribute high storage density of hard disk drive [27, 49].

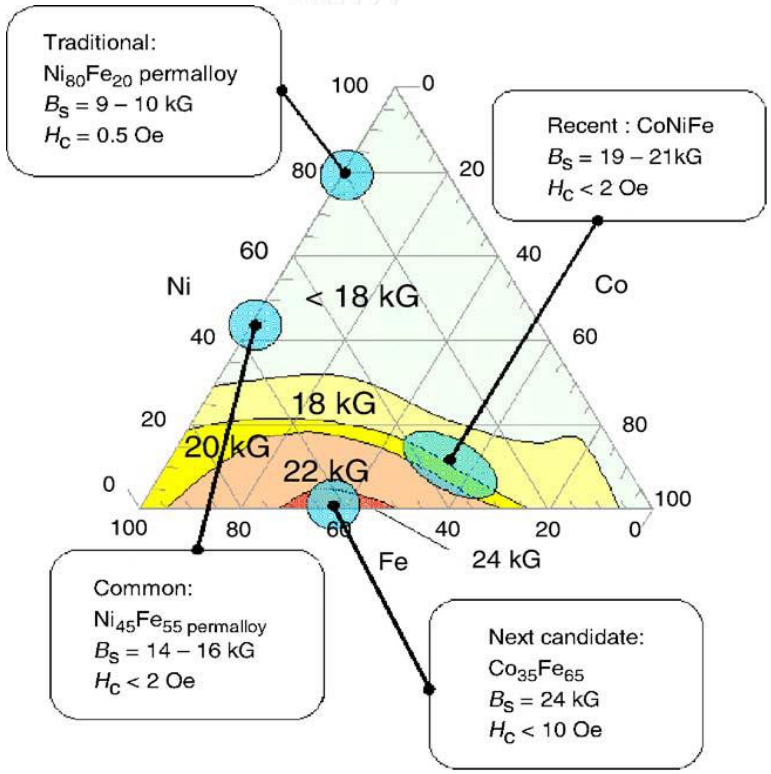

Fig. 2.11 CoNiFe ternary diagram with saturation magnetization of each area [5].

As far as electrodeposition involved hard disk drive production especially fabrication of recording head core, since 1970s, NiFe was applied as core material such as IBM storage products. For improving ultra-high density of hard disk drive, the first requirement, large saturation magnetization of the head core film is highly needed [2, 3, 50]. Thus, to consider the soft magnetic alloys map, ternary CoNiFe

phase diagram as shown in Fig. 2.11. The highest saturation magnetization alloys is focused, so CoFe alloy is taken into account but its coercivity is higher than others in the diagram. The possible method to reduce the coercivity is to fabricate the alloy's structure with very grain size which should be around 20 nm or smaller [50]. The proper composition of the CoFe alloys should be 30 – 40 at.% Co and 60 – 70 at.% Fe, with the saturation magnetization value of around 24.5 kG [44]. The key operation of the electroplating for the high saturation magnetization film is to prevent oxidation of ferrous in the electrodeposition bath. The oxide can occur in the plated film as inclusion then depletes the saturation magnetization. Furthermore, the films' soft magnetic properties are able to be enhanced by a post-annealing process applied to the electroplated film. The coercivity of the film can decline to be a small value about 6 – 8 Oe [5, 7, 51].

2.3 Electrodeposition of CoFe Based Magnetic Thin Films

Electrodeposition is an attractive process for a fabrication of a metallic coating layer onto a conductive substrate by applying electrical current onto electrodes submerged in an electrolyte. A systematic set-up of the electrodeposition system is shown in Fig. 2.12. Reduction reaction of metal ions in aqueous electrolyte is performed through an electrodeposition process, as written:

จุฬาลงกรณ์มหาวิทยาลัย
Chulalongkorn University

$$M^{z+}_{solution} + ze^{-} \rightarrow M_{lattice} \tag{2-8}$$

Electrons are induced by a rectifier, and metal ion reduction and subsequent deposition occur on a surface of the cathode. The governing thermodynamic of the reaction is represented by Nernst equation. The potential of the reaction E is a function of concentration M^{z+} as shown in the equation:

$$E = E^{0} + \frac{RT}{zF} \ln\left[M^{z+} \right] \tag{2-9}$$

Where R, T, z and F are the gas constant, the absolute temperature, the number of electrons involved in the reaction and the Faraday number (96,500 C) respectively [52].

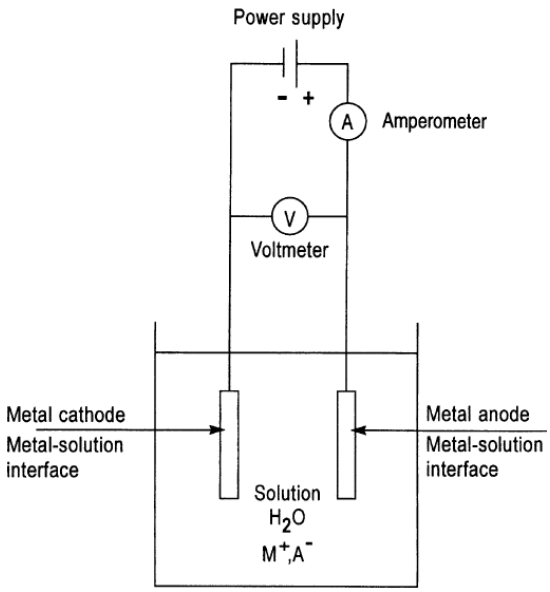

Fig. 2.12 Schematic feature of electrodeposition apparatus for metal coating from aqueous electrolyte and metal salt, MA [52].

Soft magnetic alloy is suitable to be fabricated by electroplating because high rate production of nanocrystalline structure with very fine grain size smaller than 20 nm within a substrate with complex configuration. The structure is able to attribute low coercivity and high saturation magnetization [3, 5]. The samples of soft magnetic thin films produced within the past decades are shown in Table 2.1. The CoFeNi and CoFe alloyed films are popular and proper to accomplish soft magnetic film manufacturing by both chloride bath and sulfate bath. Despite a little bit higher current efficiencies in chloride bath, the results may obtain the lower H_2 limiting current in chloride bath compared to sulfate bath [10]. In addition, the presented ammonium ion could reduce the rate of air oxidation of iron (II) ion in both sulfate and chloride baths. Other plating conditions; current density, temperature, and agitation result in obvious differences of Co content of the alloys deposited from sulfate bath. Whereas, less effects on the composition of the alloy deposited from

chloride bath [17]. However, there is an experiment exhibited that CoFe film with lower coercivity can be obtained from sulfate bath compared to chloride bath in the range of 30 — 50 wt.% Fe content in the film, whereas saturation magnetization variation depends on the Fe content of the film which is existed from both chloride and sulfate baths [10].

Table 2.1 The samples of CoFe based magnetic thin films produced by electroplating process within the past decade.

Composition	Soft Magnetic properties		Year
	B_s (kG)	H_c (Oe)	
$Co_{65}Fe_{23}Ni_{12}$ [6, 50]	21	1.2	1999
$Co_{19}Fe_{52}Ni_{29}$ [25]	20.5	1	2000
$Co_{60}Fe_{40}$ [25]	20.4	12	2000
$Co_{65.8}Fe_{13}Ni_{21.2}$ [53]	17	6.4	2001
$Co_{75}Fe_9Ni_{16}S_{0.35}$ [54]	16	4	2001
$Co_{73}Fe_{15}Ni_{12}S_{0.9}$ [54]	17	0.9	2001
$Co_{65}Fe_{23}Ni_{12}$ [54]	21	1.2	2001
CoFe, 50 wt.% Fe [10]	23	40	2003
$Co_{68.2}Fe_{18}Ni_{12}S_{1.8}$ [55]	21	0.94	2003
$Co_{29}Fe_{71}$ [56]	23	31.4	2004
$Co_{35}Fe_{65}$ [9]	24	7	2004
$Co_{26.2}Fe_{73}Ni_{0.8}$ [57]	24	40	2006
$Co_{34}Fe_{66}$ [18]	20.4	17	2007
$Co_{40}Fe_{60}$ [7]	24.3	5.6	2008

2.3.1 Effect of Additive

Various chemicals are used to be the additives to improve both morphology and soft magnetic properties of metallic deposit. There are many cases exhibiting that CoFe film contains both high saturation magnetization and coercivity simultaneously. Therefore, electroplating with additives is essential to be applied to produce the film with lower coercivity. The presence of iron (III) in plating bath can prohibit good soft magnetic properties in alloyed film because of air oxidation. The oxide is undesirable because it lowers the cathode efficiency and causes the deposited film brittle, pitted

and especially stressed that impart significantly high coercivity [56]. However the issues are possible to be prevented by appropriate conditions in operation with some additives [17].

2.3.1.1 Sulfur Containing Additive

Sulfur inclusion about 0.9 at.% in the CoNiFe film causes a decrease of crystal grain size to be smaller. Therefore it contributes favorable soft magnetic properties [5]. The inclusion of small amount of sulfur is found to be important to produce the film with fine crystals that presents low coercivity and high saturation magnetization including variation of resistivity and magnetostriction [55]. Saccharin and thiourea are practically applied as sulfur containing agents in electrochemical bath. Effects of saccharin and thiourea concentrations on the sulfur content and the coercivity of CoNiFe alloy deposited film are shown in Fig. 2.13. The sulfur content in the films from the thiourea bath is more sensitive as its concentration in electrolyte than the sulfur content in the films from the saccharin bath.

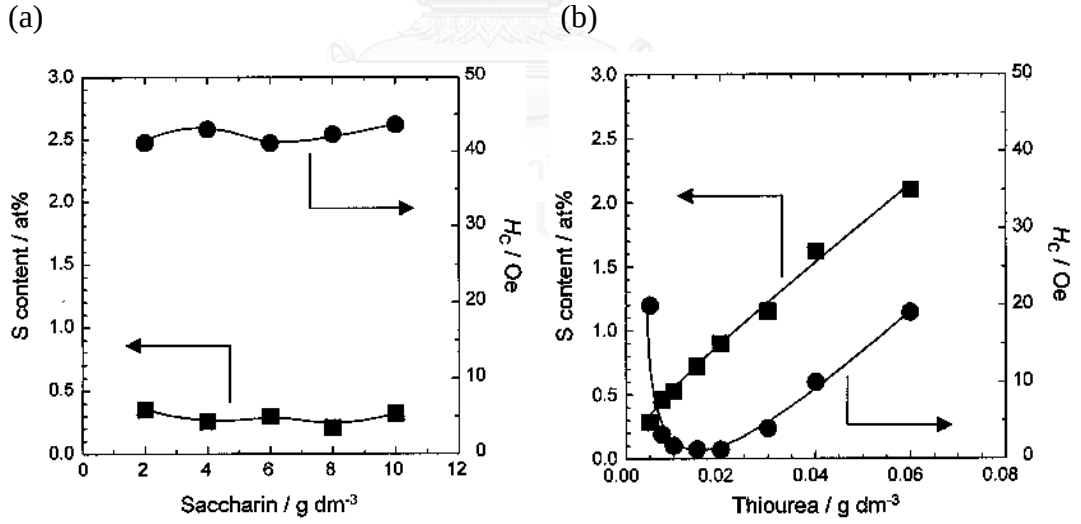

Fig. 2.13 Coercivity and sulfur inclusion of electrodeposited CoNiFe thin films deposited from the sulfur-containing additive (SCA) baths; (a) saccharin bath; (b) thiourea bath [6].

The coercivity of the films from thiourea bath reaches the lowest point at around 2 Oe at the concentration at 0.015 – 0.02 g/dm^{-3}, while the coercivity from the saccharin bath is almost constant about 40 – 45 Oe at the concentration from 2 – 10 g/dm^{-3} [3]. The CoFeNi film with the sulfur content less than 0.1 at.%, the bcc-fcc mixed phase may appear that contributes high saturation magnetization region [50]. In addition, a few research found that saccharin is able to be used as additive for $\lambda_s \sim 0$ of the CoFeNi alloy film [53]. Saccharin results in smoother, more compact and more leveled deposits as compared to phthalimide or o-toluene sulfonamide [58].

2.3.1.2 Boron Containing Additive

The B-reducer, such as dimethylamine borane [$(CH_3)_2NHBH_3$], emerging additive, can protect the CoFe film effectively from oxidization since B-reducer, acting as a reductant molecule, can reduce Fe^{3+} (produced during plating) back into Fe^{2+}:

O_2 or at anode

$$Fe^{2+} - e^- \rightarrow Fe^{3+} \text{ (by reaction)} \quad (2\text{-}10)$$

B-reducer

$$Fe^{3+} + e^- \rightarrow Fe^{2+} \quad (2\text{-}11)$$

จุฬาลงกรณ์มหาวิทยาลัย
Chulalongkorn University

A very low content of oxygen and boron present in the deposited CoFe films cannot be detected by EDX, while the boron content is less than 0.8 % after XPS analyzing. The coercivity at easy axis and coercivity at hard axis values enormously decrease while saturation magnetization increases twice in average, then film becomes very soft due to the effect of B-reducer. But too much of B-reducer leads to an unstable plating solution and a high content of boron doping (> 2 %) in the CoFe films. The films possess an amorphous texture, a decreased saturation magnetization, and poor anisotropy [7].

2.3.1.3 Wetting Agent

Although a wetting agent tends to increase deposit stress but pitting may be lowered. Many reports confirmed that sodium loauryl sulfate is proper and compatible with all types of Fe plating solution [17].

2.3.1.4 Oxidation Preventing Additive

Many agents, oxycarboxylic and dicarboxylic acid groups such as citric, malic, malonic, tartaric acid, and ascorbic acid have been used to prevent the formation of ferric hydroxide precipitation which depletes soft magnetic properties. These acids may give codeposition of an impurity element that affect the properties of an Fe-alloyed deposit. Especially for CoFe and CoFeNi based plating baths, stabilized with ammonium citrate to complicate the metal ions and prevent metal hydroxide precipitation at higher pH levels, the solutions are stable at pH values up to 5.8 and remain transparent without precipitate. Furthermore, the citrate-added baths result in a lower coercivity. Because the deposition of the metal atoms may be delayed from citrate-complexed ions that lead to more time for the atoms to fit into favored sites in the lattice. A structure with fewer defects and lower stress is able to constructed [17, 18].

จุฬาลงกรณ์มหาวิทยาลัย
Chulalongkorn University

2.3.1.5 Brightening Agent

The plate that is ‘mirror-bright’ can be deposited by adding lead salts. For examples, sodium hydrosulfite, or formaldehyde and cadmium sulfate in the cobalt ammonium sulfate bath. Sodium thiosalfate is reported as a brightening agent of Co bath. For NiCo alloy, formaldehyde, nickel formate and sodium sulfate are referred to perform as brightening agents [17].

2.3.1.6 Stress Reducing Agent

CoNi-alloyed bath for reducing stress in the deposits, for example, saccharin and sodium naphthalene trisulfonate are able to be added in plating bath. Adding saccharin can be effective to reduce the internal stress in the deposit into one-eighth for CoNi film [17, 58]. For CoFe film, stress is well control by saccharin coverage changing driving force of grain adhesion on the CoFe surface during electroplating

process. The saccharin absorption on the surface is thermodynamic attained either by control of plating potential or control of saccharin concentration in electrolyte solution. Internal stress of CoFe may be decreased into one-fourth with decreasing of coercivity into around one-third [59].

2.3.2 Current Density

In order to avoid rough and dark deposits of metal hydroxide precipitation, the low current densities should be applied for plating Co alloy in both sulfate and chloride baths [17]. For the CoFe alloyed film, the composition of Co and Fe is various with the variation of current density. The current density increment causes the Fe content in the film decreases, at the low current density; the amount of Fe content in the film is greater than the expected ratio of Co to Fe in the solution. But the Fe content approaches the ratio when higher current densities are applied. However, for the electrodeposition of CoFeNi alloy, with increasing current density, Ni content in the film increase, in contrast to Co and Fe contents which decrease [25].

The application of pulse reverse current may be used to achieving a high saturation magnetization and low coercivity as well. This result is reported that the pulse reverse current could generate the deposited film of CoFeNi alloy with the low residual stress level during the film growth in the process [53].

จุฬาลงกรณ์มหาวิทยาลัย
Chulalongkorn University

2.3.3 pH

The Fe group metals and its alloys, the electroplating reactions may take place during deposition as follows:

$$M^{n+} + ne^- \leftrightarrow M \quad (2\text{-}12)$$

$$2H^+ + 2e^- \leftrightarrow H_2 \quad (2\text{-}13)$$

$$2H_2O + 2e^- \leftrightarrow H_2 + OH^- \quad (2\text{-}14)$$

$$xM^{n+} + yH_2O \leftrightarrow M_x(OH)_y^{(xn-y)+} + yH^+ \quad (2\text{-}15)$$

$$xM_x(OH)_y^{(xn-y)+} + (xn-y)H_2O \leftrightarrow xM(OH)_n + (xn-y)H^+ \quad (2\text{-}16)$$

The reaction (2-13), the pH value near the cathode surface is become higher because hydrogen ion is performed to generate hydrogen gas. At sufficient plating potential level, water in solution is decayed as the reaction (2-14) with hydroxide iron appearing in front of electrode supporting pH increment. When the pH value is high enough, further reactions appear which produce buffering effect, hydrolysis of the metal ion as the reaction (2-15) generating hydrogen ions and reducing the pH value. But if the reaction (2-15) is not able to prevent the further increase of the pH value, precipitation of the hydroxide in the reaction (2-16) will occur then it may contaminate the deposit as inclusions [60]. For example, in sulfate bath at room temperature with pH about 3.5 results in dark-colored inclusion of iron (III) salts in deposits which reduces saturation magnetization of the deposit [5, 10]. As the justification, pH plays an important role of oxidation prevention that affects saturation magnetization value of the CoFe based magnetic thin film. However, too low pH range might results in a low cathode efficiency and increased deposit stress. On the contrary, at too high pH level, both anode and cathode efficiency are almost equal. Air oxidation of iron (II) imparts iron (III) hydroxide precipitation. Therefore, it needs to adjust pH value in electrolyte solution into proper level by adding acid, such as HCl for chloride bath, H_2SO_4 for sulfate bath or adding base such as, KOH, NaOH and NH_4OH [10]. Furthermore, the pH at the electrode surface can be reduced during plating by applied magnetic field. The magnetic flux density generated from the field induces magnetohydrodynamic phenomenon causing the Lorentz force which depletes hydrogen ion concentration at the surface, then the hydroxide formation is suppressed. This effect contributes better quality of the deposited layer [60].

Moreover, the Co and Fe proportions in the CoFe alloyed films can be modified by changing pH value of electrolyte. The content of Co significantly trends to decrease as increasing pH value, while Fe content obviously increases as shown in Fig. 2.14 [61].

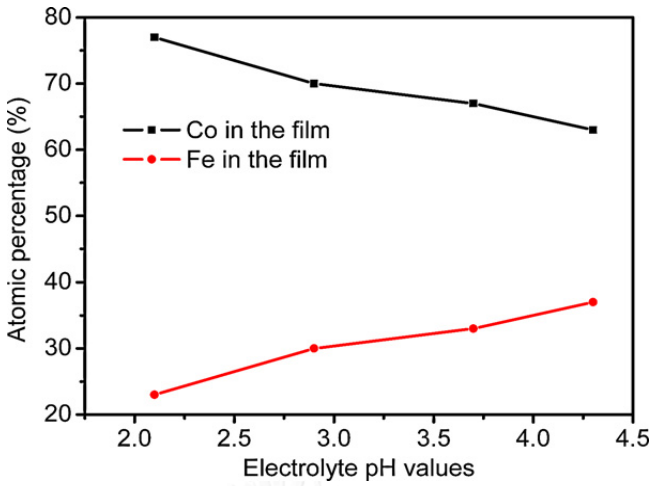

Fig. 2.14 The dependence of Co and Fe contents in the films on pH value [61].

2.3.4 Temperature

Operating at high temperature, the rapid air oxidation occurs then results in sludge during plating of Fe-rich alloys, but there is an advantage when operating at elevated temperature, the higher current density appears in plating operation. A decrease in temperature has a grain-refining effect. At the high temperature plating is able to cause somewhat rough deposited surface [17, 53].

The deposition temperature in the FeCoNi thin films, when the deposition temperature increases in plating baths, the deposited Fe proportion decreased, the deposited Co proportion increased and Ni proportion slightly increased. Current density of the deposition increases with the temperature. Furthermore, grain sizes and roughness of the film trend to enlarge with increasing temperature. In contrast to the film stress, it decreases while the temperature increases. These factors have however no significant relation to the films coercivity. The crystalline texture of the film also change by increment of plating temperature, for example, from bcc(110) to bcc(200) with slight decrement of the saturation magnetization of the deposits [57, 62]. In addition, for CoFe alloy, the composition ratio of Co to Fe and phase in films are also changed with temperature of plating. For example, Co proportion increases with plating temperature. Crystallographic structure also alters from a mixed phase of fcc and bcc with fine grain size at around room temperature to bcc α-Co_7Fe_3 around

60°C, but the largest grain size is from the plating at 40°C [63, 64]. Moreover, temperature plays an important role in magnetic anisotropy induction process, because randomizing influence is caused by high temperature during the process reducing induced anisotropy energy and magnetic properties of plated film [27].

2.3.5 Magnetic Field

In recent studies, a uniform magnetic field is performed in electrodeposition process of ferromagnetic alloyed films to modify film's structure and its magnetic properties. Lorentz force, F_L induced by magnetic field is the cross product of current density and magnetic flux density as shown in the equation 2-17:

$$\vec{F}_L = \vec{j} \times \vec{B} \tag{2-17}$$

when the force is perpendicular to current density, j and magnetic flux density or induction, B [28, 47]. The relation of theses factors' directions is exhibited in Fig. 2.15. The effect of this force in plating aqueous electrolyte called magnetohydrodynamic (MHD) effect. The effect interplays with micro-magnetic convection (MMC) in diffusion zone (δ_D) of electrolyte as shown in Fig. 2.16 leading to induced uniaxial magnetic anisotropy. Magnetic force exerts on grains in nucleation and growth processes that change deposit's structure which influence on its magnetic properties [26, 65].

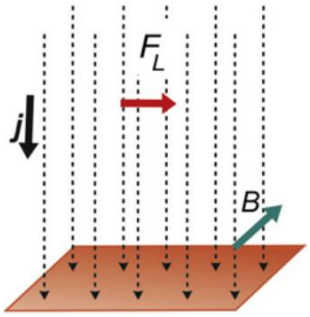

Fig. 2.15 Hydrodynamic flow system of Lorentz force as a result of current density and magnetic flux density [28].

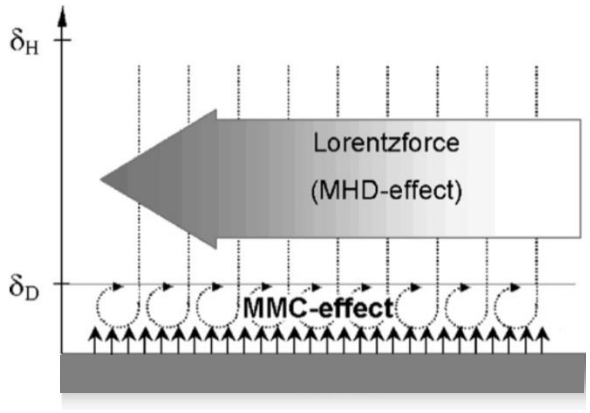

Fig. 2.16 Schematic illustration of magnetohydrodynamic (MHD) effect interplaying with micro-magnetic convection (MMC) in diffusion zone of electroplating process [65].

The field applied parallel to electrode surface during the electroplating of CoFe alloyed film in sulfate bath increases limiting current density and deposition rate. The electrode surface is also able to be smoother and more homogenous than the one obtained without the magnetic field. On the contrary, when the magnetic field applies perpendicular to the electrode surface, no any significant effects of the limiting current and deposition rate appears significantly. The morphology of the deposit is strongly affected that the roughness obviously increases with the grains grow in the shape of separated columns aligning perpendicularly to the electrode surface as shown in Fig. 2.17. However, some studies indicate that the both directions of the magnetic field not affect chemical composition and crystal structure including (110)<uvw> texture of the CoFe deposits [32, 66].

In addition, a magnetic field also affects the magnetic properties of the deposit as shown in Fig. 2.18. The coercivity of the deposits in the magnetic field applying parallel to the electrode surfaces during the electroplating is reduced, but increased in the perpendicular field because of the high stress generated under the perpendicular field. On the other hand, there is no significant influence of any magnetic field on the film's squareness [32].

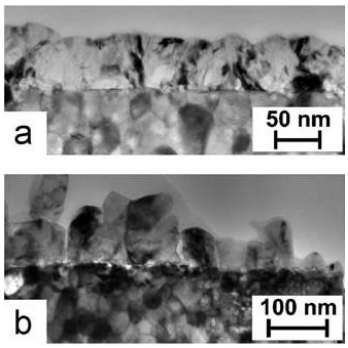

Fig. 2.17 TEM images of CoFe deposits: (a) and (b) cross sections of the deposits without and with magnetic field perpendicular to electrode surface respectively [32].

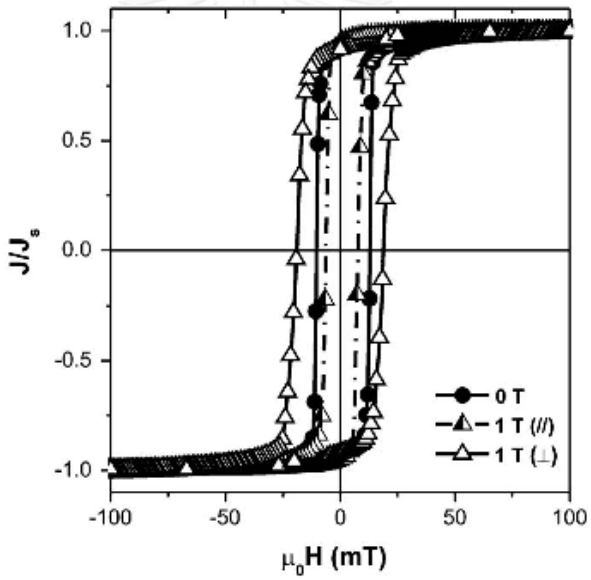

Fig. 2.18 In-plane hysteresis loops from VSM measurements of layers deposited without, with magnetic field parallel and perpendicular to electrode surface of CoFe films [32].

2.4 Thermal Annealing

The post thermal treatment applied after plating process of the soft magnetic alloyed films can also influence their structure and magnetic properties which are the function of the temperature ranges and soaking durations. The annealing by thermal heating may contribute to release internal stress, alter crystallographic orientation and

modify microstructural configurations of the films [20]. This may subsequently affect the films' magnetic responses, which are known to be dictated by interactions between magnetic domains and the films structural features. For examples, applying thermal treatment with high temperature to $Co_{50}Fe_{50}$ alloy at 700 – 850°C leads to a decrease of coercivity, despite enlargement of grain size [23]. Moreover, temperature higher than 1,000°C of annealing applied on $Co_{68}Fe_{32}$ film can releases residual stress as increasing temperature. On the other hand, low-temperature annealing can also reduce CoFe film's coercivity. For examples, annealing at 200°C can also lead to low coercivity of electroplated $Co_{40}Fe_{60}$ and $Co_{19}Fe_{52}Ni_{29}$ films as studied by Zong et al. and Liu et al. respectively [7, 25]. The low temperature annealing is a very interesting method because of it requires low energy and short duration. Therefore, low temperature annealing is expected as a potential process to improve the soft magnetic properties of CoFe films in this research.

2.5 Electroplated CoFe Based Alloy Films and Their Soft Magnetic Properties

Recently, CoFe as a material for magnetic thin film has been developed [5, 24]. It is found that proper for electronic and magnetic application, owing to its distinguished soft magnetic properties, high magnetization and low coercivity. Many researches aim to improve the magnetic behavior of the alloy which fabricated by electrodeposition, the results as shown in Table 2.1. It is generally known that coercivity is much extrinsic while saturation magnetization is so intrinsic property. Therefore, the modifications of morphology, microstructure, roughness and grain size can substantially impact on the coercivity while the chemical composition and atomic orientation of the material play an important role on the saturation magnetization. The principles are performed as key controlling approaches for the development of CoFe magnetic thin film.

Prior studies have shown that various electroplated CoFeNi based alloy films were fabricated. For examples, Liu et al. fabricated $Co_{19}Fe_{52}Ni_{29}$ (at.%) film containing bcc-fcc mixed phase with 20.4 kG saturation magnetization and 1 Oe coercivity by electroplating process with 15 mA/cm^2 current density and stress-reducing additive used [25]. Osaka et al. reported that bcc-fcc mixed phase was induced by no sulfur containing additive bath causing coercivity lower than 2 Oe and

20 – 21 kG saturation of $Co_{65}Fe_{23}Ni_{12}$ (at.%) [6, 50]. Rasmussen et al. revealed that pulse reverse electrodeposition could reduce internal stress and grain size of around 10 – 20 nm of $Co_{65.8}Fe_{21.2}Ni_{13.1}$ film caused low coercivity around 160 A/m and fairly saturation magnetization of 17 kG [53]. Nam et al. revealed that interaction between bcc and fcc phases in CoFeNi thin films contributed very fine grain size smaller than grain size of each single phase and thiourea bath supported a smaller grain size than that of saccharine bath [54]. Sulitanu et al. applied 4 mA/cm^2 current density which produced good soft magnetic $Co_{68.2}Fe_{18}Ni_{12}S_{1.5}$ film with thickness about 2.1 – 2.7 μm and grain size of 10 – 14 nm including low coercivity of 75 A/m and high saturation magnetization of 21 kG [55]. Kim et al. discovered that anion type of electrolyte obviously affected the film's coercivity because of different in crystallite plane pattern and grain size. $Co_{80}Fe_{15}Ni_5$ (wt.%) from chloride bath with 26 Oe coercivity consisted of 22 nm average grain size and hcp(100), fcc(111) and bcc(110) planes, while $Co_{76}Fe_{17}Ni_7$ (wt.%) from sulfate bath with 9 Oe coercivity consists of 42 nm average grain size with bcc(110) and bcc(200) planes [10]. Park et al. found that Ni content influenced on the saturation magnetization decrement of CoFeNi films. Increasing in plating temperature from 23 to 70°C in 0.3-pH bath resulted in grain growth from around 50 to 65 nm and internal stress reduction from 260 MPa to 28 MPa including change of texture from bcc(110) to bcc(200), while pH increment from 0.3 to 2.15 in 70°C-bath leaded to lower internal stress from about 40 MPa – 0 MPa and texture changed from bcc(200) to bcc(110) [57]. Zhang et al. presented that Fe higher than 20 at.% in CoFeNi film induced bcc-fcc mixed phase with 10 – 20 nm grain size and coercivity decreased from about 30 to 15 Oe with increment and Fe content from 17 to 35 at.%. In addition, an increase of plating temperature from 15 to 55°C gave a fall of coercivity from 23 to 16 Oe and saturation magnetization close to 20 kG [18].

Recently, many applications require high flux density of magnetic film, such as data storage device for small sizing design. CoFeNi alloyed film is limited in its saturation magnetization. CoFe alloyed film is taken into account because of its high saturation magnetization as shown in Fig. 2.11. There are some researches of CoFe magnetic alloy; however, the systematic study is still significantly limited. For examples, Liu et al. produced plated $Fe_{40}Co_{60}$ film with low coercivity of 12 Oe and

saturation magnetization of 20.4 kG including coexistence of bcc and fcc [25]. Osaka et al. revealed that separated anode and cathode cells could be applied to prevent oxidation of Fe^{2+} and fabricate $Co_{35}Fe_{65}$ film with high saturation magnetization of 24 kG and coercivity of the film was reduced from 15 Oe to 9 Oe by post annealing at 400°C [1]. Kim et al. reported that saturation magnetization of CoFe plated film increased as Fe content then reached a plateau, while coercivity of the film with Fe more than 30 wt.% from sulfate bath was lower than that from chloride bath. The saturation magnetization and coercivity of the film with 48 wt.% Co reached a limitation about 20 kG and 18 Oe respectively with bcc(110) and bcc(200) including around 40 nm average grain size [10]. Myung et al. found that plated CoFe films' soft magnetic response improved as Fe content increment. $Co_{29}Fe_{71}$ film contained good magnetic properties with 23 kG saturation magnetization and around 30 Oe coercivity. In addition, higher Fe content could cause lower internal stress which resulted in low coercivity [56]. Yokoshima et al. fabricated $Co_{35}Fe_{65}$ film plated by dual cell system that suppressed oxidization of Fe^{3+} contributed to its high saturation magnetization of about 23 kG and high coercivity around 15 Oe reduced to 7 Oe by annealing at 400 °C because magnetoelastic anisotropy played an important role on the film with 65 wt.% Fe. Whereas, there was negligible change of coercivity by the annealing in the films with Fe content higher than 65 wt.% Fe, indicating higher magnetocrystalline anisotropy which effectively influenced on its coercivity [9]. Zhang et al. proved that plating temperature influenced on grain growth leading to high coercivity of CoFe films, in contrast to current density increment which supported fine grain size promoting low coercivity. Crystallographic planes of the films were coexistence of bcc(110) and fcc(111) resulting in fine grain size about 10 – 20 nm leading to low coercivity, but fcc(111) was the texture of the film with Fe content more than 69 at.%. Good soft behavior film was $Co_{34}Fe_{66}$ with its saturation magnetization of 20.4 kG and 17 Oe coercivity [18]. Zong et al. manufactured $Co_{40}Fe_{60}$ films with amorphous texture and prevented Fe^{2+} from oxidation by boron doping and applying 280 Oe magnetic field in plating bath, resulting in high saturation magnetization of around 24.5 kG with bcc(110) texture and low coercivity of 6.5 and 2.5 reduced to 5.6 and 1.8 Oe in easy axis and hard axis by 200°C annealing [7]. Koza et al. discovered that magnetic field perpendicular to CoFe film's

surface strongly affected grain growth, rise of roughness and internal stress inducing high coercivity, while the magnetic field parallel to the electrode achieved smooth and homogeneous surface of the film because of magnetohydrodynamic effect. The preferred orientation of the films was bcc(110) at any composition. The good soft magnetic film of the report was $Co_{77}Fe_{23}$ deposit with squareness of around 0.85 and coercivity of 4.15 Oe [32]. Qiang et al. reviewed that rise of plating pH value contributed to high Fe atomic content ratio and roughness increment including grain size enlargement with (110) preferred orientation. The good magnetic properties were 2,974.03 emu/cm^3 saturation magnetization and 42.72 Oe of $Co_{70}Fe_{30}$ film [61].

As discussed above, the $Co_{40}Fe_{60}$ film with the best soft magnetic properties was fabricated by Zong et al. The sample fabrication process comprises electrodeposition with 280 Oe magnetic field followed by 200°C. However, the study did not study the effect of important processing variables, including alloy composition, annealing, and magnetic field on the developments of the CoFe films' microstructure and soft magnetic properties. In this dissertation, these points will be investigated in detail to obtain some mechanistic view of the process of soft magnetic CoFe films' fabrication.

จุฬาลงกรณ์มหาวิทยาลัย
Chulalongkorn University

CHAPTER III
EXPERIMENTAL PROCEDURE

The properties of magnetic materials are influenced from the many factors of fabrication, film structure and character as described in principles of magnetic materials including the results from the researches in chapter II. It can be presented the relation between the factors which influence on the magnetic properties of CoFe film for the experiment of the study by the diagram in Fig. 3.1

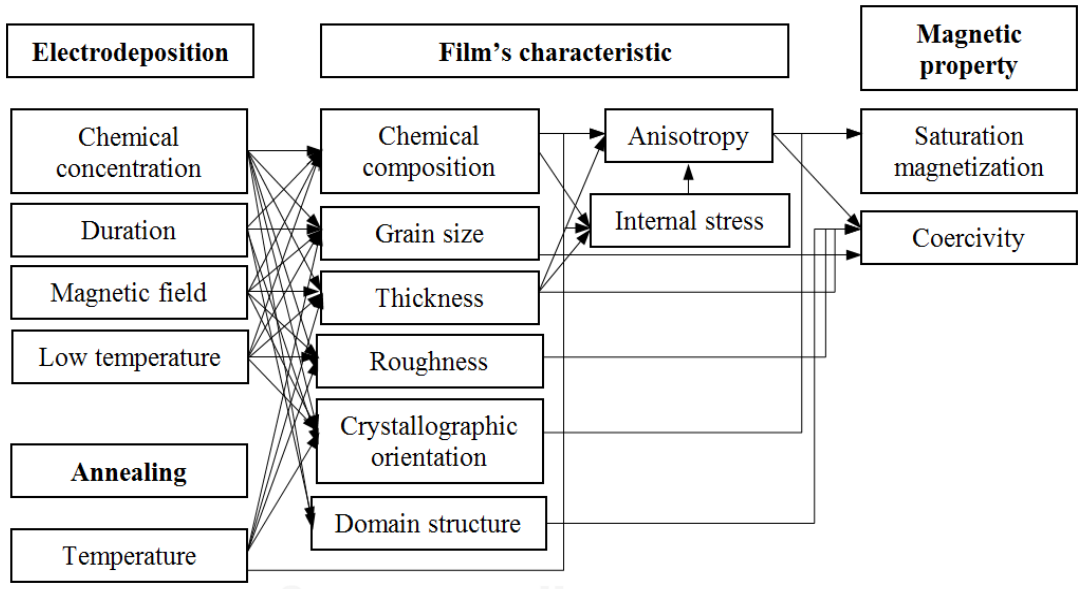

Chulalongkorn University

Fig. 3.1 The relation of plating factors, film characteristic and magnetic properties.

The several parameters affected the magnetic properties of CoFe film. However, the systematic and continuous study of the dependence is still limited. Hence, there are the separated three parts of the experiment in this research consisting of;

- Part I – Effects of composition and thickness,
- Part II – Effects of annealing,
- Part III – Effects of magnetic field and low temperature.

As the relation above, the microstructure and characteristic of the film can be manipulated by plating method that result in the film's magnetic behavior. The

plating conditions and the factors of the film are investigated. The understanding can contribute the basic knowledge of soft magnetic property and shed the light on the development of soft magnetic material.

3.1 Part I – Effects of Composition and Thickness

As described in Chapter I, magnetic properties of magnetic films are sensitive to its composition and thickness. An interesting research of the soft magnetic properties of CoFe film was performed by Zong et al. [7]. The electroplated CoFe film with high magnetic moment of 24.5 kG and low coercivity of 6.5 and 2.5 Oe in easy and hard axes, respectively, were developed. However, the effects of the composition and thickness have yet to studied in detail. Hence, in this chapter, a wide range of composition, particularly above 55 wt.% Fe, and different thicknesses of CoFe films will be taken into account to understand the relation between these factors and the films' properties. The results from this experiment should disclose some mechanistic view of how composition and thickness influence the soft magnetic properties of the alloys.

In this part, the effects of composition and thickness of electroplated CoFe films were systematically investigated on their structures' changes simultaneously with the differences of their magnetic properties, saturation magnetization and coercivity in the in-plane direction of the films which is relevant to general electromagnetic applications.

3.1.1 Electrodeposition

The CoFe specimens were provided on resin mounted copper plates (32 × 10 mm^2) as anodes which were mechanically polished to mirror-like finishing, while platinum rod was used as a cathode. The electrodeposition was employed in 300 mL acidic sulfate baths at room temperature (25°C) with natural pH of the plating solution. The plating durations were performed of 0.5 hour and 4 hours which provide thin and thick films respectively. Oxidation of Fe^{2+} easily occurs during a plating process, especially when a relative content of Fe^{2+} in the electrolyte is high. This could be prevented by nitrogen gas blasting to decrease oxygen in the electrolyte with agitation by rotation of a magnetic stirrer at around 400 rpm to maintain the

electrolyte's homogeneity and push bubbles away from a surface of the substrate. From a preliminary experiment, this technique was found to help assisting the stability of the plating process, and yielded the Fe content in CoFe film as high as 80 %wt. Fe. To achieve various films' composition for investigation in this study, a proportion of Co and Fe salts' concentration were systematically varied, as showin in Table 3.1.

Table 3.1 Composition of the plating bath for Co-Fe electrodeposition

Chemicals	**Concentration (mol/L)**				
$CoSO_4 \cdot 7H_2O$	0.05	0.09	0.12	0.15	0.18
$FeSO_4 \cdot 7H_2O$	0.31	0.28	0.24	0.21	0.18
NH_4Cl	0.50				
H_3BO_3	0.50				
saccharin	0.006				

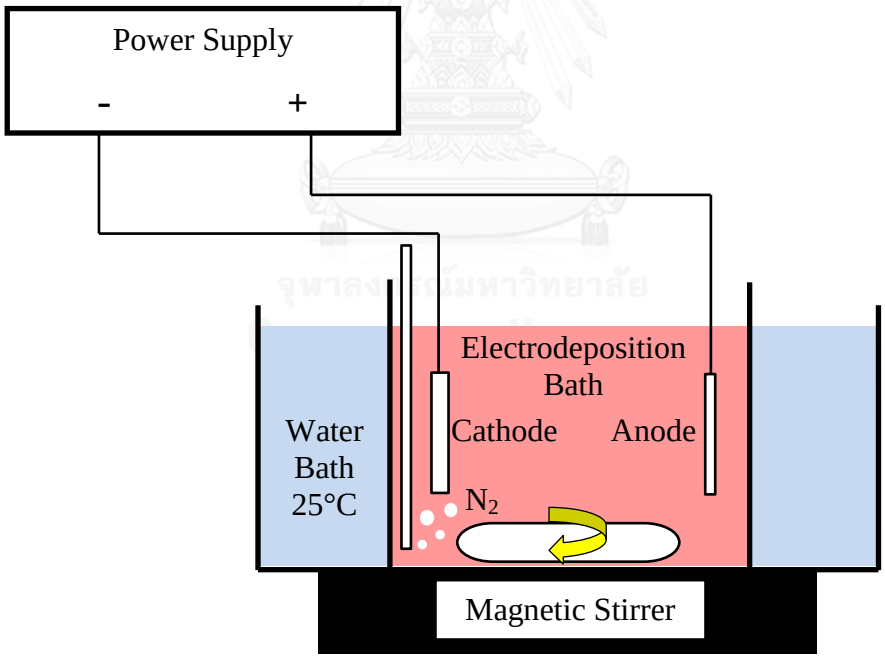

Fig. 3.2 Schematic illustration of the set-up of electrodeposition for CoFe deposits production.

Plating complexity of Co and Fe ions in electrolyte was produced during the process by boric acid [67]. Stress and grain size of the films were reduced by saccharin added in the solution [5]. The electrodeposition was carried out by a rectifier (Dynatronix DuPR10-3-6, United States) for 0.5 hour and 4 hours using a platinum electrode as the anode of the system. DC current density was charged of 0.03 A/cm^2. The system is illustrated as shown in Fig. 3.2.

3.1.2 Characterization

In this part, the objective is to observe the influences of chemical composition, grain size, crystallographic planes and surface morphology on the magnetic properties of as-deposited CoFe films. Optical microscope was used for investigation of surface configuration. XRD profiles were used for phase and crystallographic plane determination. Chemical composition analysis and film thickness measurement were performed with X-ray fluorescent spectroscopy (XPS). Vibrating sample magnetometer (VSM) was employed to determine magnetization properties, saturation magnetization and coercivity, of the samples as a function of magnetic field. Nodule size and roughness of the films were measured by atomic force microscopy (AFM), and magnetic domains were observed by means of magnetic force microscopy (MFM). The specimens were taken into account of these characterization methods.

จุฬาลงกรณ์มหาวิทยาลัย
Chulalongkorn University

3.1.2.1 Surface Configuration

Optical microscope (Carl Zeiss, Germany) was employed for configuration of CoFe specimens' surface.

3.1.2.2 Film Composition and Thickness

Co and Fe contents of specimens were measured by X-ray fluorescence spectroscopy (XRF, Fischerscope XRAY XUV-773, Germany). Furthermore, the method also was performed to measure films' thickness for computation of films weight. The XRF measurement was employed hundred times on hundred points of each film as shown in Fig. 3.3. The each point was spent 5 second a time of the measurement.

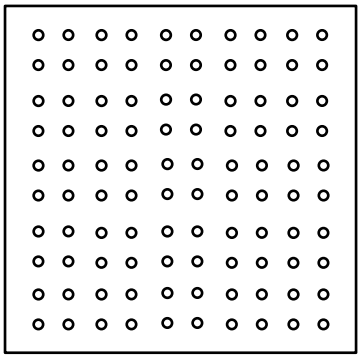

Fig. 3.3 XPF measurement points on each CoFe sample.

3.1.2.3 Structural Analysis

3.1.2.3.1 Grain Size

Grain size was estimated from the average of crystallite sizes of all crystallographic planes of each CoFe film. X-ray diffraction (XRD) was operated for nanometer scale of grain size measurement from XRD peak broadening by the basis of Scherrer equation that was performed by JADE version 6.5 software of XRD apparatus (Rigaku x-ray diffractometer model TTRAX-III, Japan). XRD scan on CoFe specimen that started from 30° to 100° in the 2θ range with sampling 0.02° and scan speed of 5° per minute at power of 50 kV and 300 mA.

3.1.2.3.2 Roughness and Cluster Size

Atomic force microscopy (AFM, Asylum Research MFP-3D, United States) was applied to measured roughness profile and nodule size. Magnetic force microscopy (MFM), as an option of AFM, was employed to investigate magnetic domain structure of the samples.

3.1.2.3.3 Crystallographic Plane

CoFe specimens' crystallographic planes were identified by XRD technique (Rigaku x-ray diffractometer TTRAX-III, Japan) with angle range from 35° to 100° in

the 2θ range with sampling 0.02° and scan speed of 5° per minute at power of 50 kV and 300 mA.

3.1.2.4 Magnetic Properties

Saturation magnetization and coercivity, of in-plane direction of the specimens as a function of magnetic field were performed by a vibrating sample magnetometer (VSM). Magnetic field was generated to magnetize parallel to surface of CoFe specimen inducing its intensity of magnetization then hysteresis loop happened. The magnetic field was applied until the magnetization reached maximum level which is saturation magnetization and the field achieved zero intensity of magnetization called coercivity.

3.2 Part II – Effects of Annealing

As mentioned in Chapter I, annealing is a post heat treatment method that can release the internal stress in a magnetic film and thus help improve its soft magnetic properties. Low temperature annealing around 200 – 300°C is an attractive technique to enhance the soft magnetic properties of CoFe film. An outstanding study done by Zong et al. shows that annealing at 200°C for 4 hours results in a reduction of electroplated CoFe film's coercivity from 6.5 to 5.6 and 2.5 to 1.8 Oe in easy and hard axes respectively, while the process slightly affects a change of magnetic moment from 24.5 to 24.3 kG [7]. However, the study of low temperature annealing for electroplated CoFe film is still limited.

In this part, the annealing effects of electroplated CoFe films were investigated on their structures' changes simultaneously with the alterations of their magnetic properties. Furthermore, it is well known that internal stress of plating film will be changed due to annealing process. Hence, the change of the films' internal stress was investigated with the modification of magnetic response of the films. The results from this experiment should disclose the mechanistic view of how low temperature annealing alters soft magnetic properties of electroplated CoFe film.

3.2.1 Thermal Annealing

The modification of the CoFe films providing by thermal annealing were investigated. The samples of 4-hour plating from Part I were selected to be annealed for 1 hour either at 200°C and 300°C in a tube furnace with a controlled atmosphere by 99.999% pure nitrogen gas with flow rate of 2,000 cm^3/min to prevent oxidation on the surface of specimens.

3.2.2 Characterization

In Part II, the objective is not only to observe the changes of the films' structure and their magnetic response due to annealing process, but also the alterations of internal stress of the deposits. Therefore, internal stress measurement was required for the investigation.

3.2.2.1 Young's Modulus

To determine the films' internal stress, Young's modulus of specimen has to be measured. Nanoindenter (CSM TTX-NHT, Switzerland) with a diamond indenter using maximum load of 10 mN, loading rate of 20 mN/min, unloading rate of 20 mN/min, pause of 5 second, approach speed of 2,000 nm/min, was applied for the Young's modulus. The measurement was randomly performed on five points for each specimen. The Young's modulus value was computed from the average of the five-point measurements.

จุฬาลงกรณ์มหาวิทยาลัย
Chulalongkorn University

3.2.2.2 Internal Stress

The residual stress measurement was obtained by XRD analysis operated in the conditions of 300 mA and 50 kV (15 kW), a rotating Cu K_α anode applied with a Ni filter by the parallel beam in the inclined measurement method. The samples could be tilted to set ψ angles: -50°, -40°, -30°, -20°, -15°, -10° and 0°. Scan speed of 1° per minute and start-stop angles of 116° to 118° continuously. The residual stress of the films can be calculated from the equation [68]

$$\sigma = \left(\frac{m}{d_0}\right)\left(\frac{E}{1+\nu}\right) \tag{3-1}$$

where σ is the residual stress, m is the slope of linear plot of lattice spacing (d) of the (310) plane versus $\sin^2\psi$, ψ is the XRD tilted angle, d_0 is the lattice spacing of the (310) plane of a stress-free CoFe film (d_0 = 0.9035 Angstrom), E is Young's modulus of the CoFe films as measured by nanoindentation and ν is Poisson's ratio of the CoFe alloyed film (ν = 0.208) [59].

3.2.2.3 Film Composition and Thickness

The analysis of composition and thickness follows the procedure and parameters as explained in Part I.

3.2.2.4 Structural Analysis

All measurements of grain size, roughness and crystallographic plane follow the same instruction and variables as described in Part I.

3.2.2.5 Magnetic Properties

Both of saturation magnetization and coercivity observation of the films are implemented as clarified in Part I.

3.3 Part III – Effects of Magnetic Field and Low Temperature

As discussed in Chapter I, magnetic field running parallel to an electrode surface contributes to good soft magnetic properties because of the magnetohydrodynamic effect, as confirmed by a number of researches. The outstanding work done by Zong et al. exhibits that an electroplated CoFe film with high saturation magnetization of 24.5 kG and low coercivity of 6.5 and 2.5 Oe in easy and hard axes can be developed by applying 280 Oe magnetic field in a plating bath during electroplating [7]. However, the study of magnetic field effect with a wide range of composition is still limited. Moreover, there is no study of low temperature plating with magnetic field for electroplating of CoFe films, especially below 0°C, as it is challenging to consistently control the temperature level and homogeneity of the electrolyte.

In this part, it is well known that magnetic field induces anisotropy energy which attributes magnetic domain and grain orientation resulting in modification of soft magnetic properties. In addition, the anisotropy energy stimulated in magnetic film has to be larger than the thermal energy which is a function of the temperature of film preparation process. Due to vibration created from the thermal energy can interrupt the orientation [26, 27]. Therefore, low temperature of plating bath is able to contribute the easy alignment of induced orientation along applied magnetic field. The plating phenomena by magnetic field and low temperature influences on the electrodeposition to modify the CoFe films' structure and magnetic properties which would be elucidated.

3.3.1 Electrodeposition with Magnetic Field and Low Temperature

The couple of magnets would be put in electrolyte to generate a magnetic field of 6 kG parallel to the electrode's surface during the plating process as the set-up in Part I at room temperature of 25°C with the plating duration of 4 hours. The specimens from this step would be taken to characterization for their structure and properties modification. After that, plating would be operated at the temperature as low as possible with the same magnetic field.

From a preliminary experiment, the test exhibited that the plating could be carried out with a good control for a temperature as low as -2°C. Below this temperature, precipitation and segregation took place, even when a stirrer ran with a high speed.

Therefore, for the next step, the electrolyte would be cooled to reach -2°C by a refrigerator of cooling system while the magnetic field still existed in the plating for 4 hours. The concentration of electrolyte in plating bath followed as Table 3.1, current density and stirring rate followed as Part I. However, magnetic stirrer could not work in this part because of the attraction force from the couple of magnets in the plating bath, so a mechanical stirrer would be applied instead. The systematic set-up of experimental apparatus is shown in Fig. 3.4. The results of this part would be compared to the films from 4 hour-plating in Part I.

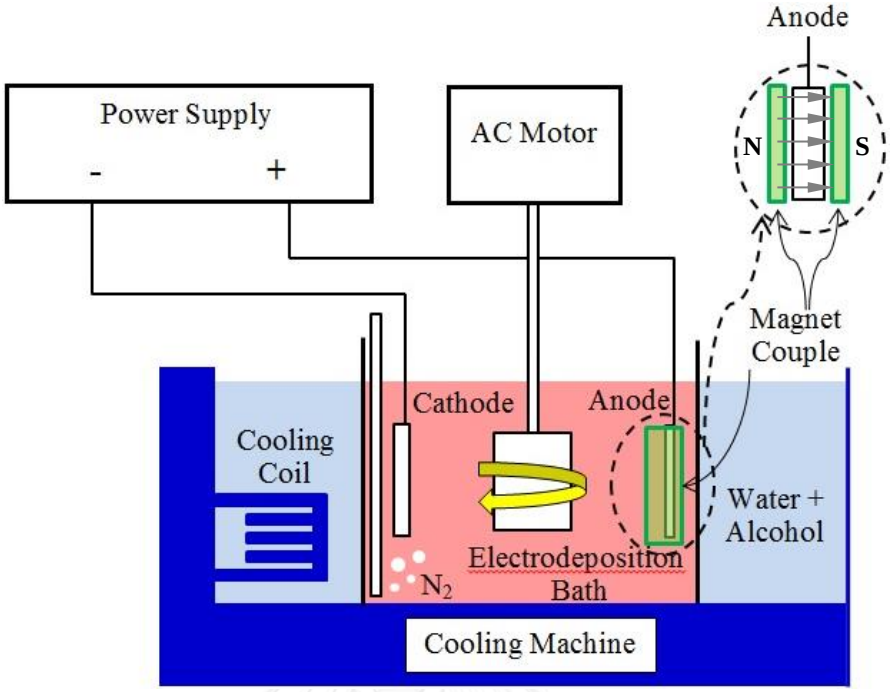

Fig. 3.4 Schematic illustration of the set-up of magnetic-field electrodeposition for CoFe deposits production.

3.3.2 Characterization

All characterization procedures followed as that of Part II.

จุฬาลงกรณ์มหาวิทยาลัย
Chulalongkorn University

CHAPTER IV
EXPERIMENTAL RESULTS

This chapter is divided into three parts of experimental results in the chapter;

- Part I – Effects of composition and thickness,
- Part II – Effects of annealing,
- Part III – Effects of magnetic field and low temperature.

4.1 Part I – Effects of Composition and Thickness

4.1.1 Plating Films and Compositions

The CoFe deposits, with the relative Fe contents ranging around 55 – 81 wt.%, were successfully fabricated with uniform surface morphology. By increasing the ratio of Fe^{2+} in the bath, the Fe contents in the deposits are enhanced as shown in Fig. 4.1. The Fe content in the relatively thin and thick CoFe films fabricated with 0.5 hr and 4 hr plating durations show similar dependency on bath composition. However, as presented in Fig. 4.2, the thick film from 4 hr plating exhibits more homogeneous than the thin film from 0.5 hr plating. In addition, the thin film contains many defects on its surface. It indicates that the long duration plating, the more completed and homogeneous in plating film surface. The increment of thickness of the film can suppress the surface incompleteness that is 'leveling' phenomenon in electrodeposition [52]. The 0.5-hour plating produces the thin films with thickness in the range of 0.5 – 1 μm, while the thickness of 4-hour plating films is around 1 – 2.5 μm. Noticeably, the thickness of the 4-hour plating films with low and high Fe content are relatively higher than that of the films with moderate Fe content, as shown in Fig. 4.3.

จุฬาลงกรณ์มหาวิทยาลัย
CHULALONGKORN UNIVERSITY

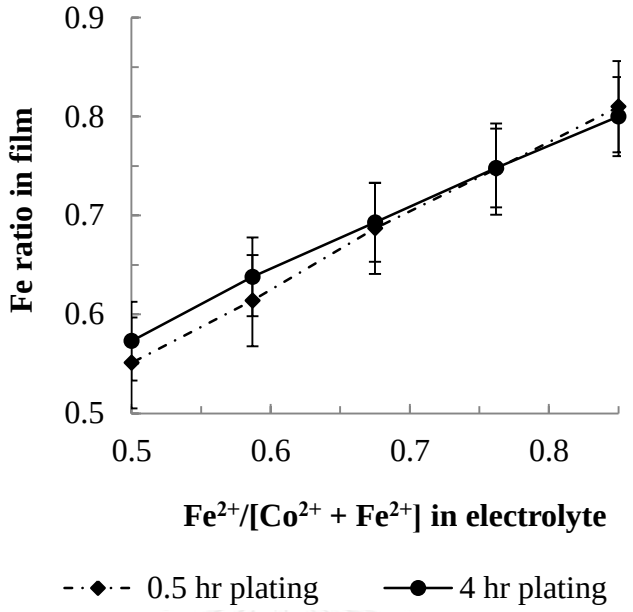

Fig. 4.1 The Fe content in the deposits as a function of Fe^{2+} /(Co^{2+} + Fe^{2+}) ratio in the plating baths with 0.5-hour and 4-hour plating durations.

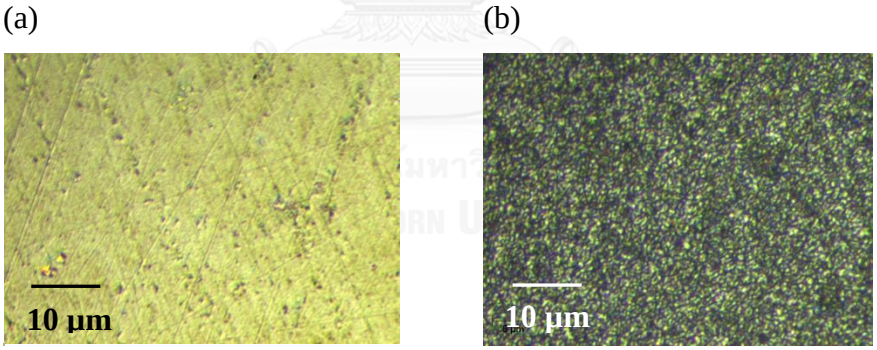

Fig. 4.2 The optical micrographs of surface morphology of (a) 0.5-hour plating and (b) 4-hour plating films from the bath of electrolyte with 85 % Fe^{2+}.

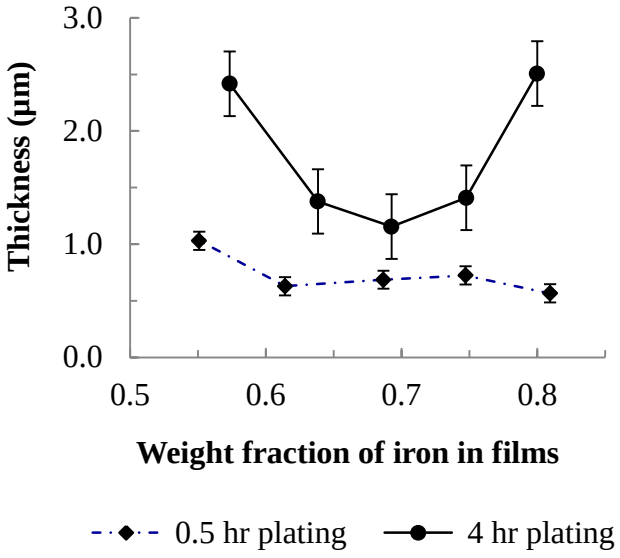

Fig. 4.3 XRF results of the films' thickness.

4.1.2 Magnetic Properties

The in plane hysteresis loops of selected CoFe films measured from VSM are shown in Fig. 4.4. The coercivity of the CoFe specimens were determined from the hysteresis loops and the saturation magnetization is calculated from the equations (2-1) and (2-2) [27].

Fig. 4.5(a) and (b) show the saturation magnetization and coercivity of the CoFe deposits as a function of Fe content respectively. It is observed that the two properties of the relatively thick films (4-hour plating) are well-influenced by the Fe content. With an increase in the Fe content, the saturation magnetization and the coercivity are generally reduced. The highest saturation magnetization of 27.5 kG and the lowest coercivity of 18 Oe are found in the deposits that comprise 57.3 wt.% and 80 wt.% Fe, respectively. On the other hand, the relatively thin films (0.5-hour plating) exhibit poorer soft magnetic responses, with relatively low saturation magnetization and high coercivity that does not clearly depend on the Fe content in the deposits.

(a)

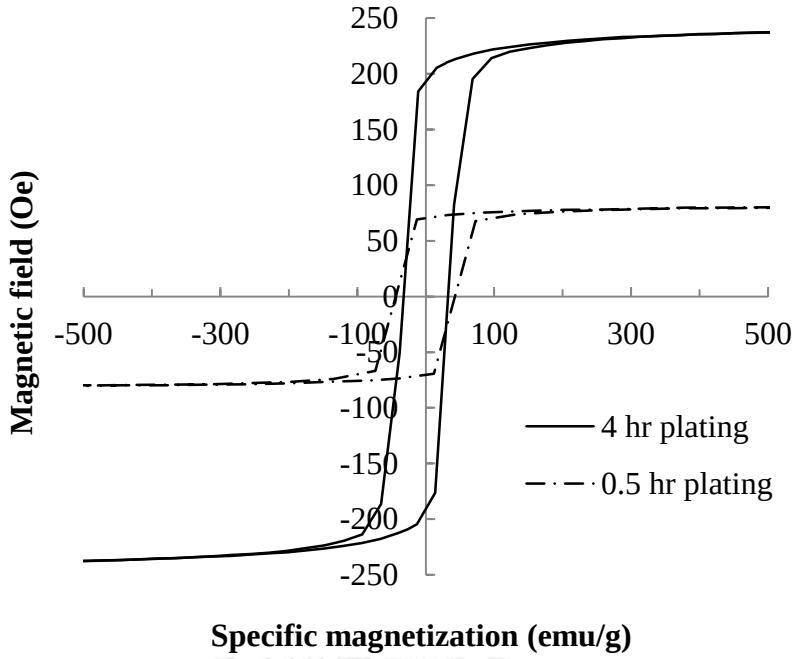

(b)

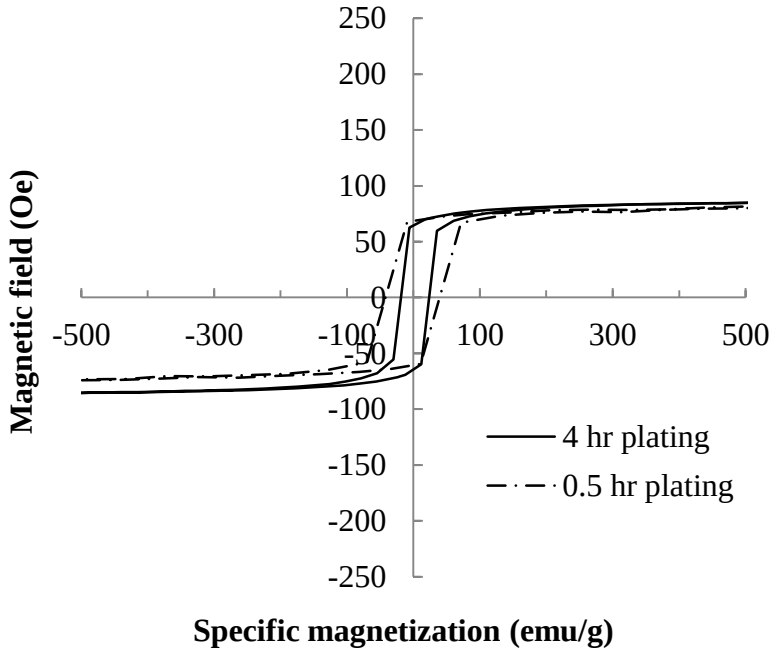

Fig. 4.4 The VSM measurement of in-plane magnetic hysteresis loop of the as-deposited CoFe films with (a) low Fe content; 55.1 and 57.3 wt.% Fe from 0.5-hour and 4-hour plating, and (b) high Fe content; 80.9 and 80.0 wt.% Fe, from 0.5-hour and 4-hour plating, respectively.

(a)

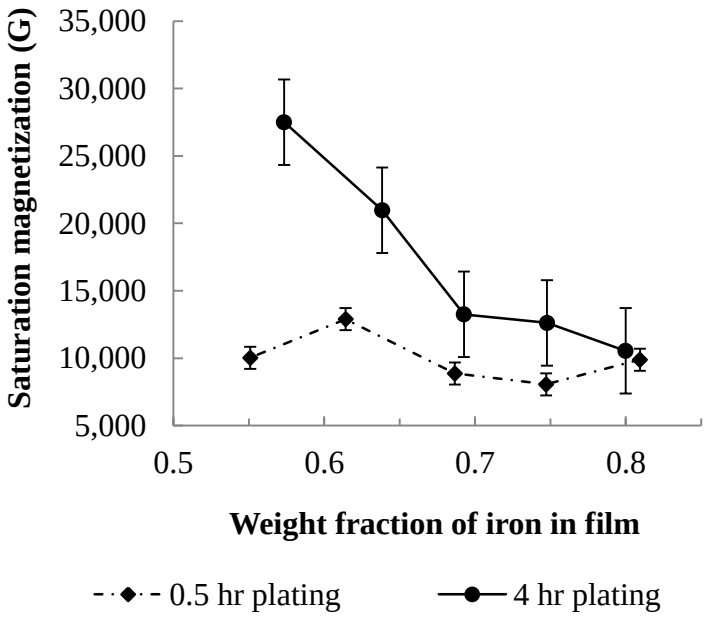

(b)

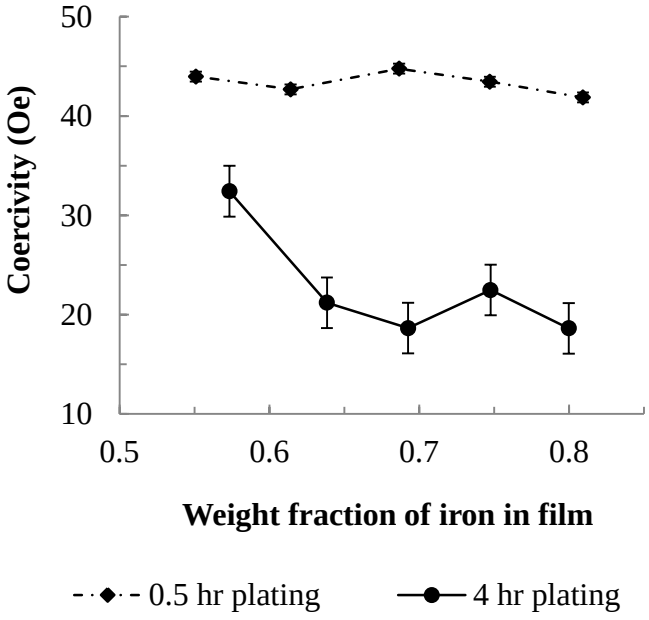

Fig. 4.5 The in-plane magnetic properties of the 0.5-hour and 4-hour plated CoFe films as measured by VSM: (a) saturation magnetization, and (b) coercivity.

4.1.3 Films' Characteristics

The 0.5-hour films exhibit preferred orientation in the direction of (110) planes, as shown in Fig. 4.6. On the other hand, the 4-hour films are marked by the additions of (200) and (211) peaks in the XRD profiles. In general, an increase of Fe content leads to a preferential orientation of (200) planes. The results from XRD profiles are used to calculate the texture coefficient of electroplated CoFe films are able to be calculated from the equation (4-1) [69]

$$T_{hkl} = \frac{\left(\frac{I_m(hkl)}{I_0(hkl)}\right)}{\frac{1}{n}\sum\left(\frac{I_m(hkl)}{I_0(hkl)}\right)} \qquad (4\text{-}1)$$

Where $I_m(hkl)$ is the measured relative intensity of (hkl) plane, $I_0(hkl)$ is that of the standard reference of (hkl), n is the number peaks reflected from the measured film. The texture coefficient values of the specimens are shown in Fig. 4.7.

จุฬาลงกรณ์มหาวิทยาลัย
Chulalongkorn University

(a)

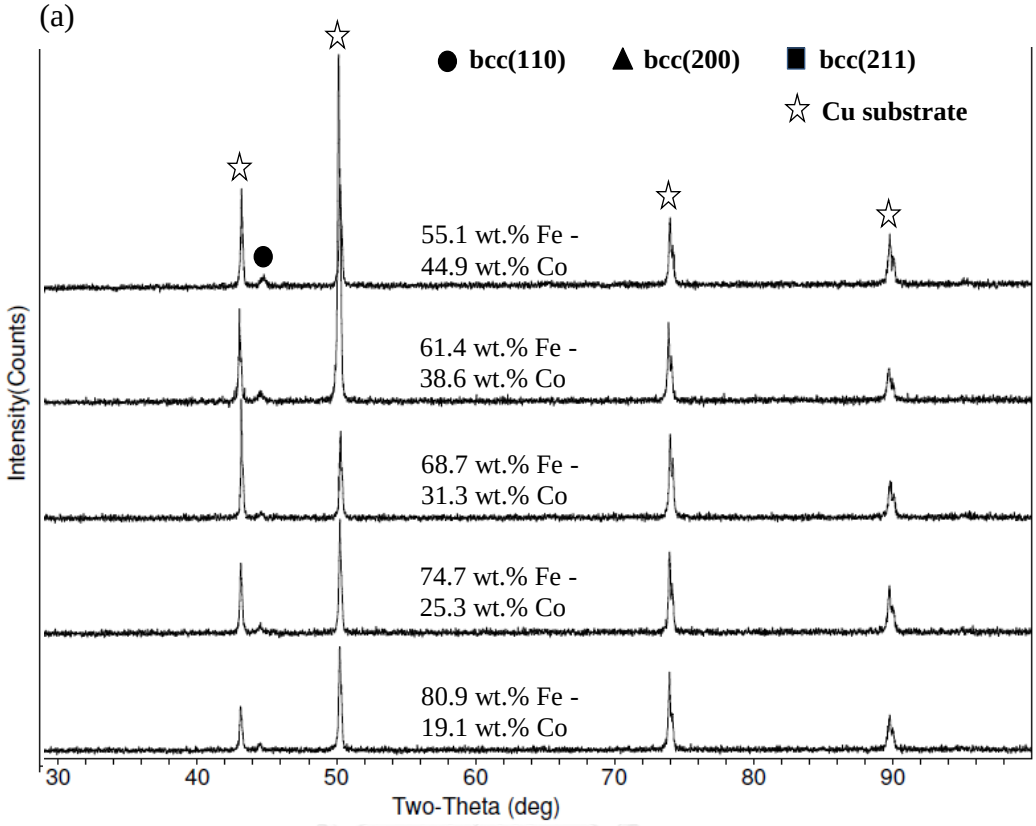

จุฬาลงกรณ์มหาวิทยาลัย
Chulalongkorn University

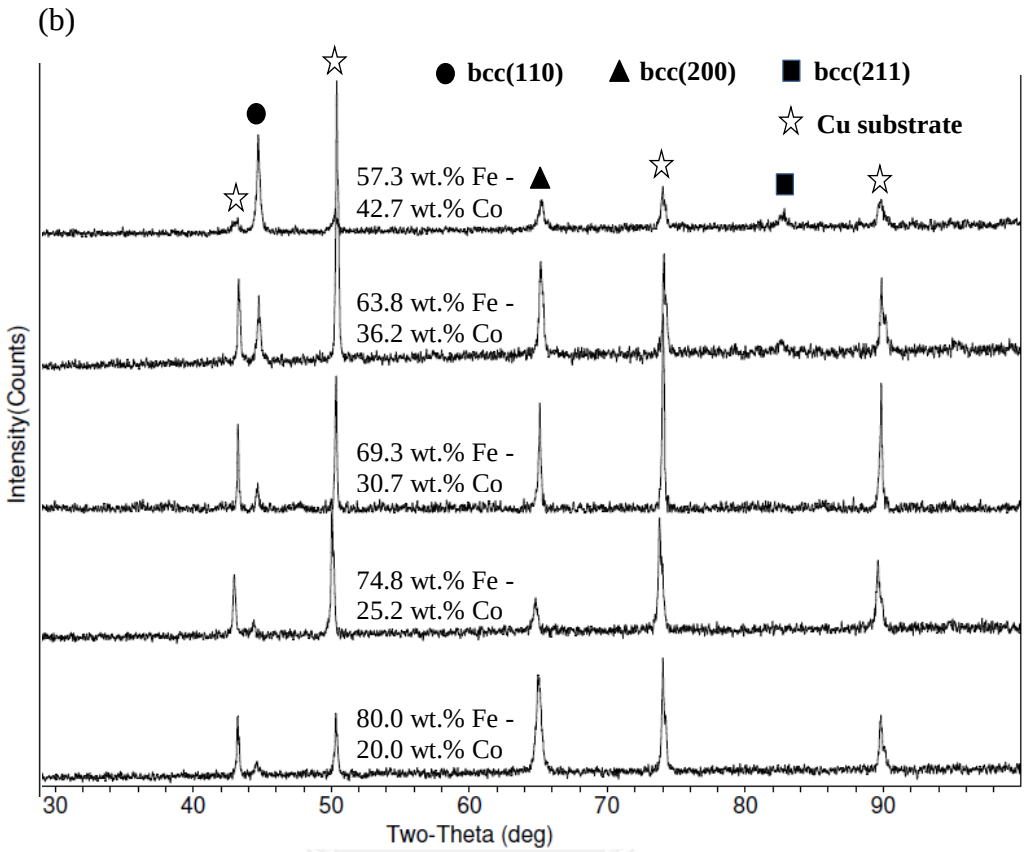

Fig. 4.6 The XRD profiles of the CoFe deposits electroplated for (a) 0.5 hour and (b) 4 hours.

จุฬาลงกรณ์มหาวิทยาลัย
Chulalongkorn University

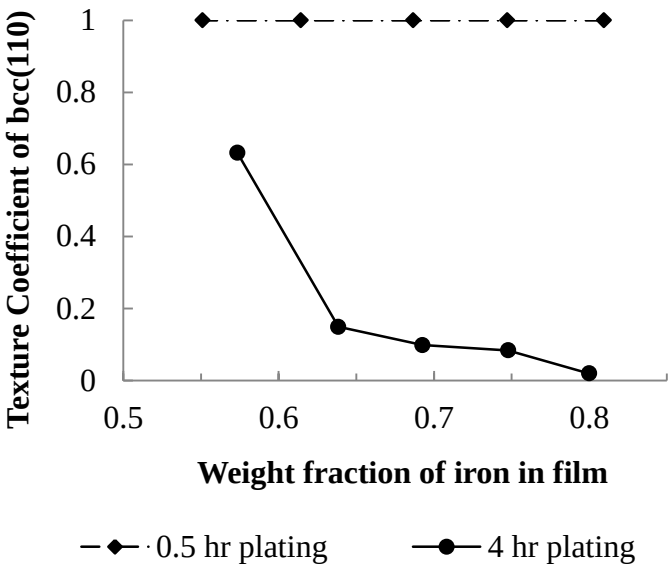

Fig. 4.7 Texture coefficient of bcc (110) plane of the CoFe deposits as determined from XRD analysis.

A cluster is defined as a distinct group of grains. A contour of a collection of clusters establishes surface roughness of the deposits. Both the size of the clusters and surface roughness can be determined by AFM. Fig. 4.8 shows AFM images of the deposits with minimum and maximum Fe contents. It is observed that the 0.5-hour plating films generally exhibit relatively large cluster size, and relatively low surface roughness, as compared to the 4-hour plating films. Fig. 4.9(a), which summarizes the cluster size and roughness of the deposits, shows the minimal effect of the Fe content on these parameters. Fig. 4.9(b) shows the estimated grain sizes calculated from the XRD profiles. From the observations, it can be elucidated that the films grow in the form of columnar shape perpendicular to the substrate surfaces. Over time, the mesoscaled columns grow and entangle one another and correspondingly induce the formations of clusters with smaller size and increased surface roughness.

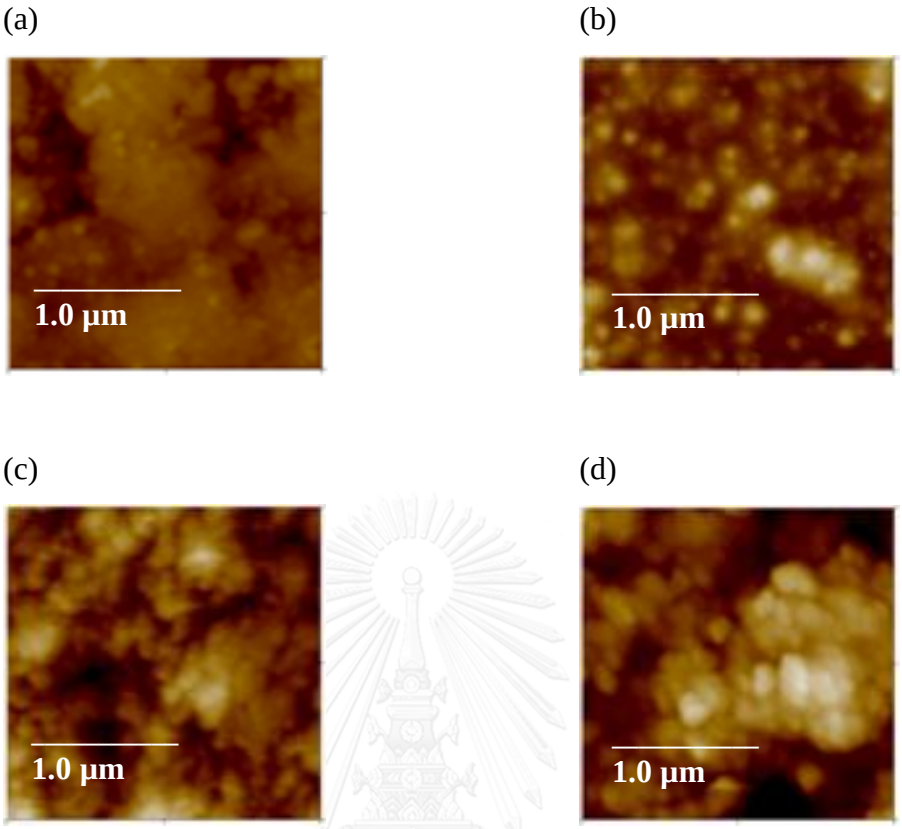

Fig. 4.8 AFM images of the surface of the deposits with (a) 55.1 wt.% Fe and (b) 80.9 wt.% Fe of the 0.5-hour plated CoFe films, and the deposits with (c) 57.3 wt.% Fe and (d) 80.0 wt.% Fe of the 4-hour plated CoFe films.

Chulalongkorn University

(a)

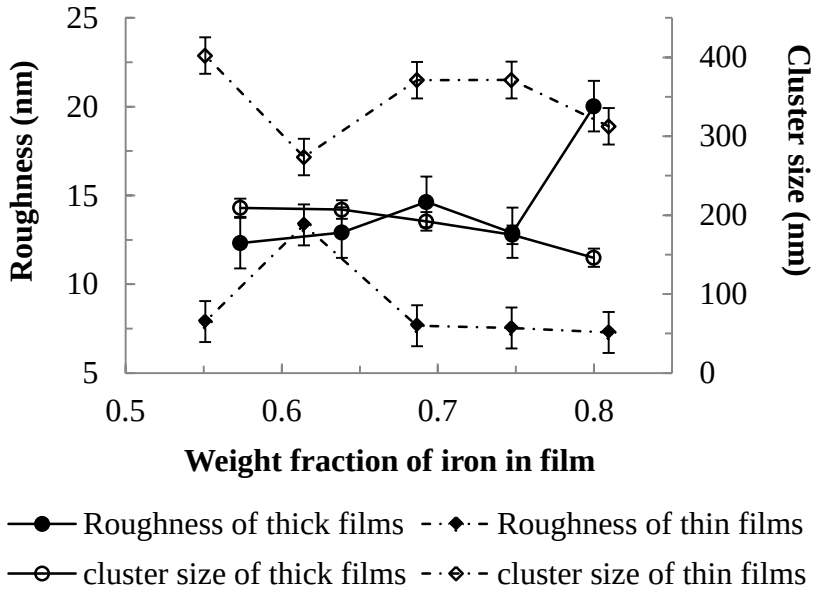

(b)

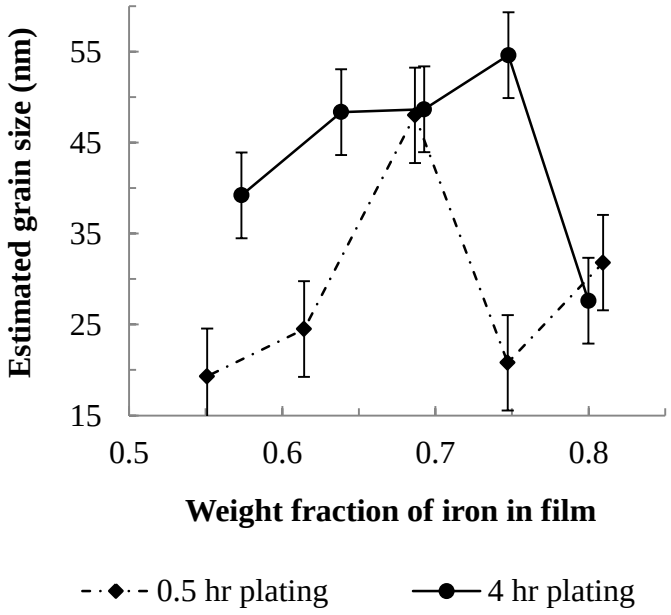

Fig. 4.9 (a) Roughness and cluster size, and (b) XRD grain size of the CoFe films electroplated for 0.5 hour and 4 hours.

4.1.4 Magnetic Domain Structure

The domain structures of the CoFe deposits with the highest and lowest Fe contents from the two groups are illustrated in Fig. 4.10. It is observed that the magnetic domain pattern of the 0.5-hour deposits is "stripe-liked", whereas that of the 4-hour plated films is "bubble-liked". The relatively thick films have relatively large domain size, which appears to grow with the Fe content. An influence of Fe content on domain size is minimal in the case of the relatively thin films.

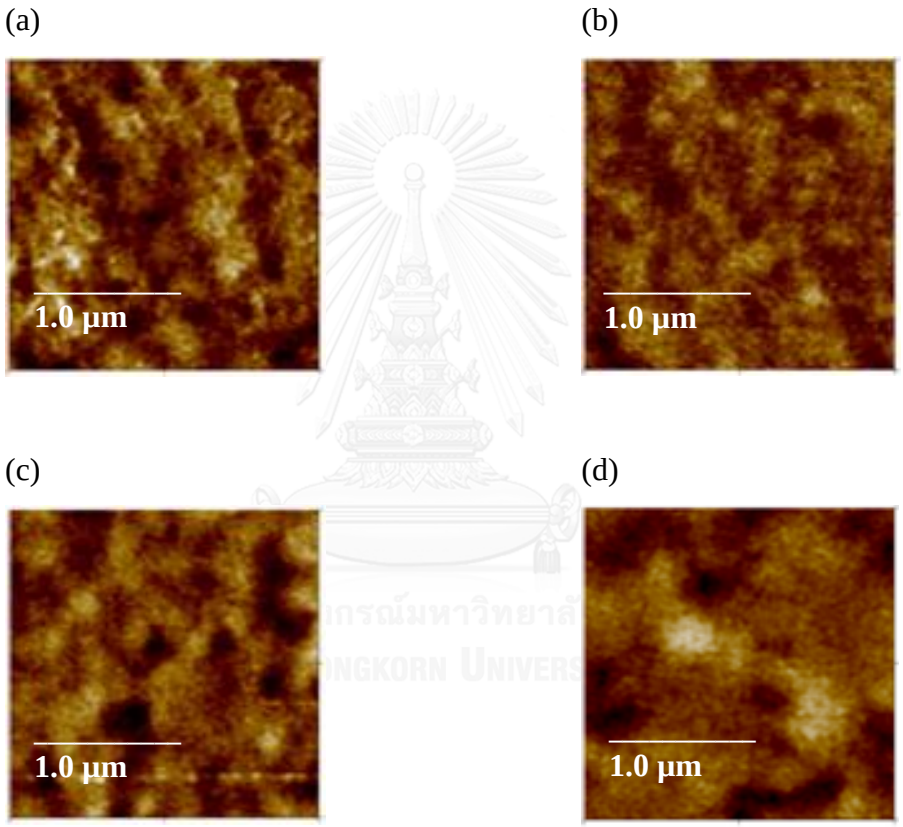

Fig. 4.10 MFM images of the magnetic domain structure: (a) 55.1, (b) 80.9 wt.% Fe of 0.5-hour plated CoFe films and (c) 57.3, (d) 80.0 wt.% Fe of 4-hour plated CoFe films.

4.2 Part II – Effects of Annealing

The data of 4-hour plating films in Part I are taken into account for comparison in this part, the results would be re-called ‘as-deposited’ films’ data. The sample of 4-hour plating in Part I would be annealed at 200 and 300°C under nitrogen atmosphere. The effect of annealing on the films’ structure and soft magnetic properties were investigated.

4.2.1 Magnetic Properties

The hysteresis loops of the CoFe films with minimum Fe content (57.3 wt.% Fe) and maximum Fe content (80.0 wt.% Fe) obtained from the study are exemplified in Fig. 4.11(a) and (b), respectively. The coercivity of the CoFe specimens were determined from the hysteresis loops and the saturation magnetization is calculated from the equations (2-1) and (2-2) [27].

The saturation magnetization and coercivity of the CoFe deposits are shown in Fig. 4.12(a) and (b) respectively. In general, the saturation magnetizations of the specimens follow the same trend, having monotonic decrement with the increase of Fe content in the films. These values of the as-deposited and the 300°C annealed specimens are comparable, whereas the 200°C annealed specimens exhibit slightly higher saturation magnetizations when the Fe content is above 65 wt.%. On the other hand, the results show that the coercivity of the specimens is affected significantly by annealing temperature. As for the as-deposited specimens, their coercivity ranges from about 20 Oe – 30 Oe when the Fe content is reduced from 80 to 57 wt.%. Reductions of the coercivity to below 20 Oe are observed when the films were annealed at 200°C. Interestingly, an increase of the annealing temperature to 300°C results in the increase of coercivity to about 40 Oe for all chemical compositions examined.

(a)

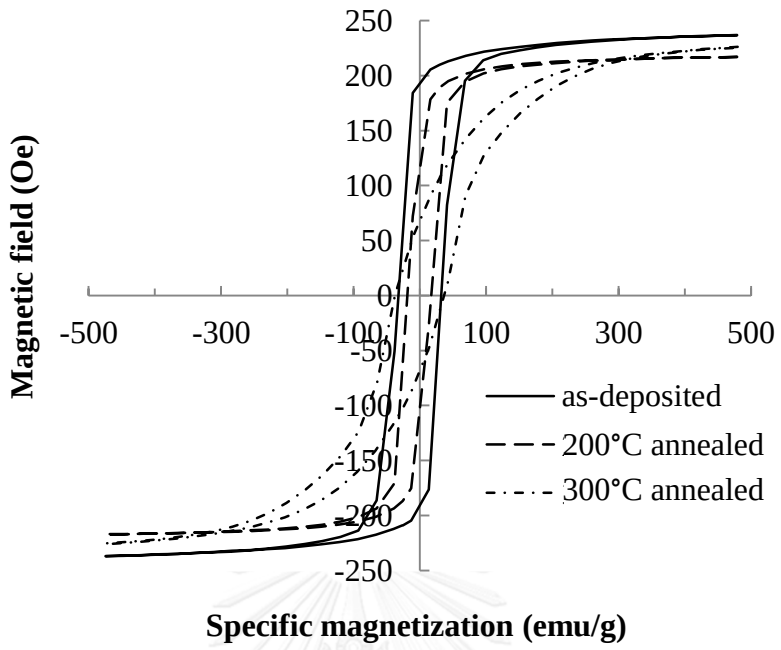

(b)

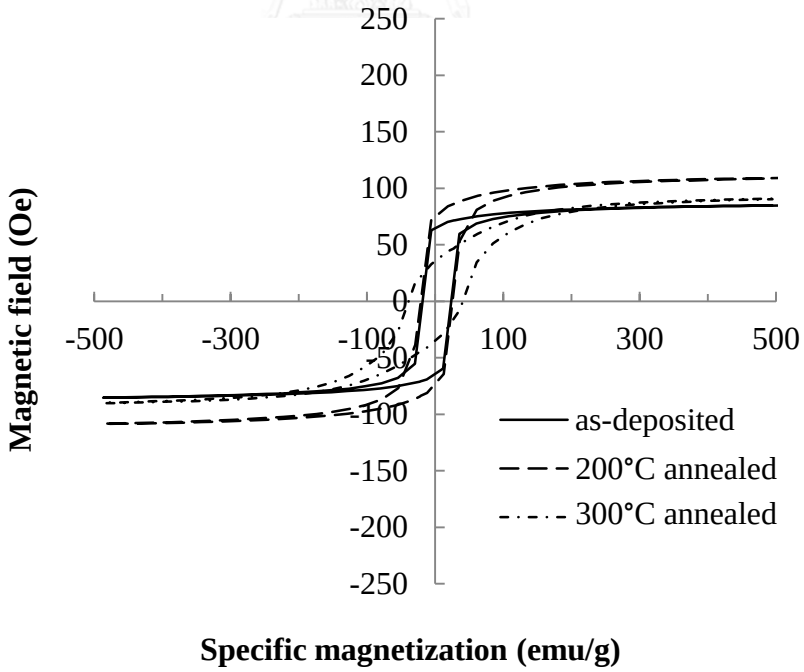

Fig. 4.11 The VSM measurement of in-plane magnetic hysteresis loop of the as-deposited, 200°C annealed and 300°C annealed CoFe films with: (a) 57.3 wt.% Fe, and (b) 80.0 wt.% Fe.

(a)

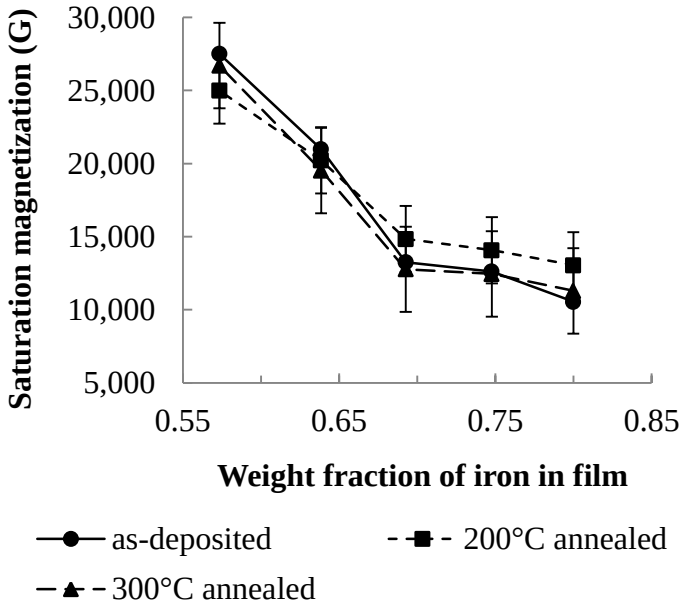

(b)

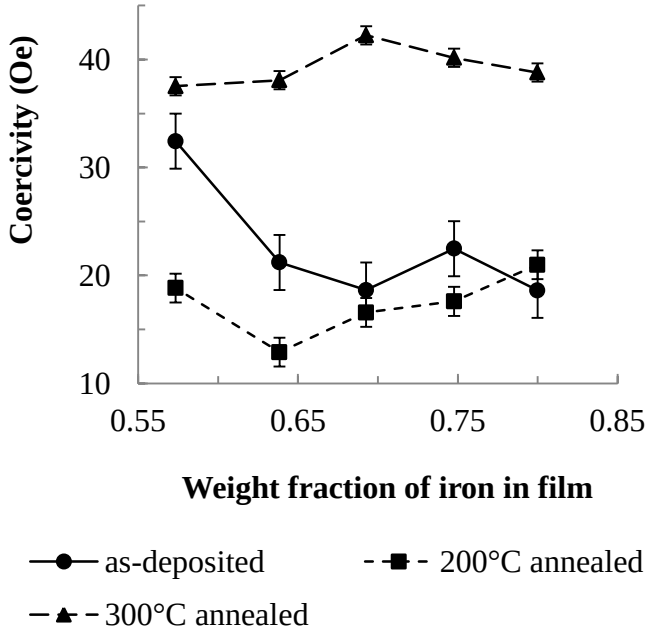

Fig. 4.12 The in-plane magnetic properties of the as-deposited, 200°C and 300°C annealed CoFe films as measured by VSM: (a) saturation magnetization, and (b) coercivity.

4.2.2 Films' Characteristics

As illustrated in the AFM images in Fig. 4.13, all fabricated specimens under investigation exhibit a uniform coating layer without a presence of crack formation, and the crystallite features of the specimens appear in the nanometer regime. Using the AFM, the roughness of the specimens is also quantified to be in the nano-scale for all films' compositions considered. Slight differences of surface roughness levels are observed, with the relatively high and low roughness being found in the 200°C and the 300°C annealed specimens, respectively, suggesting the influence of heat treatments on the development of films' morphology.

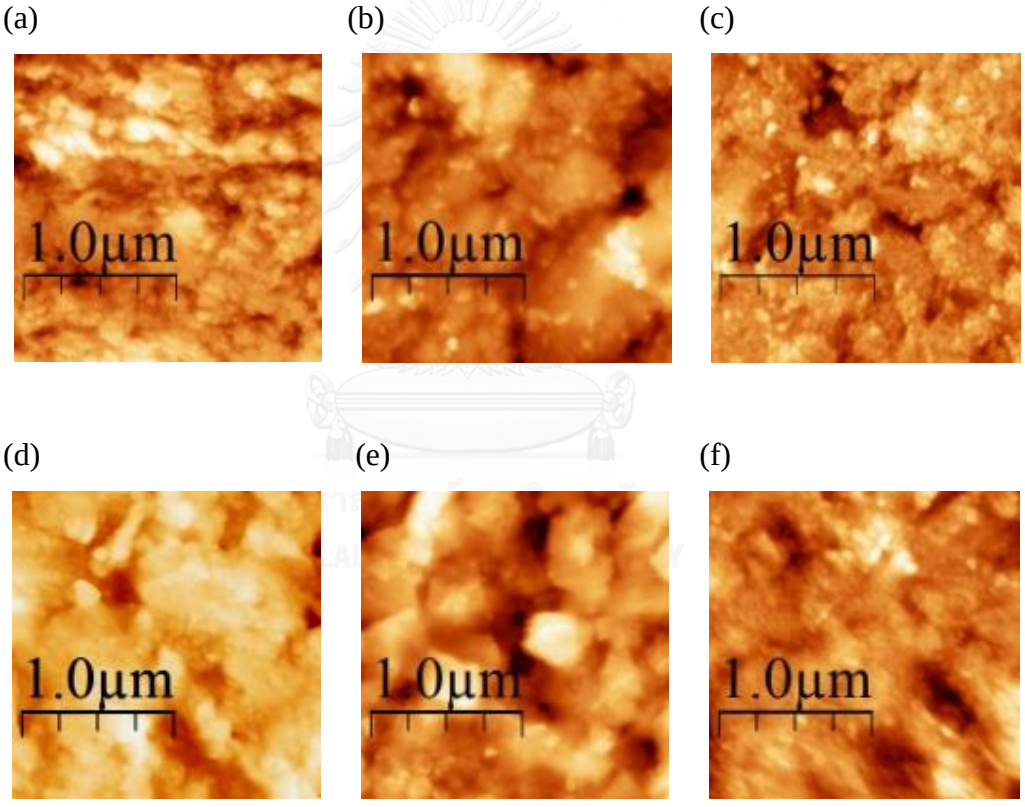

Fig. 4.13 The AFM images of the surface of CoFe deposits with 57.3 wt.% Fe; (a) as-deposited, (b) 200°C annealed, (c) 300°C annealed, and the films with 80.0 wt.% Fe; (d) as-deposited, (e) 200°C annealed, (f) 300°C annealed.

XRF provides the information on the thickness of the films. As illustrated in Fig. 4.14, the thickness of the films is parabolically related to the Fe content. The

optical microscopy, as shown in Fig. 4.15, was employed to confirm validity of the film thickness measured from the XRF. Furthermore, the film thickness of the specimens is reduced with the increment of annealing temperatures occurring plainly in the films with high Fe content. This should be owed to densification of the films during thermal treatments.

The XRD profiles of the specimens with the Fe contents of 57 wt.% and 80 wt.% are exemplified in Fig. 4.16. A range of important information can be deduced from these profiles, namely crystallite size, crystal orientation, and texture coefficient. The crystallite size is used as estimated grain size, which is calculated from XRD analysis is a function of the Fe content and annealing temperature, as shown in Fig. 4.17. The results show that the films exhibit nano-scaled grain size which is in agreement with the microscopic features observed from the AFM. Furthermore, grain growth is apparently detected as the annealing temperature reaches 300°C. In contrast to the films' roughness, as shown in Fig. 4.18, the 300°C annealing results in the smallest roughness, while the roughness seems to propagate larger roughness comparing to that of as-deposited films.

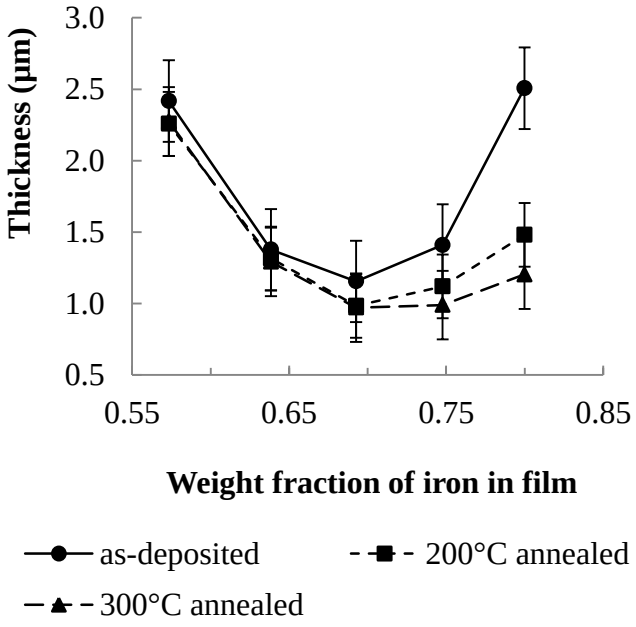

Fig. 4.14 Measurement of the films' thickness by XRF.

(a)

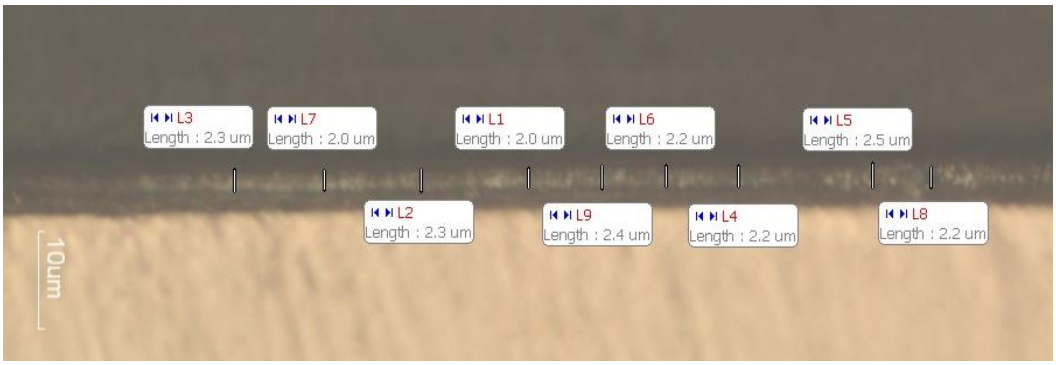

(b)

Fig. 4.15 Thickness measurement by optical microscope of the selective specimen; (a) as-deposited and (b) 300°C annealed CoFe film with 80.0 wt.% Fe.

The XRD profiles shown in Fig. 4.16 also indicate that both the high-Fe and low-Fe films exhibit solid solution bcc structure of CoFe alloys. The 80 wt.% Fe film preferentially oriented in the (200) direction, whereas the 57 wt.% Fe film has the (110) preferred orientation. It should be noted that it is prior study revealed that the plane (110) is well-related to strong saturation magnetization of CoFe composites [7]. Determining the (110) texture coefficients of the films from the XRD profiles and the equation (4.1), as presented in Fig. 4.19, it is observed that the texture coefficient of bcc(110) plane is a strong function of the Co and Fe contents. Generally, the coefficient is reduced with the increase of the relative Fe content. Considering Fig. 4.16 and Fig. 4.19, it can be also observed that for the most parts, the applications of heat treatments on these specimens, do not significantly affect the films'

crystallographic orientation, texture coefficient, and the development of a new phase, except for the films with relatively low Fe content.

(a)

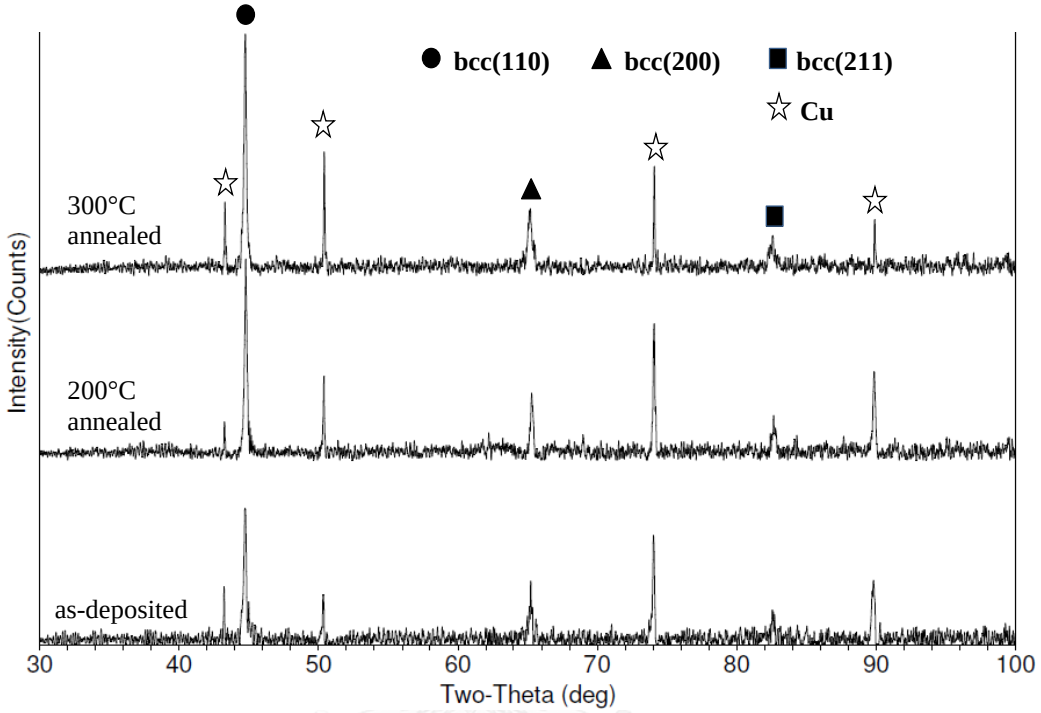

จุฬาลงกรณ์มหาวิทยาลัย
Chulalongkorn University

(b)

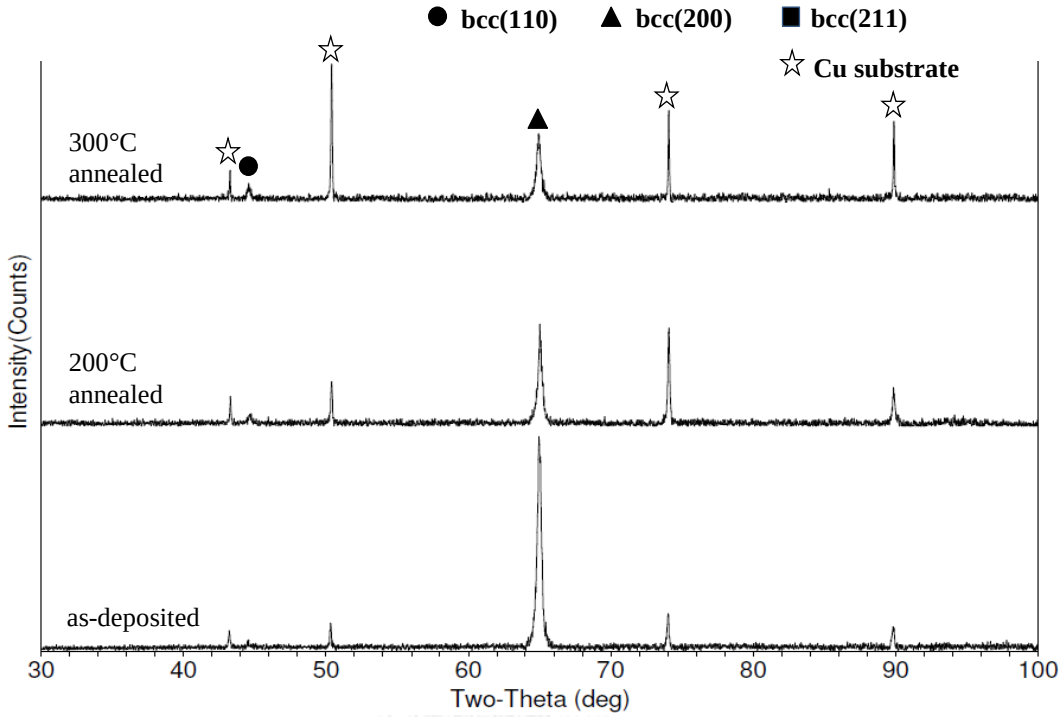

Fig. 4.16 XRD analysis of the CoFe deposits of: (a) 57.3 wt.% Fe, and (b) 80.0 wt.% Fe.

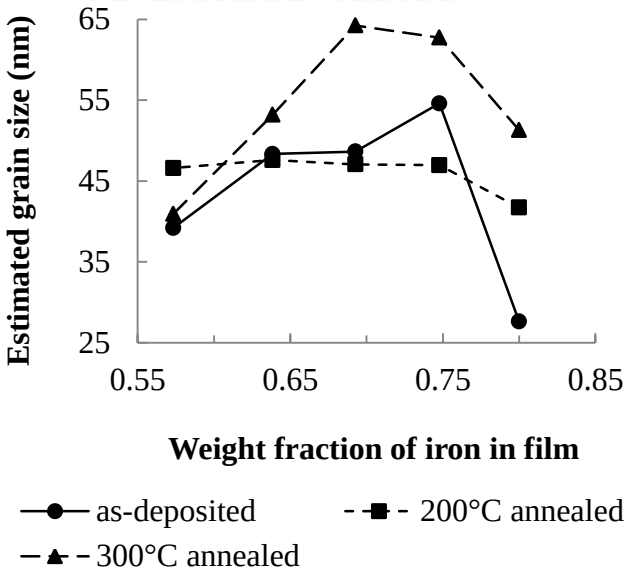

Fig. 4.17 Estimated grain size of the films by XRD.

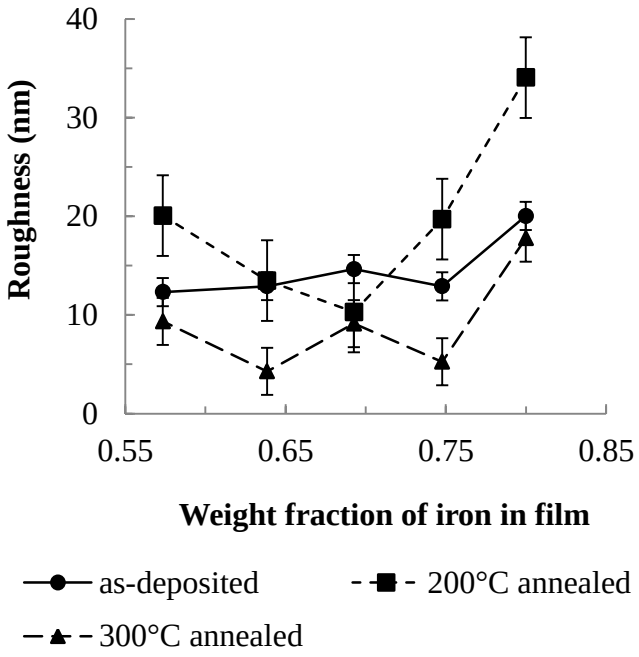

Fig. 4.18 AFM measurement of the films' roughness.

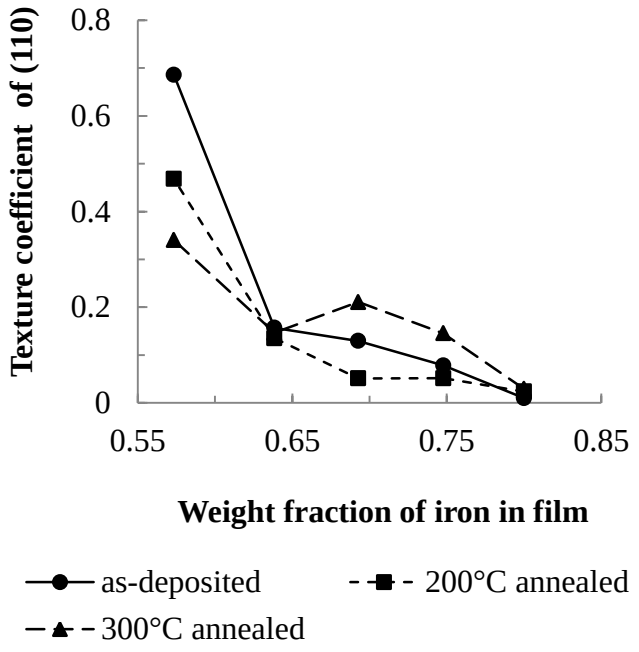

Fig. 4.19 Texture coefficient of bcc(110) plane of the films by XRD analysis.

4.3 Part III – Effects of Magnetic Field and Low Temperature

The magnetic field of 6 kG would be applied during electrodeposition process at room temperature (25°C) and low temperature (-2°C). The investigation for the influences of both magnetic field and low temperature on the films' structure and magnetic properties were elucidated.

4.3.1 Plating Films' Compositions

The relative contents of Co and Fe in the electroplated CoFe deposits from magnetic-field plating at room temperature and at -2°C were shown in Fig 4.20.

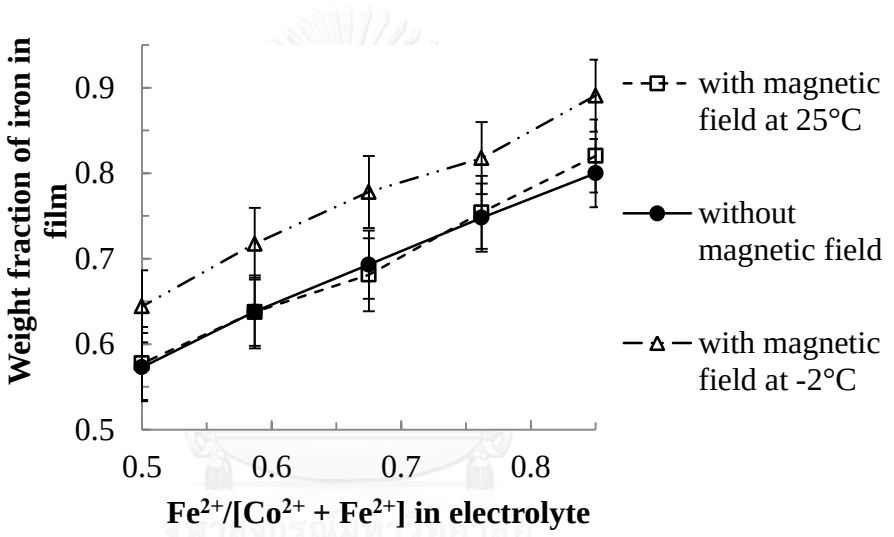

Fig. 4.20 The Fe content in the deposits as a function of $Fe^{2+}/(Co^{2+} + Fe^{2+})$ ratio in the plating baths with and without 6 kG magnetic field at room temperature and with 6 kG magnetic field at -2°C.

By increasing the ratio of Fe^{2+} in the baths, the Fe contents in the deposits are enhanced. Comparing to the CoFe films from 4-hour plating in Part I which has no magnetic field at room temperature, the results show that magnetic field slightly affects Fe content in CoFe films while low temperature significantly impacts on the content which increases in its ratio around 0.07 – 0.09. This means that low temperature supports the deposition rate of Fe^{2+} in the electrolyte on the surface of the

electrode. The low and high Fe-content films are produced from the plating of the electrolyte with low and high Fe^{2+} proportion respectively.

4.3.2 Magnetic Properties

The electroplated CoFe films are measured their magnetic properties by VSM presenting the hysteresis loops' shapes. The hysteresis loops of the selected low and high Fe-content films are shown in Fig. 4.21.

(a)

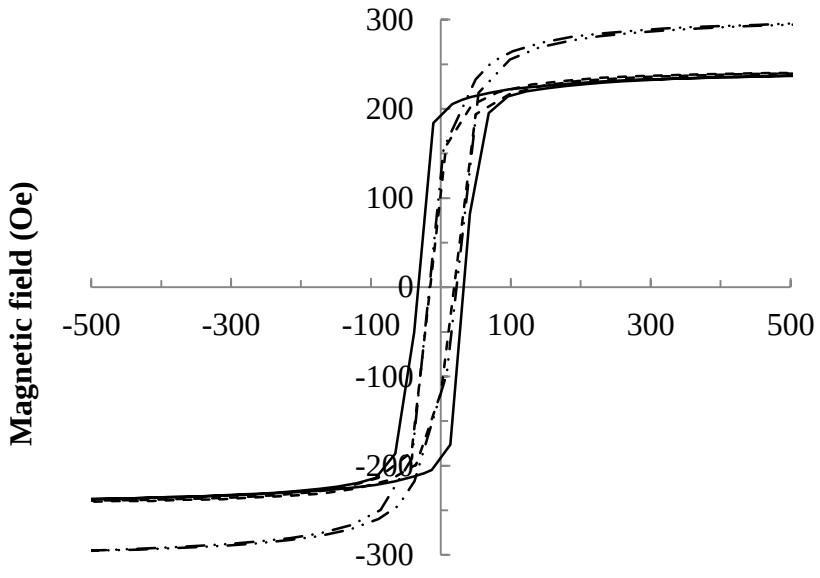

(b)

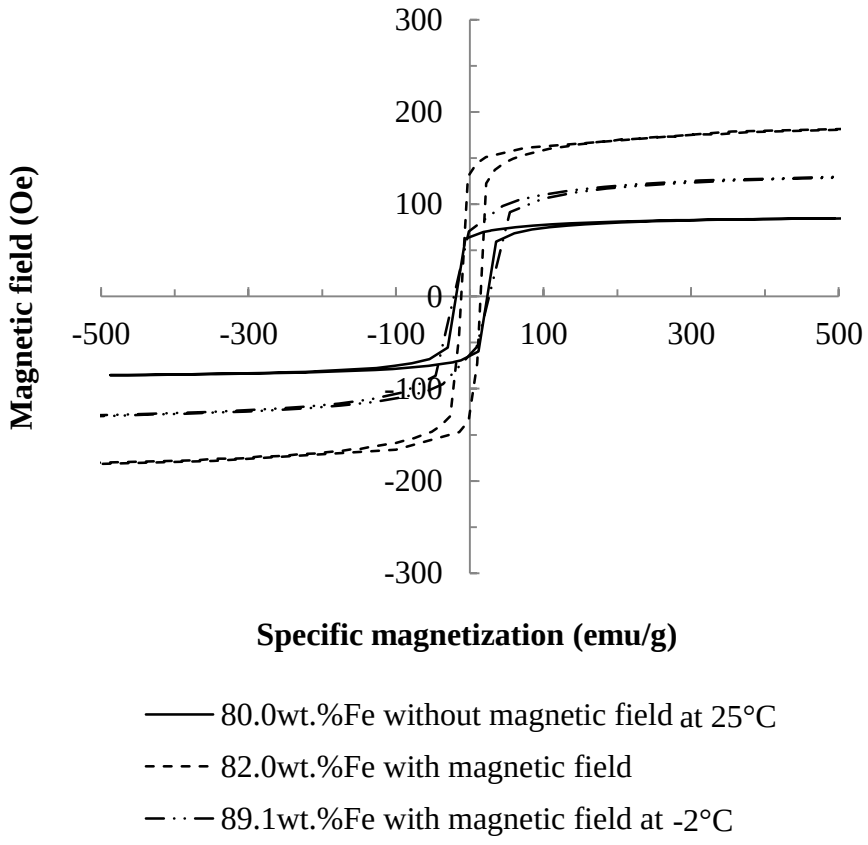

Fig. 4.21 The VSM measurement of in-plane magnetic hysteresis loops of (a) high Fe content, and (b) low Fe content of the CoFe films from plating: without magnetic field, with 6 kG magnetic field at room temperature and the field at -2°C.

It seems that the plating with magnetic field can induce soft magnetic properties of the films. The data of intensity of magnetization from hysteresis loops are transformed to saturation magnetization by the equation (2-1) and (2-2) as described in Part I and II. Both parameters: saturation magnetization and coercivity, of the specimens are exhibited in Fig. 4.22 (a) and (b) respectively.

The Fig. 4.22 presents that the magnetic-field plating significantly induces higher saturation magnetization and lower coercivity of CoFe films comparing to the results of the plated films without magnetic field. The very high saturation magnetization of 42.3 kG is attained from the film with 64.4 wt.% Fe plated at -2°C in the magnetic field.

For the plated films with magnetic field, the low temperature condition in plating contributes to the increment of saturation magnetization and obvious inversely relate to Fe content in the films. In addition, the condition supports the coercivity returns to be higher than that of the magnetic-field plated films at room temperature.

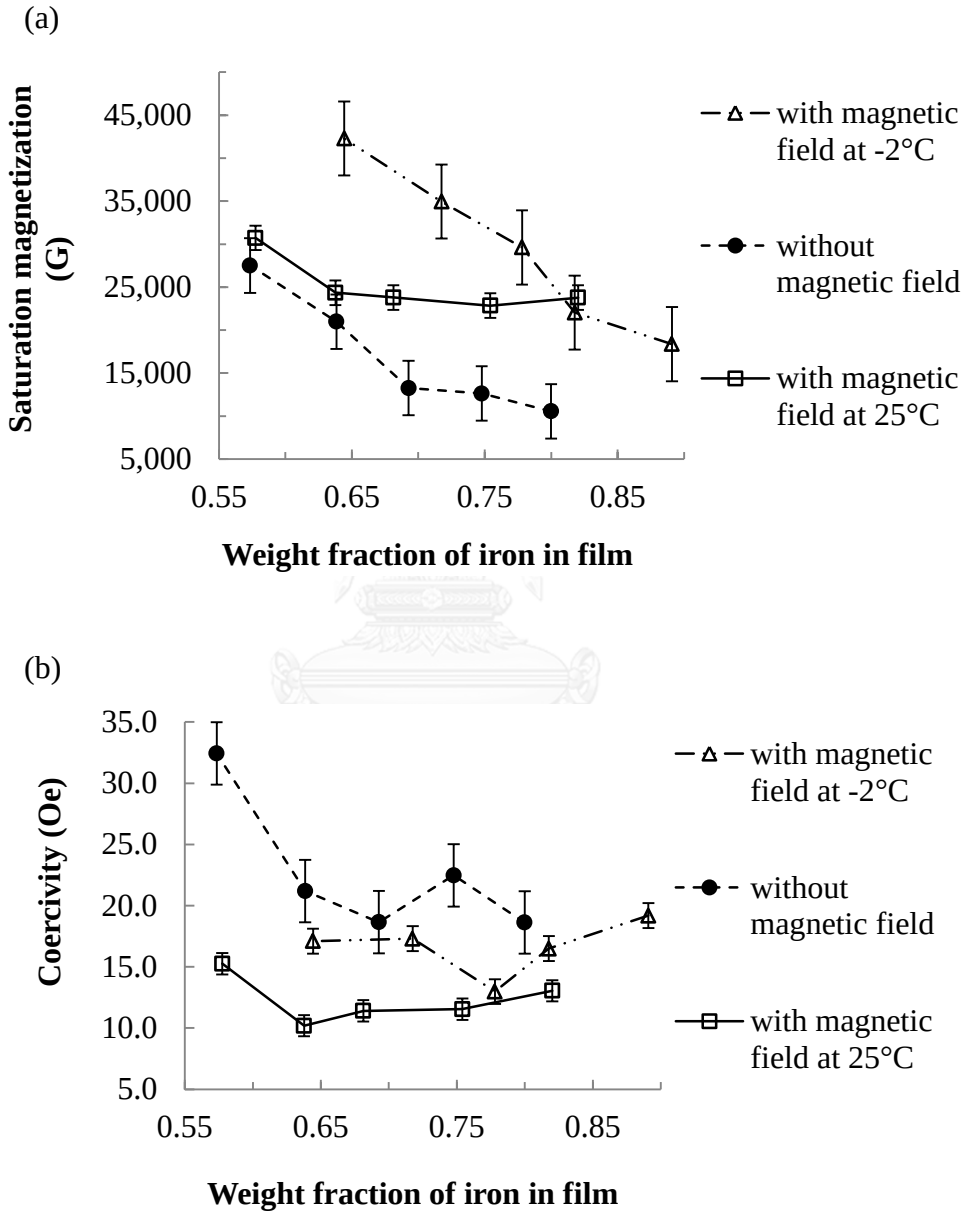

Fig. 4.22 The in-plane magnetic properties: (a) saturation magnetization, and (b) coercivity measured by VSM of the CoFe films from plating: without magnetic field, with 6 kG magnetic field at room temperature and the field at -2°C.

4.3.3 Films' Characteristics

All specimens are measured their surface configuration in nanoscale length by AFM as shown in Fig. 4.23. Nodules of grains appeared clearly in the films of plating with magnetic field and slight difference of the nodules' size of the films from plating with magnetic field at -2°C, significantly suggesting that the magnetic field effects on the surface's films morphology.

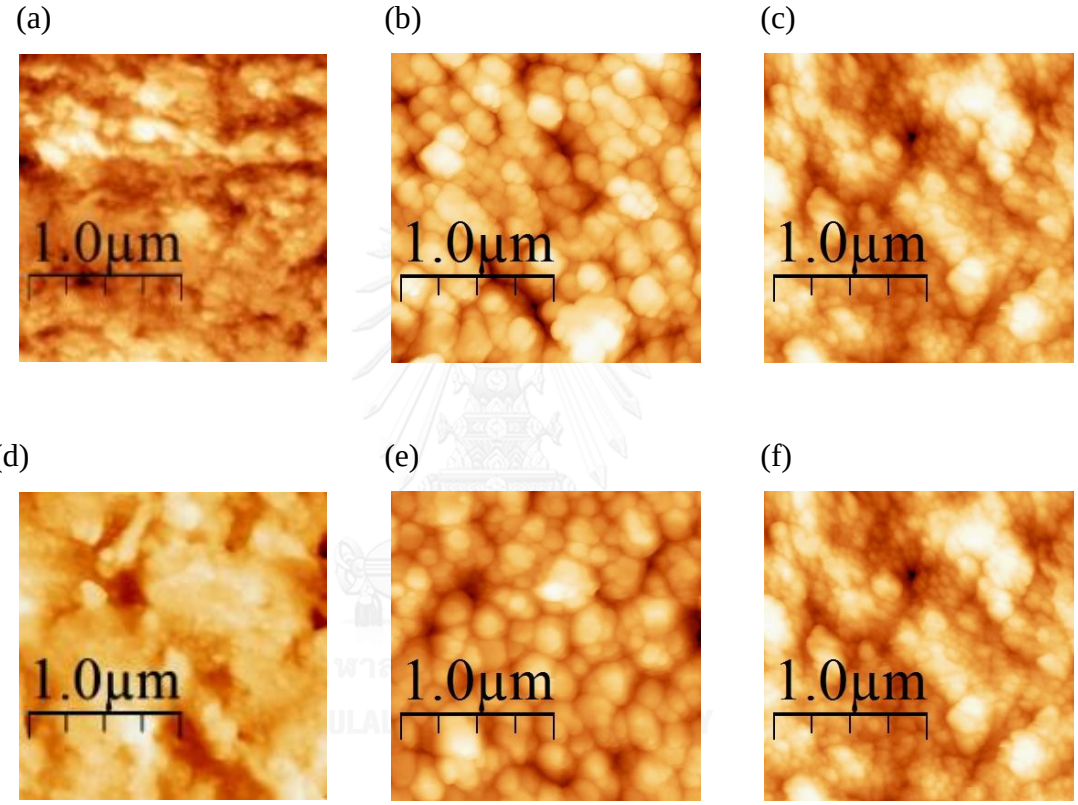

Fig. 4.23 The AFM images of the surface of CoFe deposits with; (a) 57.3 wt.% Fe as-deposited, (b) 57.8 wt.% Fe with magnetic field at room temperature, (c) 64.4 wt.% Fe with magnetic field at -2°C , and the films with; (d) 80.0 wt.% Fe as-deposited, (e) 82.0 wt.% Fe with magnetic field at room temperature, (f) 89.1 wt.% Fe with magnetic field at -2°C.

The XRD profiles of the deposits from electroplating with magnetic field at room temperature and at -2°C are presented in Fig. 4.24. All films' structure is bcc solid solution. The magnetic-field plating induces high intensity of bcc(200) as

predominated plane, while the magnetic-field plating at -2°C also creates bcc(200) as predominated plane, except bcc(110) is the easy plane of the 89.1 wt.% Fe film from the magnetic-field plating at -2°C. It means that low temperature of plating supports high intensity of bcc(110) and low intensity of bcc(200) plane in high Fe content film. While, the films from no magnetic-field plating as shown in Part I in Fig 4.6 and Fig. 4.16 in Part II, bcc(110) is predominate in 57.3 wt.% Fe film and bcc(200) for other films.

(a)

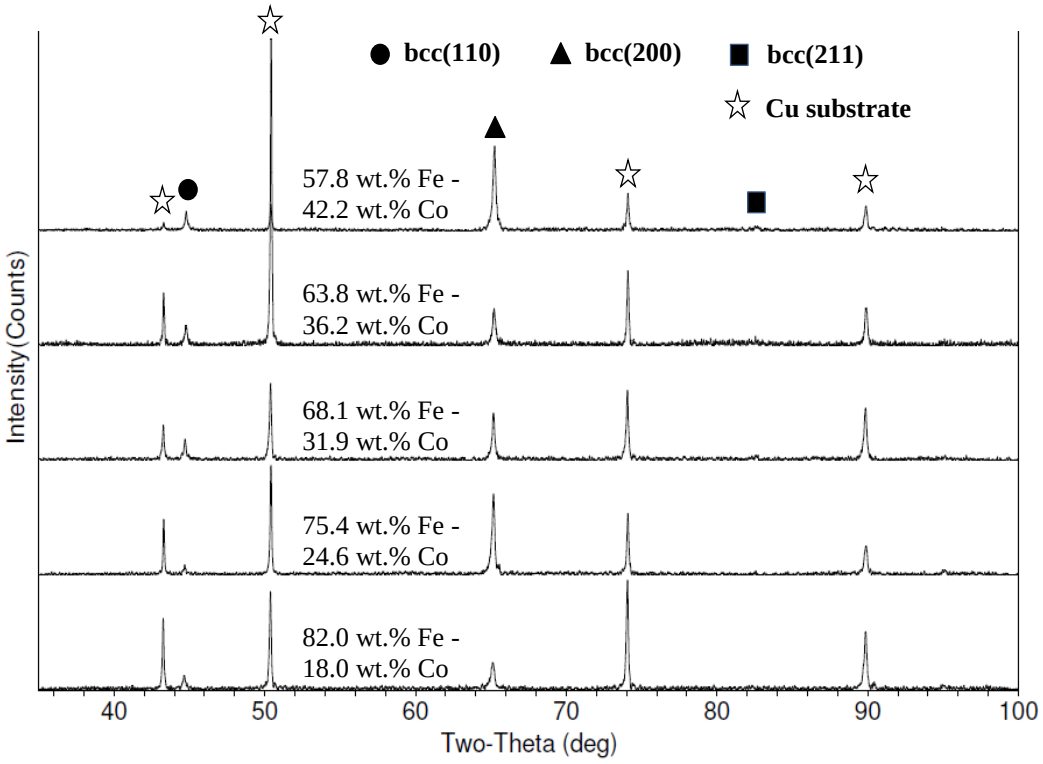

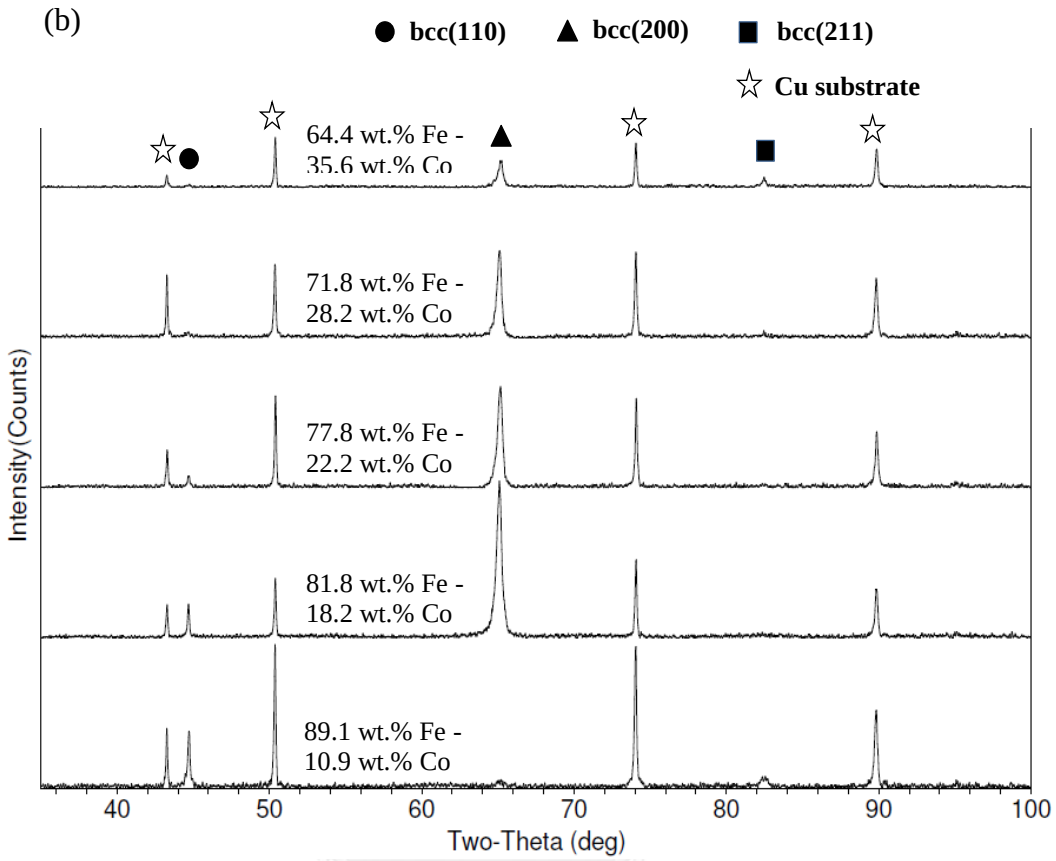

Fig. 4.24 The XRD profiles of the CoFe deposits electroplated with magnetic field at (a) room temperature and (b) -2°C.

Considering the texture coefficient of the CoFe films determined from XRD profiles as exhibited in Fig. 4.25. For bcc(110), the texture coefficient decrement is a function of Fe content in the films from no magnetic plating, but slightly trends to decrease and increases for the magnetic-field plated films and -2°C magnetic-field plated films, respectively. For the texture coefficient of bcc(200), it increases as Fe content in the films of no magnetic-field plating and that of -2°C magnetic plating films which is opposite to bcc(110) and relatively high but sharply drop at high Fe content at 89.1 wt.%, while it fluctuates and trends to decrease for magnetic-field plated films. Whereas the bcc(211) texture coefficient occurs only in 57.3 wt.% Fe film from no magnetic-field plating process and appears at low level in a few films

with 68.1 and 57.8 wt.% Fe from magnetic-field plating. However, the value decreases as Fe content increment except 89.1 wt.% Fe that the coefficient returns to high in the films from -2°C magnetic-field plating.

(a)

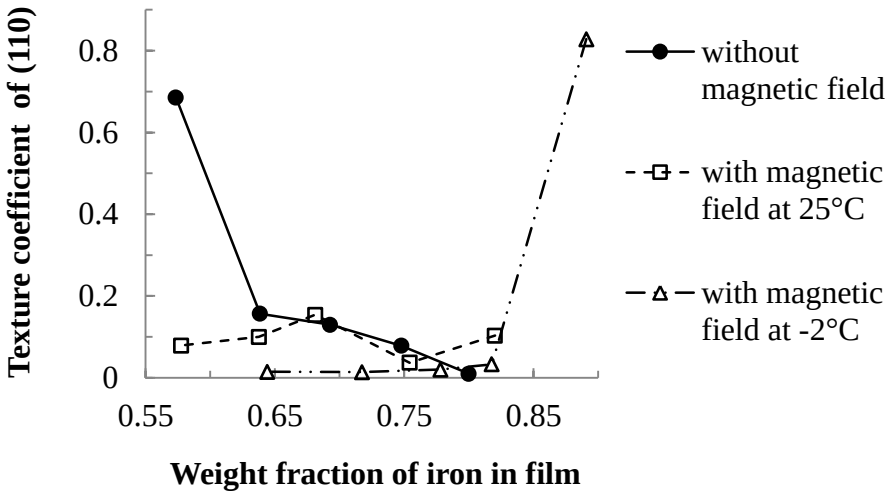

(b)

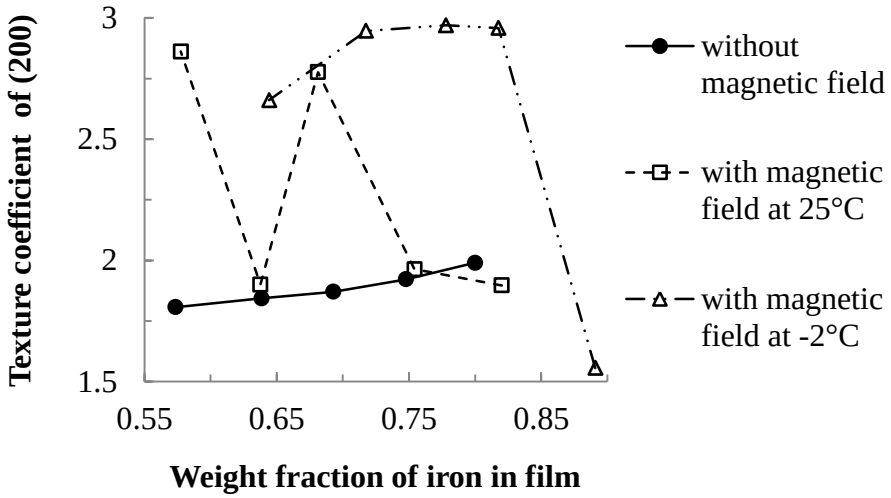

(c)

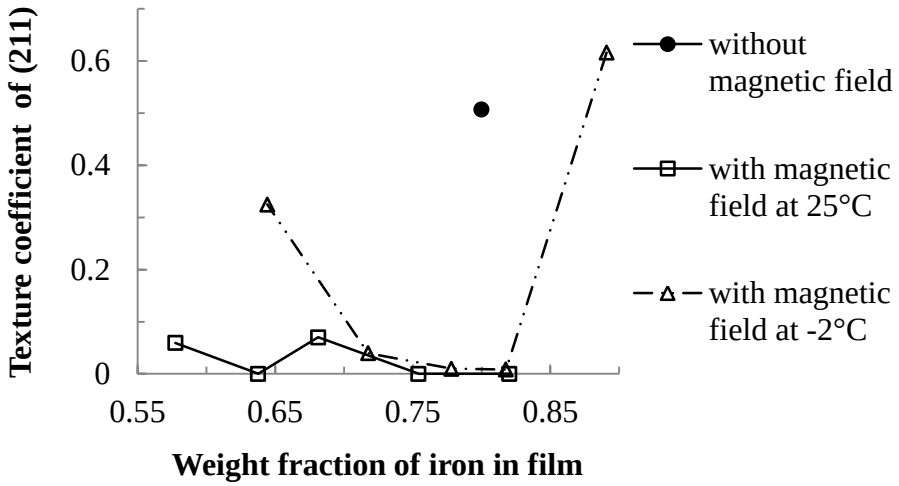

Fig. 4.25 Texture coefficient of bcc: (a) (110), (b) (200) and (c) (211) planes of the CoFe films by XRD analysis.

The XRD profiles of the CoFe films are used for the calculation of the estimated grain size as exhibited in Fig. 4.26. The results show inverse parabolic relation of the three processes and the largest estimated grain size appears in the film with Fe content about 70 – 75 wt.%. In the overall, the plating with magnetic field at -2°C creates the largest estimated grain size.

The surface roughness measured by AFM analysis is shown in Fig. 4.27. The magnetic-field plating induces the films' roughness fluctuating around 15 – 30 nm, while -2°C magnetic-field plating creates the parabolic relation between roughness and Fe content also in the same ranges. In overall, the roughness of the films from no magnetic plating process is a function of Fe content and lower than that of the films from magnetic-field plating. It can imply that magnetic field applied in plating bath induces high surface roughness of CoFe films.

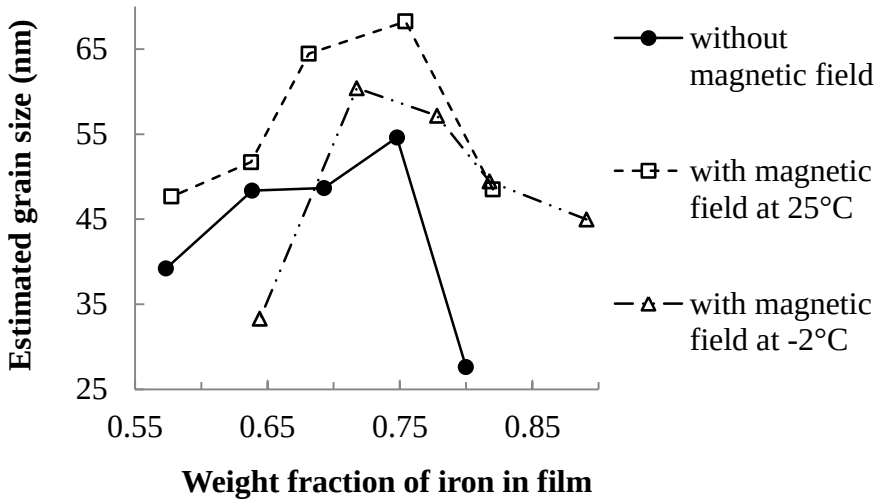

Fig. 4.26 Estimated grain size of the CoFe films by XRD.

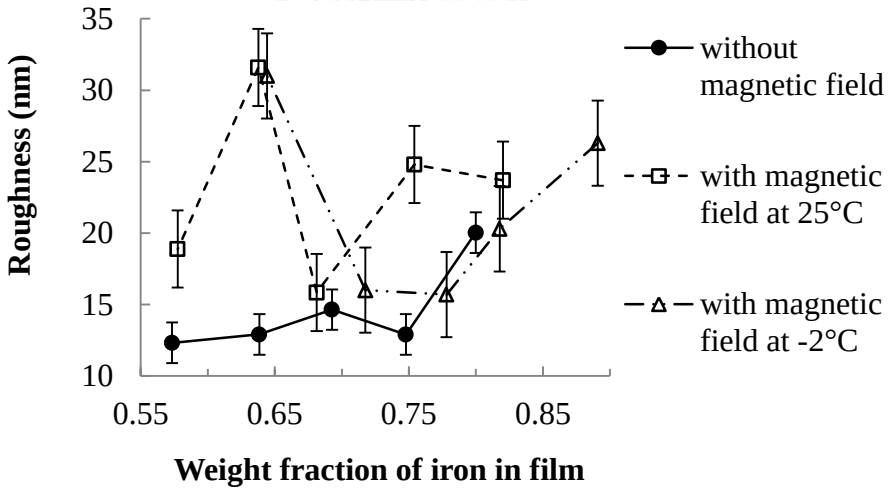

Fig. 4.27 AFM measurement of the films' roughness.

The XRF measurement provides the films thickness as illustrated in Fig. 4.28. The thickness of the films from no magnetic-field plating parabolically related to their Fe content. Whereas, the thickness of the films from magnetic-field plating decreases as Fe content increment, which is opposite to the films from -2°C magnetic-field plating; the roughness is a function of Fe content.

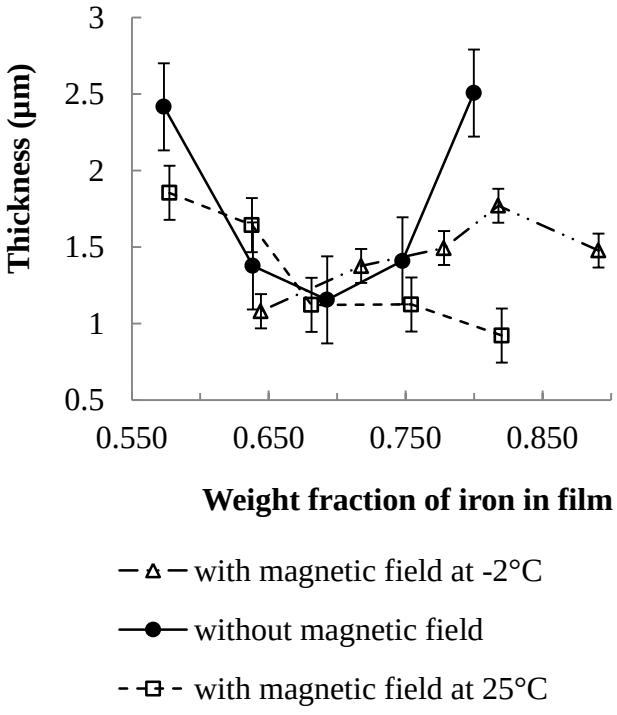

Fig. 4.28 XRF measurement of the films' thickness.

จุฬาลงกรณ์มหาวิทยาลัย
Chulalongkorn University

CHAPTER V
DISCUSSION

There are three parts of discussion in the chapter;

- Part I – Effects of composition and thickness,
- Part II – Effects of annealing,
- Part III – Effects of magnetic field and low temperature.

5.1 Part I – Effects of Composition and Thickness

The magnetic properties, namely, saturation magnetization and coercivity, are influenced by chemical composition and growth of films [5, 27, 62, 70]. In particular, these parameters may affect surface roughness and crystallographic orientation, which in turn influence saturation magnetization. On the other hand, chemical composition and films' growth may control grain size, surface roughness and morphology, cluster size, and domain structure. This subsequently induces changes in coercivity. The details of these influences of the CoFe deposits are discussed below in relation to the obtained results.

5.1.1 Coercivity

It is generally understood that, grain size and roughness are predominant factors affecting coercivity [71]. In general, small sized grains exhibit relatively high coercivity owing to their high volume of grain boundaries, which act as pinning sites for magnetic domain wall movement [37, 72]. However, the coercivity of nano-sized grains may be reduced to a low value because of its low and random magnetic anisotropy [36, 38, 41]. Additionally, roughness which is related to cluster size plays a role in obstructing domain wall's movement and rotation that leads to coercivity increment. Finally, a domain pattern may also influence the coercivity of soft magnetic materials [71, 73]. Fig. 5.1 presents the relationship of coerivity and grain size of the CoFe films. For the thick films, it can be observed that grain size of about 40 nm, which belongs to the deposits with 57.3 wt.% Fe, acts like the critical grain size.

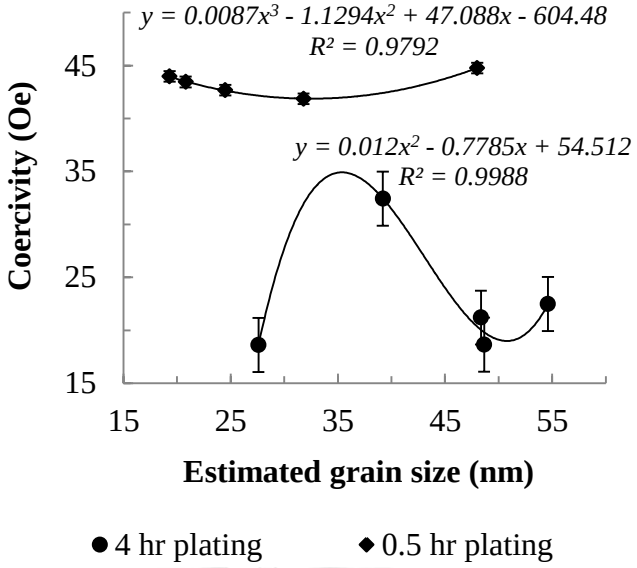

Fig. 5.1 Coercivity as a function of the XRD grain size of the CoFe deposits.

As for the thin CoFe deposits, their coercivity values are relatively high and depend on grain size but fluctuate in very small range of 42 – 45 Oe. Other influences, such as surface roughness and thickness, also become dominant. Particularly, the uniform films with minimal roughness of the thin CoFe deposits may obstruct the domain wall's motion more effectively than the thick film with high roughness. In addition, the thin films contain low homogeneity because of porous defects as shown in Fig. 4.2. The defects can also obstruct domain wall movement [71, 73]. The both obstruction caused by roughness and defects result in high coercivity. Furthermore, the difference of domain patterns observed in the thin and thick films (Fig. 4.10) may imply that the stripe-liked and bubble-liked domain patterns are related to high and low coercivity, respectively.

Furthermore, the uniaxial anisotropy constant of the films is taken into account, because it can support high coercivity due to difficult change in domain mechanism [27]. The constant is able to be computed for non-magnetized films or isotropy films by the equation (2-4) and anisotropy field can be estimated by the equation which is based on Stoner-Wohlfarth model

$$H_k = \left(\frac{2}{3}\right)\left(\frac{M_s}{\chi}\right) \tag{5-1}$$

when χ is susceptibility determined by the slope of coercivity line from in-plane hysteresis loop [74]. In addition, the exchange stiffness which is estimated by the equation (2-5) [4]. The number of atoms in unit cell (for bcc, $n = 2$), the total spin of electron assumed 1 for CoFe, the lattice constant determined from XRD analysis, the exchange integral for CoFe it is estimated by the equation (2-6) [44], the Curie temperature of CoFe is about 1,390 K [44]. The domain wall width is related to the exchange length by the equation (2-7) [27, 41].

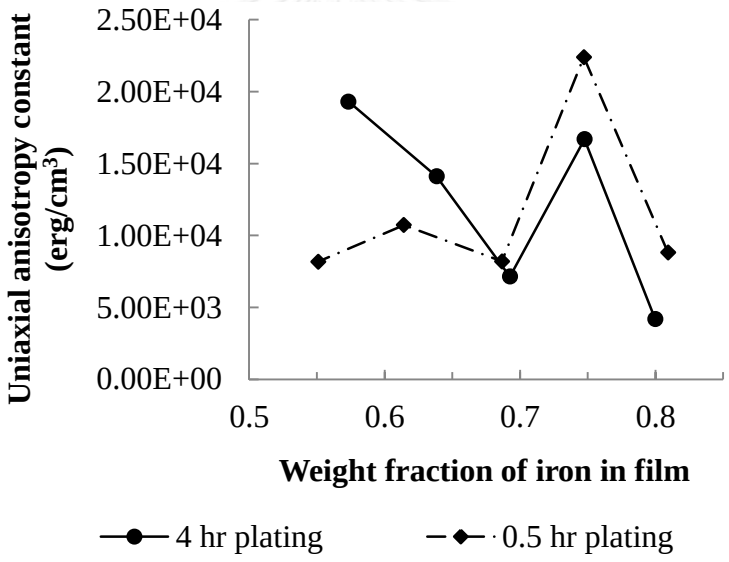

Fig. 5.2 Uniaxial anisotropy constant as a function of Fe content in CoFe films.

Fig. 5.2 depicts the uniaxial anisotropy constant values which of the thin and thick films are slightly different, but varies in a huge range of 2,500 – 22,500 erg/cm^3. It is described that Fe content affects change of pair of atoms orientation in the films. Moreover, Fig. 5.3 shows that the coercivity of the thick films significantly depends on the uniaxial anisotropy constant, but not in the thin films.

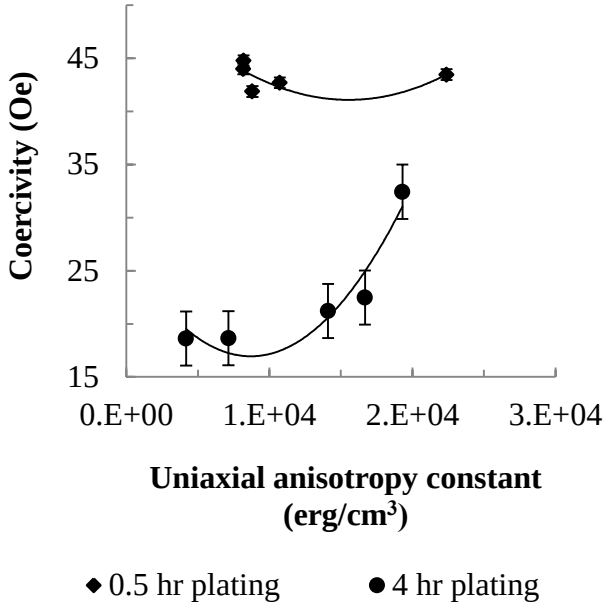

Fig. 5.3 The coercivity of the CoFe films as a function of uniaxial anisotropy constant.

The domain types: single domain and multi domain, can be indicated from the ratio of the estimated grain size to the exchange length (d / L_{ex}) given in the equation (2-3). Fig. 5.4 expresses that all films contain only a single domain type, so the effects of random anisotropy mechanism as Herzer's model with the relation $H_c \alpha d^6$ should be expected [38, 71, 73]. However, Fig. 5.1 exhibits the relation of $H_c \alpha d^2$ and $H_c \alpha d^3$ for the thin and thick films, respectively. In addition, a uniaxial anisotropy constant in Fig. 5.2 represents rather high anisotropy of the films. These reasons thus indicate that the relation between coercivity and grain size from the experiment is rather different from Herzer's model, especially for the thin films.

As justification above, it can conclude that thickness plays an important role on the films' coercivity. Thickness contributes to homogeneity of the films and then easy domain wall movement which suppresses coercivity, then develops soft magnetic behavior. In addition, thickness promotes two factors which plays an important role on coercivity, grain size and uniaxial anisotropy constant of thick

films, while grain size and homogeneity are dominant factors for the thin films. The lowest coercivity is obtained in the thick film with 80.0 wt.% Fe, which has the lowest uniaxial anisotropy constant and the smallest grain size, leading to the low coercivity of 18.6 Oe.

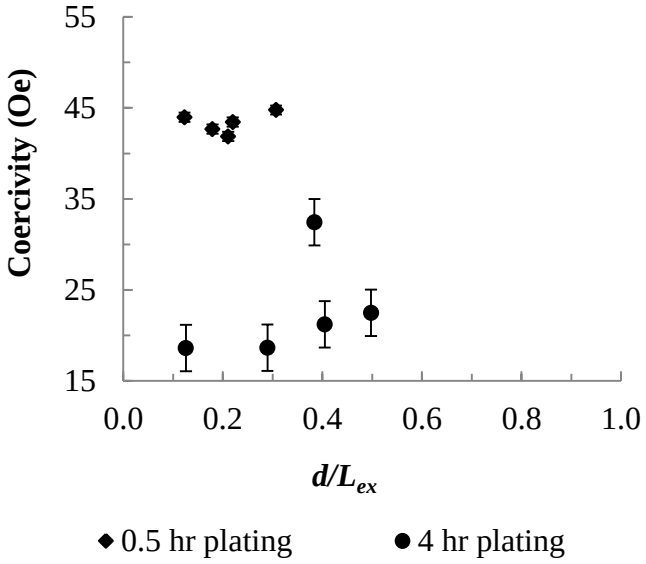

Fig. 5.4 The relation of coercivity and the ratio of estimated grain size (d) to exchange length (L_{ex}) of the CoFe films.

จุฬาลงกรณ์มหาวิทยาลัย
Chulalongkorn University

5.1.2 Saturation Magnetization

The highest saturation magnetization of 27.5 kG is obtained from the thick 57.3wt.% Fe films. This value is somewhat higher than what obtained by the prior studies [5, 6, 50, 75], and is found in the deposit with a relatively low Fe content, in contrast to some studies [56].

According to crystallographic structure which interacts with spin and orbit coupling plays an important role on magnetization behavior of magnetic materials [2, 27]. For the thick CoFe films, the relatively high saturation magnetization is associated with the high volume of (110) crystallographic orientation. Interestingly, the thin CoFe films, which are predominated by (110) planes, show relatively low saturation magnetization. This should be reasoned by the homogeneity increased by thickness of the films, which leads to the improvement of the films saturation

magnetization. It implies that defect or imperfection of the films doesn't affect only the coercivity of the films, but also influences on the films' saturation magnetization. Due to the loss by demagnetizing field created in the films' defects, such as voids or pores [76]. The energy reduces the magnetization in the films as shown in Fig. 5.5.

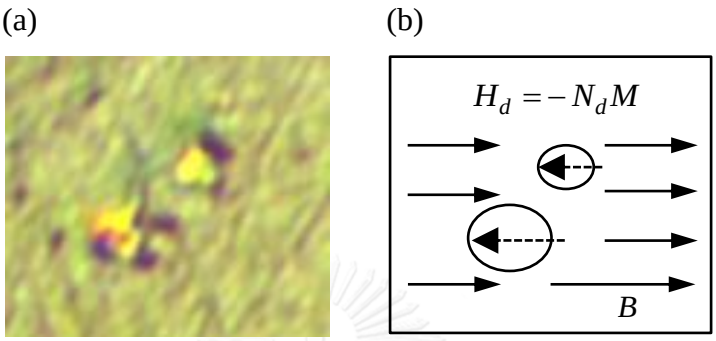

Fig. 5.5 Demagnetization of defects in the CoFe thin film, (a) porous defects in CoFe thin film (extended from Fig. 4.2) and (b) schematic view of demagnetizing field generated inside the pores.

The demagnetizing field aligns in the opposite direction to the magnetization in the film. The relation can be derived as the equations:

$$B = -H_d + 4\pi M \tag{5-2}$$

$$H_d = -N_d M \tag{5-3}$$

when $-H_d$ is the demagnetizing field and N_d is the demagnetizing factor which depends on the defect shape [27].

As discussed above, porous defects in CoFe films, especially the thin ones, plays an important role on the CoFe films' saturation magnetization. In contrast, the thick films are more homogeneous and their saturation magnetization depends on (110) preferred orientation. The thick film with 57.3 wt.% Fe contains the highest number of (110) crystallographic plane, leading to the saturation magnetization of 27.5 kG.

5.2 Part II – Effects of Annealing

As shown in the results section, the application of heat treatment of 200°C and 300°C under nitrogen atmosphere on the CoFe films affect both the alloys' characteristics and soft magnetic properties, namely coercivity and saturation magnetization. The connections between these parameters will be elucidated herein.

5.2.1 Coercivity

It is generally known that microstructural features of magnetic films dominate coercivity. Particularly, defects, surface roughness, and grain boundaries act as pinning sites for domain wall movement [18, 37]. For a bulk material, by increasing the surface roughness, an enhancing of coercivity would be expected as the movement of domain walls could be obstructed. For a thin film, however, an increase of roughness may decrease the coercivity, due to ease of domain rotation in a Bloch wall [71]. Similarly, a reduction of film thickness signifies densification of the films and hence defect annihilation, leading to anticipated reduction of coercivity. However, the relations of the roughness, thickness and coercivity, as shown in Fig. 5.6 and 5.7, are subtle and inconclusive. Surface roughness and thickness are apparently not the key controlling factor of coercivity in this system.

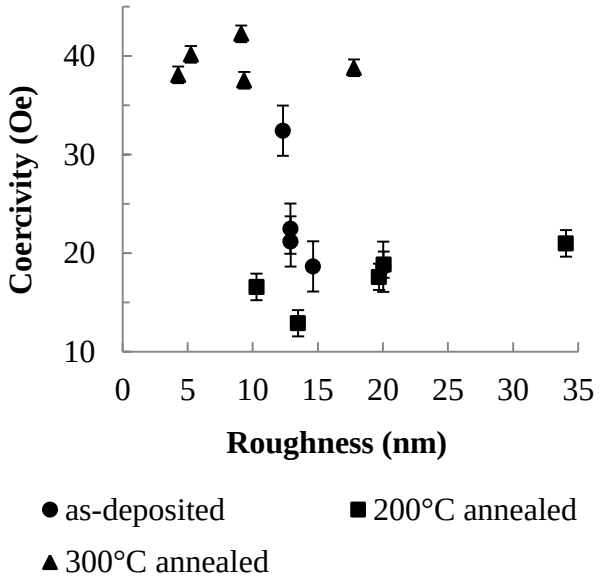

Fig. 5.6 Plots of coercivity and roughness of the CoFe films.

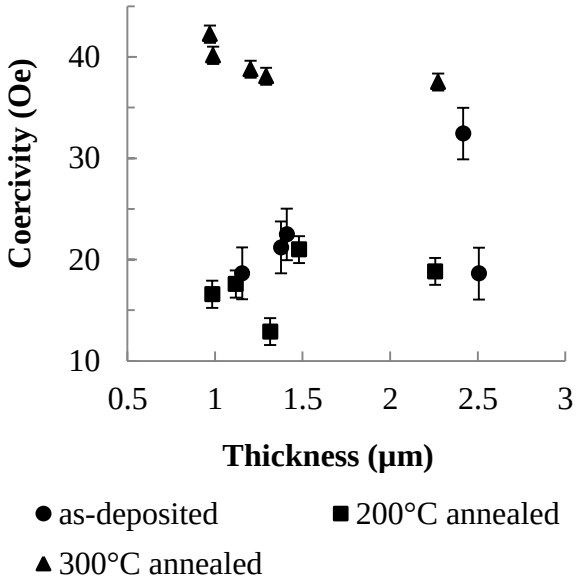

Fig. 5.7 Plots of coercvity and thickness of the CoFe films.

Turning now to grain size, generally, the influence of grain size on coercivity depends on the size of the grain with respect to exchange length and domain wall width. In particular, for grain size smaller than exchange length, it follows that $H_c \alpha\, d^6$ due to the presence of random anisotropy [36]. On the other hand, if grain size is larger than domain wall width, the coercivity is reversely related to grain size by the relation of $H_c \alpha\, d^{-1}$, owing to domain wall pinning mechanism by grain boundaries [4, 21, 41].

According to annealing affects the films' internal stress change which presents stress anisotropy along with other anisotropies, uniaxial anisotropy should be taken into account as the representative of all anisotropies; magnetocrystalline, magnetoelastic and shape anisotropies, in the films [27]. The exchange length and domain wall width can be calculated by the equation (2-3) and (2-7), the uniaxial anisotropy constant determined by the equation (2-4) [27], the saturation magnetization is are measured from hysteresis loop and anisotropy field is calculated from the equation (5-1). In addition, the exchange stiffness which is estimated by the equation (2-5) [4]. The number of atoms in unit cell (for bcc, $n = 2$), the total spin of electron assumed 1 for CoFe, the lattice constant determined from XRD analysis, the

exchange integral for CoFe it is estimated by the equation (2-6) [44], the Curie temperature of CoFe is about 1,390 K [44]. The domain wall width is related to the exchange length by the equation (2-7) [27, 41].

Following the calculations above, the relation between uniaxial anisotropy constant and Fe content for the CoFe films is exhibited in Fig. 5.8. The figure presents that the uniaxial anisotropy constant tends to reduce is as a function of Fe content in the as-deposited films, but it returns to high for the 74.8 wt.% Fe film in all conditions. Furthermore, the annealing alters the uniaxial anisotropy constant and distinctively increases the value at 300°C. It may be attributed from complexity of crystallographic change affecting crystal anisotropy due to annealing, because of crystal anisotropy is a type of uniaxial anisotropies of magnetic material [27].

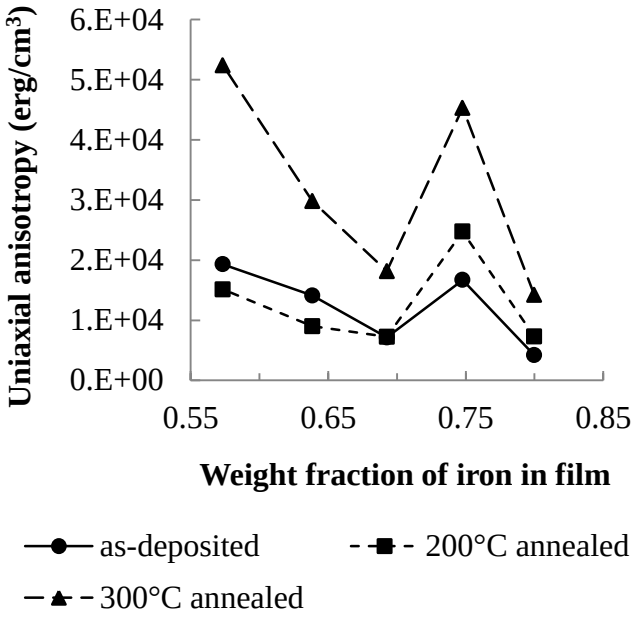

Fig. 5.8 In-plane uniaxial anisotropy constant of the CoFe films.

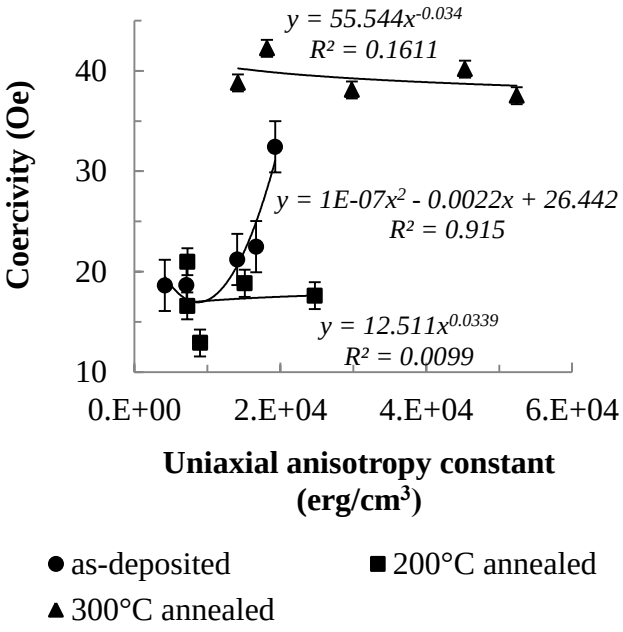

Fig. 5.9 Plots of coercivity and uniaxial anisotropy constant of the CoFe films.

Moreover, the uniaxial anisotropy constant is increased by annealing temperature. The effect is obviously seen as the results of 300°C annealing. This indicates that diffusion due to annealing leads to more directional order of like-atom pairs in the annealed films [27, 39, 69]. Nevertheless, 200°C annealing gives the opposite results in 57.3 and 63.9 wt.% Fe films.

In general, anisotropy affects domain wall mechanism leading to coercivity change [27] as the results of the as-deposited films exhibited in Fig. 5.9, but the relation is very slight for the annealed specimens. It implies that other factor plays a role on the coercivity of the annealed films.

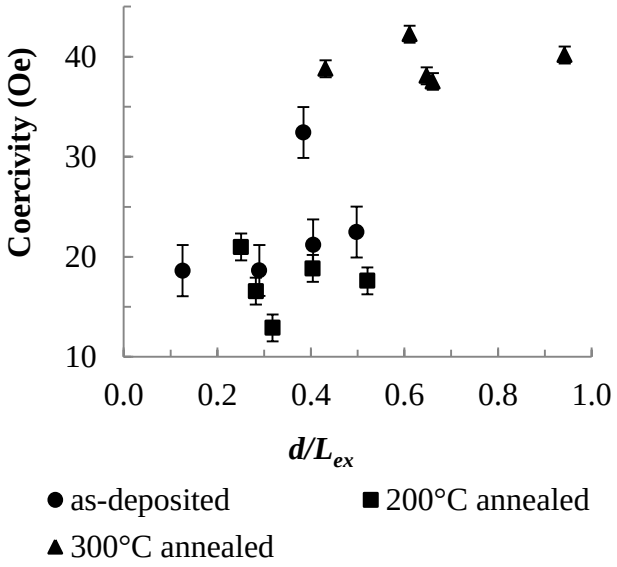

Fig. 5.10 The comparisons between coercivity and ratio of estimated grain size (d) to exchange length (L_{ex}) of the CoFe films.

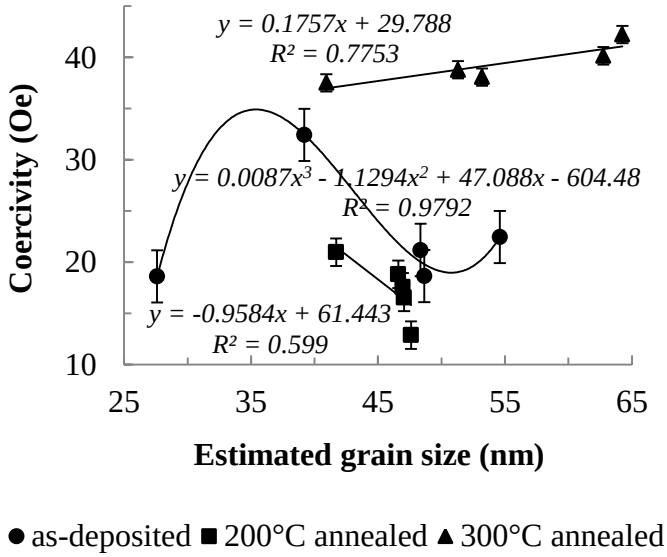

Fig. 5.11 The coercivity of the CoFe films as a function of grain size.

The dependence of the coercivity and the ratio of the estimated grain size to the exchange length of the investigated CoFe films can be determined as shown in Fig. 5.10. It is observed that for the most part, the grains of the specimens are of single domain type, and that their sizes are lower than exchange lengths and also domain wall widths. The random anisotropy mechanism of the films' magnetization process should be established [27, 36].

When the grain size is then plotted as a function of coercivity (Fig. 5.11), as expected, the typical relationship of $H_c \alpha\, d^6$ for single-domain grain as Herzer model [39] is not established. Instead, the coercivity of as-deposited and 200, 300°C annealed films exhibit similar correlation with the grain size following $H_c \alpha\, d^3$ and $H_c \alpha\, d^1$ respectively. These results signify that the heat treatments induce the changes of grain sizes with respect to exchanged lengths, and in turn influence the coercivity of the materials. However, the distinctions of the results of the specimens from different groups suggest that other influences of coercivity may also be presented.

Finally, the residual stress of the films was assessed using the XRD lattice spacing measurement. The CoFe films with 57.3 and 80 wt.% Fe of different annealing conditions were selected for examinations, as they have similar grain size of 40-50 nm but show somewhat distinct levels of coercivity. The residual stress of the films can be calculated from the equation (3.1) [68], where σ is the residual stress, ψ is the XRD tilted angle, d_0 is the lattice spacing of the (310) plane of a stress-free CoFe film ($d_0 = 0.9035$ Angstrom), E is Young's modulus of the CoFe films as measured by nanoindentation method (for 57.3 and 80 wt.% Fe films is 195.94 and 211.18 GPa respectively), ν is Poisson's ratio of the CoFe films (ν = 0.208) and m is the slope of a linear plot of lattice spacing (d) of the (310) plane versus $\sin^2\psi$ as shown in Fig. 5.12 [59]. Despite some scattering of data, this method is proved reliable for relative residual stress comparison [15]. The conclusion of the results from the residual stress measurements is presented in Fig. 5.13.

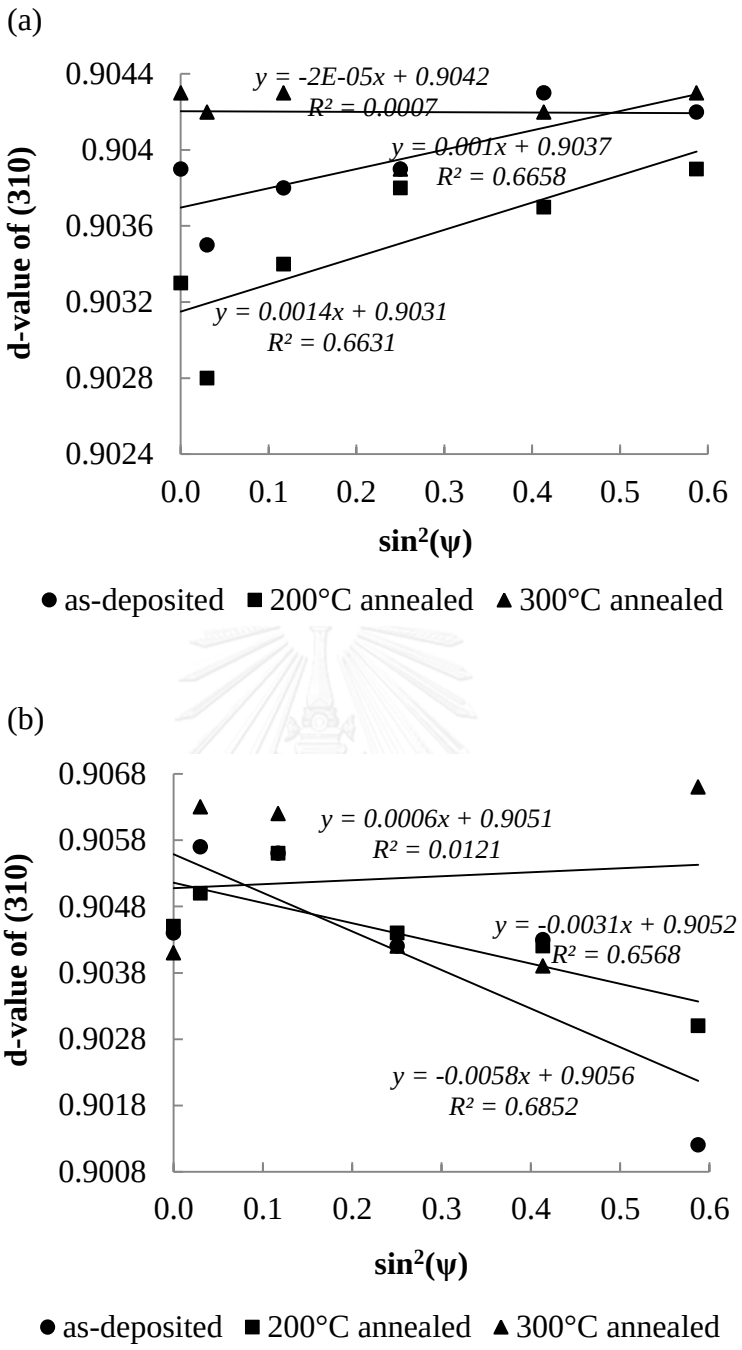

Fig. 5.12 Linear dependence of lattice spacing (d) versus $\sin^2\psi$ of the CoFe films with (a) 57.3 and (b) 80.0 wt.% Fe.

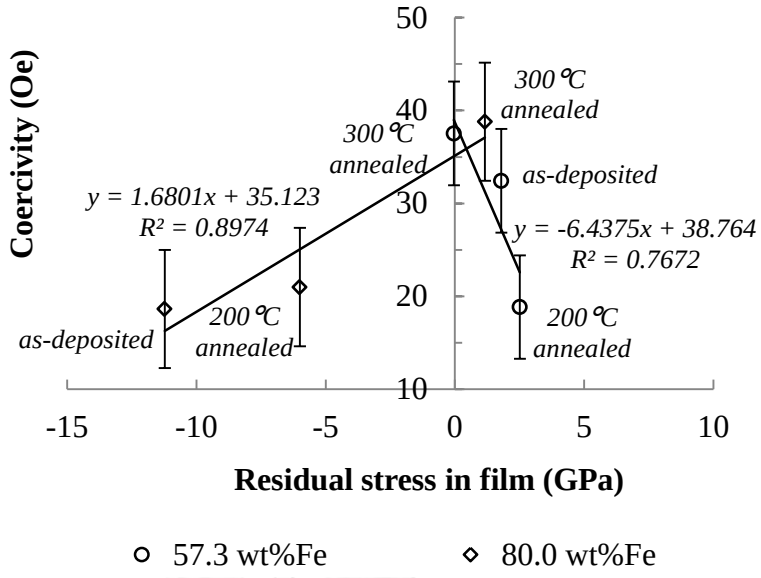

Fig. 5.13 Residual stress and coercivity of 57.3 and 80.0 wt.% Fe films.

In general, a typical stress developed in electrodeposited Co or Fe alloys is tensile. The stress can be generated by distortion of crystal lattice in atomic scale as observed by the lattice constant change. Furthermore, deposition is a non-equilibrium process of atomic diffusion with inadequate time. This may therefore results in a high density of defects and metastable structure of the films [77]. The lattice constant of the films with the low Fe content (57.3 wt.% Fe) and high Fe content (80 wt.% Fe) are shown in Table 5.1. Comparing the lattice constant values, it is found that the lattice constant values of these selective CoFe films are slightly larger than the original lattice constant of the film. This indicates that the tensile stress may be induced in the films. However, the summary of the results from the residual stress measurements presented in Fig. 5.13 reveals that the films with the low Fe content, 57.3 wt.% Fe and high Fe content, 80 wt.% Fe, exhibit tensile and compressive internal stress respectively. Therefore, there should be some other factors that contribute to stress development in the films and lattice constant.

Table 5.1 Lattice constant of the CoFe films with 57.3 wt.% Fe and 80 wt.% Fe from XRD analysis

CoFe films	Condition	Lattice constant (Å)	Original lattice constant of CoFe (Å)
57.3 wt.% Fe	As-deposited	2.863	2.855
	200°C	2.860	
	300°C	2.861	
80.0 wt.% Fe	As-deposited	2.869	
	200°C	2.865	
	300°C	2.865	

In this case, porosity in the films with high Fe content needs to be taken into account, because the observably significant reduction of the films' thickness upon annealing, as presented in Fig. 4.14 and 4.15. These pores should be generated by hydrogen gas product from the reactions (2-13) to (2-16) in the electrodeposition of high Fe-content films. Pores or voids are known to be an important factor altering stress in films [78]. They may act as inclusions which are interstitially trapped inside the films and result in the compressive stress. Upon annealing, stress relaxation occurs through diffusional re-ordering of crystal structures and suppression of defects and dislocations [79, 80]. Subsequently, films' thickness and compressive stress could be reduced. Furthermore, thermal annealing also provides the coalescence of grains, leading to grain size enlargement (Fig 4.17) and a reduction of the compressive stress towards low tensile stress inside the films [77, 78, 81].

Similarly, the tensile stress in the low Fe-content films could also be altered by thermal annealing. Annealing at 200°C also generates grain size enlargement, which may contribute to the increment of tensile stress. On the contrary, the 300°C annealing refines the grains to smaller size, inducing decrement of the tensile stress.

In general, stress in deposited films is expected to enhance film's coercivity, because of difficulty of switching magnetization [27, 77]. According to the compressive and tensile stresses can create magnetoelastic anisotropy, as the relation in the equation

$$K_\sigma = \left(\frac{3}{2}\right)\lambda_{si}\sigma \tag{5.4}$$

Here, λ_{si} is magnetostriction at saturation state of film and σ is stress in film [27].

However, it is noticeably that the coercivity is inversely proportional to the amount of both tensile and compressive stresses as shown in Fig. 5.13. The results reverse the expectation of the effect of stress supports the increment of coercivity in the films by magnetoelastic anisotropy [11, 27]. Hence, the uniaxial anisotropy is considered again. As shown in Fig. 5.14, it is interestingly that the films' coercivity depends obviously on the uniaxial anisotropy constant in accordance with the expectation of anisotropy principle. It can indicate that although the magnetoelastic anisotropy decreases as a result of the internal stress reduction by annealing, the uniaxial anisotropy still plays an important role on the films' coercivity between the conditions of as-deposited, 200°C and 300°C. Moreover, the effect of uniaxial anisotropy defeats that of magnetoelastic anisotropy in the competition.

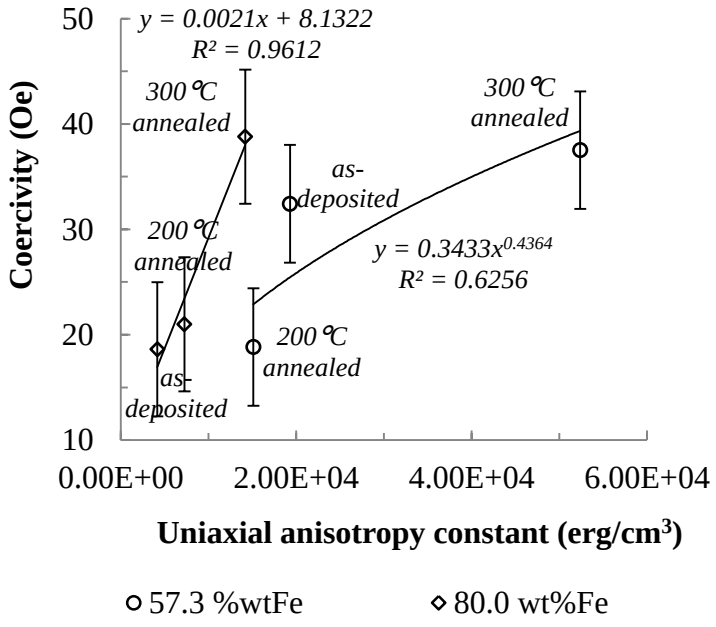

Fig. 5.14 The relation of coercivity and uniaxial anisotropy constant of the CoFe films with 57.3 and 80.0 wt.% Fe.

5.2.2 Saturation Magnetization

It is well-known that saturation magnetization of soft magnetic materials is a strong function of the chemical composition of the alloys and their corresponding crystallographic texture [5, 6]. For CoFe alloys, specifically, it has been shown that the saturation magnetization is controlled by the (110) crystallographic plane [82]. This is well-resonated by the comparable trends of the results shown in Figs. 4.12(a) and 4.19. With the increase of the relative Fe content, the (110) texture coefficient is generally decreased, leading to the monotonic reduction of saturation magnetization. The low Fe alloy (57.3 wt.%), on the other hand, exhibits somewhat high saturation magnetization of 27.5 kG, as compared to the prior studies [1, 50]. The reduction of residual stress by annealing slightly affects the films' saturation magnetization, which is in agreement with the prior studies [42, 44].

5.3 Part III – Effects of Magnetic Field and Low Temperature

As described in Chapter II that anisotropy is possible to be induced by magnetic field or magnetic field with low temperature which modify grain orientation that affects the CoFe films' characteristics and soft magnetic properties, coercivity and saturation magnetization. In this part, a couple of magnets with magnetic field of 6 kG was applied parallel to samples' surface in room temperature (25°C) and low temperature (-2°C). The elucidation will be done to reveal the relation between the films' structure and their magnetic properties.

5.3.1 Coercivity

It is well known that coercivity can be dominated by microstructure of magnetic films: roughness, defects and grain boundaries which act as pinning obstruction for domain wall movement in bulk material while for thin film, surface roughness may induce ease of Bloch wall's rotation [37, 71]. Similarly, the film thickness also influences on coercivity, due to high thickness contains more homogeneity of film and more film's volume contributing easy movement of domain walls [82]. However, the influence of roughness and thickness as shown in Fig. 5.15 and 5.16 are subtle and inconclusive for the magnetic-field plating deposits. Hence,

surface roughness and thickness are apparently not the key dominating parameter of coercivity for the CoFe films.

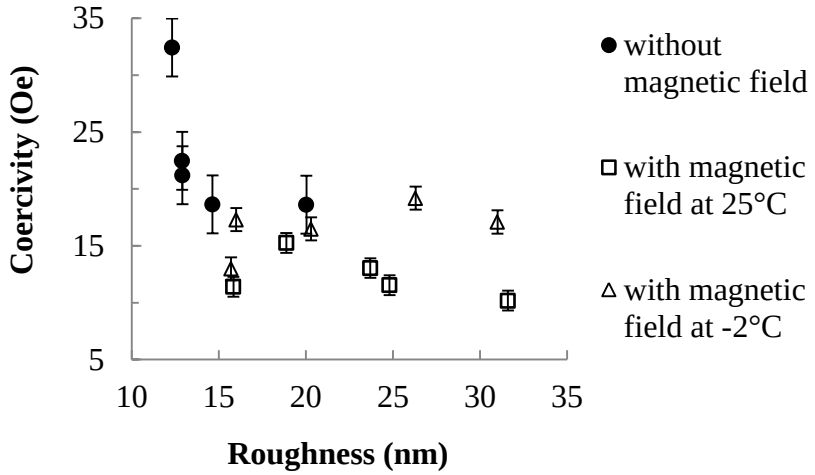

Fig. 5.15 Relation between coercivity and the CoFe films' roughness.

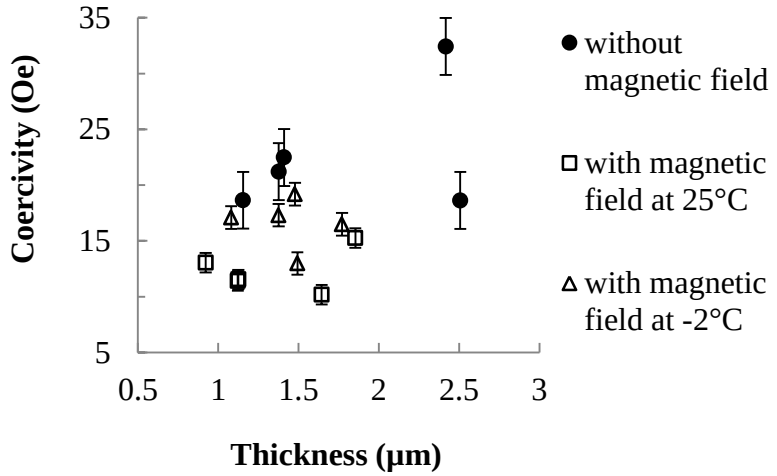

Fig. 5.16 Plots of coercivity and thickness of the CoFe films.

Considering the effect of grain size, in general, grain size plays an important role on coercivity upon the size of the grain with respect to exchange length and domain wall width. In particular, for grain size smaller than exchange length, it follows that $H_c \alpha d^6$ due to the presence of random anisotropy [36]. On the other hand, if grain size is larger than domain wall width, the coercivity is reversely related

to grain size by the relation of $H_c \alpha d^{-1}$, owing to domain wall pinning by grain boundaries [4, 21, 41].

The exchange length and domain wall width can be calculated by the equation (2-3) and (2-7) respectively. The uniaxial anisotropy constant, in this part it is the term of magnetic field induced anisotropy, determined by the equation (2-4) [27]. The anisotropy field and saturation magnetization can be measured from hysteresis loop [27, 41]. The specimens in this part are magnetized in the direction of magnetic field during plating, which is easy direction of the films, so directional induced anisotropy is created in the films [69]. The anisotropy field can determined by extrapolation of susceptibility to reach saturation magnetization from the hysteresis loop measured in hard direction by VSM [52]. The example of the method is shown in Fig. 5.17.

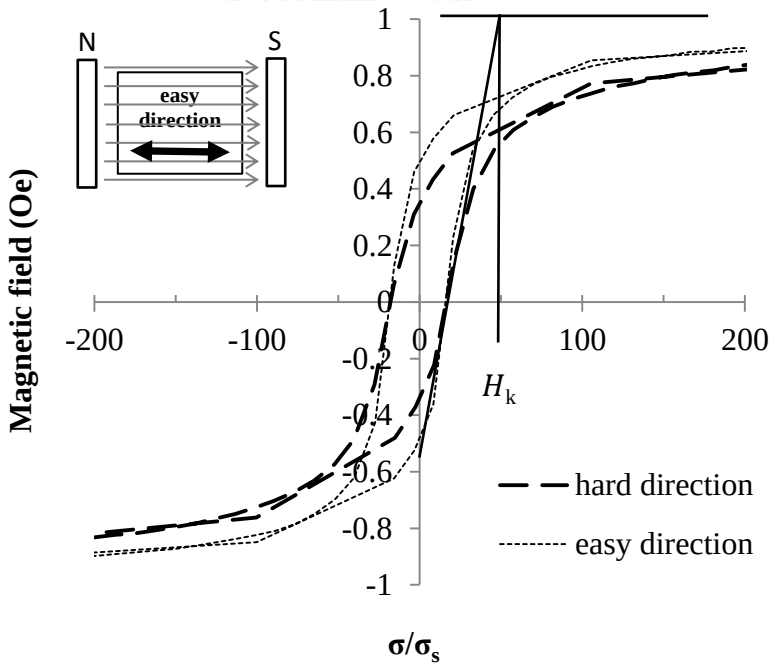

Fig. 5.17 The determination of anisotropy field (H_k) estimated from hysteresis loop of hard direction of 64.4 wt.% Fe film from magnetic-field plating at -2°C, easy and hard directions of specimen are the direction along and perpendicular to the magnetic field direction during plating respectively.

The exchange stiffness which is estimated by the formula (2-5) [4]. Here, the number of atoms in unit cell for bcc, $n = 2$, the total spin of electron assumed 1 for CoFe, the lattice constant determined from XRD analysis, the exchange integral, for CoFe it is estimated by the relation (2-6) [44], Curie temperature is 1,390 K for CoFe [44]. The domain wall width δ is related to the exchange length by the equation (2-7) [27, 41].

Following the calculations above, the uniaxial anisotropy constant (K_u) of the films was plotted versus the Fe content of the films to investigate the effect of the Fe content in the films on the directional induced anisotropy generated by magnetic field, as exhibited in Fig. 5.18. The illustration shows that the uniaxial anisotropy constant decreases with the Fe content in the films. It follows the expectation that uniaxial anisotropy depends on the number of like atom-pair ordering which is suppressed when the composition of the alloy approaches to pure metal [27]. In addition, it's found that magnetic field and low temperature promote the uniaxial anisotropy increment. It also implies that low temperature and magnetic field induce more crystalline ordering of like-atom pairs in the film cause resulting in higher uniaxial anisotropy [27].

In general, it is known that coercivity depends on anisotropy in magnetic film because of difficulty of switching magnetization [27, 77]. Their relationship obtained from the study is shown in Fig. 5.19. Even though the films from magnetic-field plating exhibit relatively high uniaxial anisotropy constants, their coercivity values are significantly low compared to those of the films from non-magnetic-field plating. Furthermore, the total range of uniaxial anisotropy constant of the annealing process in Part II as shown in Fig. 5.9 is not much different from that of the magnetic-field plating as shown in Fig. 5.19, but their coercivity values are obviously different. This can imply that the direction of anisotropy plays an important role on coercivity.

It can be explained that the induced anisotropy in the film is created by magnetic field during plating with in-plane direction or easy axis, resulting in like-atom pair ordering in this direction. When VSM measurement is also applied on the film in the same direction, the dipole moments in each domain are easily switched their magnetization direction, leading to low coercivity. In contrast, the anisotropy is

naturally generated without directional control in the electrodeposition and enhanced by the annealing process due to atomic diffusion favoring like-atom pairs ordering but with no certain direction. Therefore, when a VSM measurement is applied in the in-plane direction, not all dipole moments but only some dipole moments align in the same direction of the applied-VSM field. The result is high coercivity.

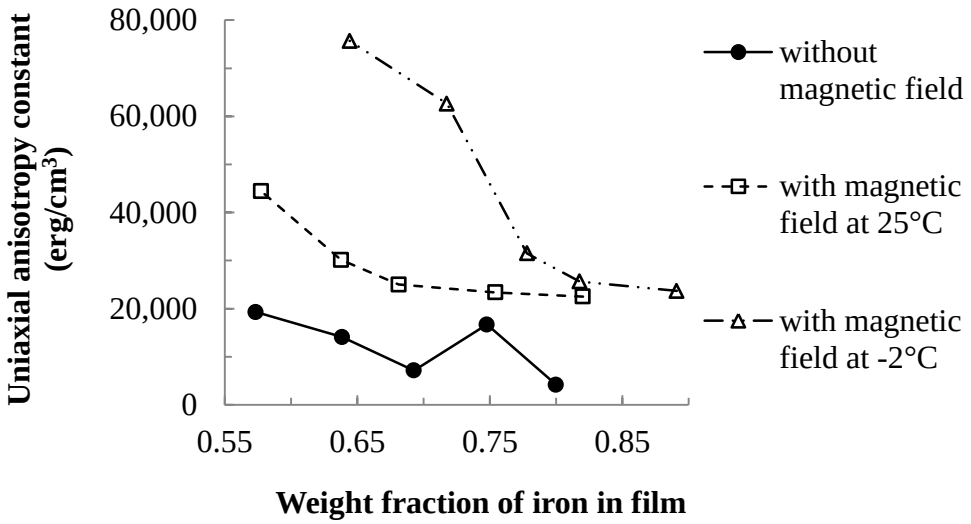

Fig. 5.18 In-plane uniaxial anisotropy constant of the CoFe films.

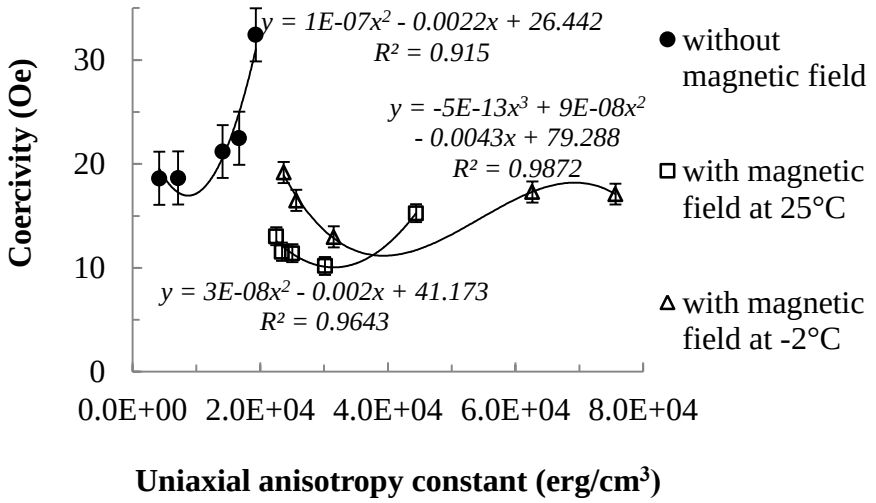

Fig. 5.19 Plots of coercivity and uniaxial anisotropy constant of the CoFe films.

Another factor, grain size, may have an influence on the films' coercivity. The relation between the coercivity and the ratio of the estimated grain size to the exchange length of the investigated CoFe films can be determined as shown in Fig. 5.20. The results present that the grain size of the films is smaller than their exchange length, so domain type of all specimens is single domain, except the film with 71.8 wt.% Fe but its grain size is very close to its exchange length ($d \cong L_{ex}$). The relation between coercivity and grain size, as shown in Fig. 5.21, exhibits $H_c \alpha\, d^3$ instead of $H_c \alpha\, d^6$ as Herzer model. The grain size around 40 nm acts as critical grain size. Furthermore, the estimated grain sizes of the films from magnetic-field plating and with low temperature are averagely larger with lower coercivity than those of the non-magnetic-field plated films. It indicates that low temperature and magnetic field generate magnetohydrodynamic effect, as described in the section 2.3.5, which leads to enlargement of grain size and in turn reduces coercivity.

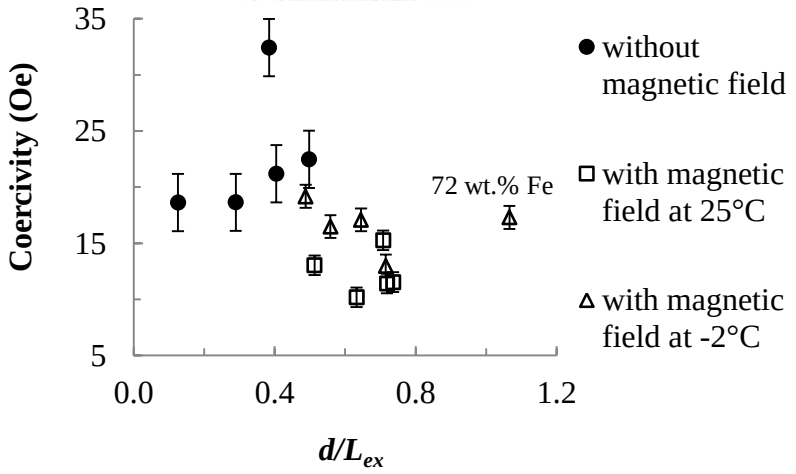

Fig. 5.20 The comparisons between coercivity and ratio of estimated grain size (d) to exchange length (L_{ex}) of the CoFe films.

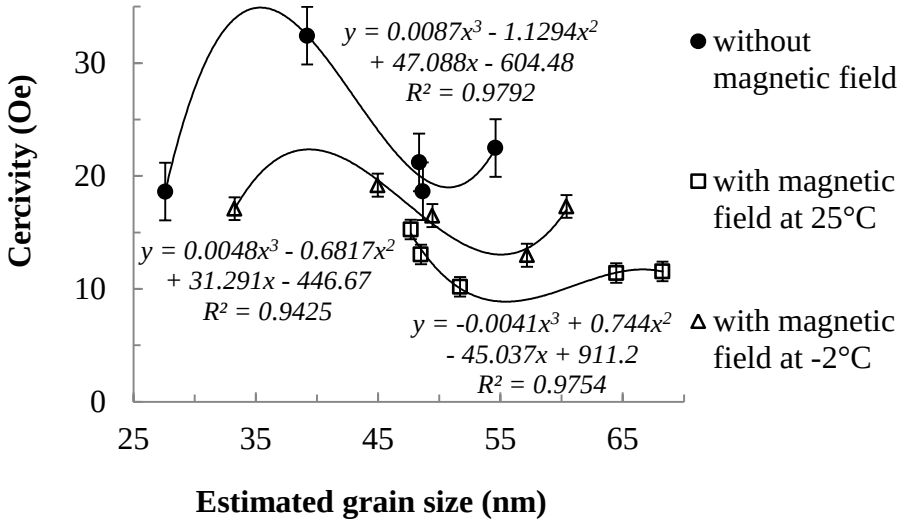

Fig. 5.21 The coercivity of the CoFe films as a function of estimated grain size.

5.3.2 Saturation Magnetization

It is well known that saturation magnetization depends on crystallographic orientation and atomic ordering. In addition, the magnetic-field induction is applied to the films' during plating process leading to rearrangement of crystallographic orientation with directional ordering of like-atom pairs in the direction of the applied field, then induced anisotropy appears, which plays an important role on the property [27, 37]. Hence, saturation magnetization significantly relates to induced anisotropy which is measured as the uniaxial anisotropy of the films.

The effect of crystallographic orientation on saturation magnetization is shown in Fig. 5.22. The saturation magnetization of the as-deposited films closely relate to (110) texture and inversely relate to (200) texture, but the results are subtle and inconclusive for the magnetic field plated films. However, the saturation magnetization of the -2°C magnetic field plated films inversely depend on (110) texture, but the results of (200) and (211) textures are inconclusive. Hence, other factor ought to play an important role in the saturation magnetization of the magnetized films.

(a)

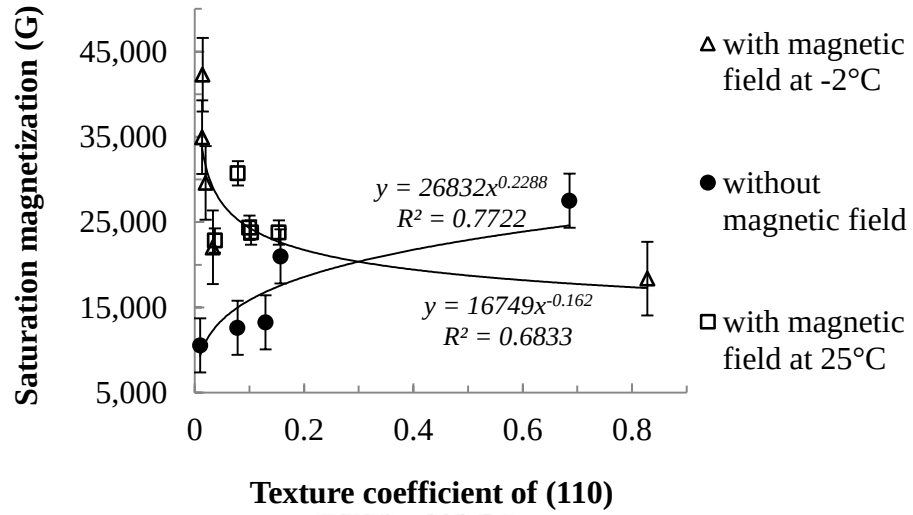
Saturation magnetization (G)
45,000
35,000
25,000
15,000
5,000
0
0.2
0.4
0.6
0.8
y = 26832x^0.2288
R² = 0.7722
y = 16749x^-0.162
R² = 0.6833
with magnetic field at -2°C
without magnetic field
with magnetic field at 25°C
Texture coefficient of (110)

(b)

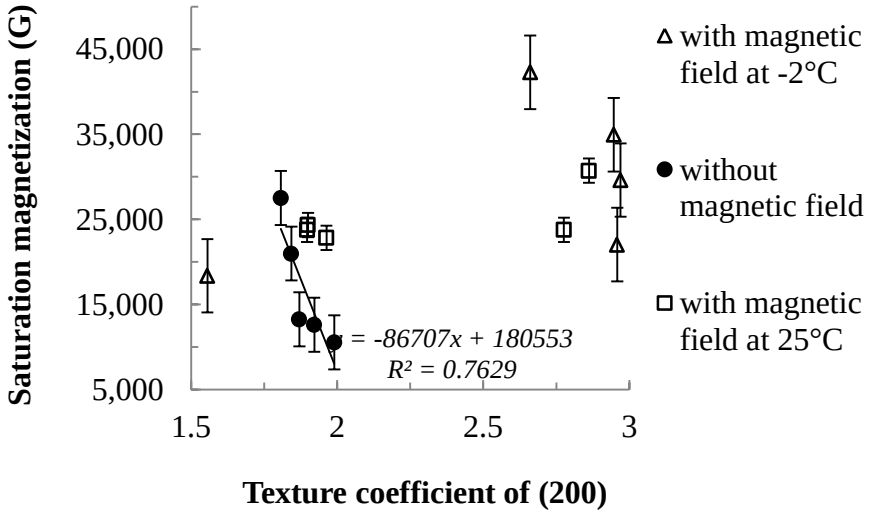
Saturation magnetization (G)
45,000
35,000
25,000
15,000
5,000
1.5
2
2.5
3
= -86707x + 180553
R² = 0.7629
with magnetic field at -2°C
without magnetic field
with magnetic field at 25°C
Texture coefficient of (200)

(c)

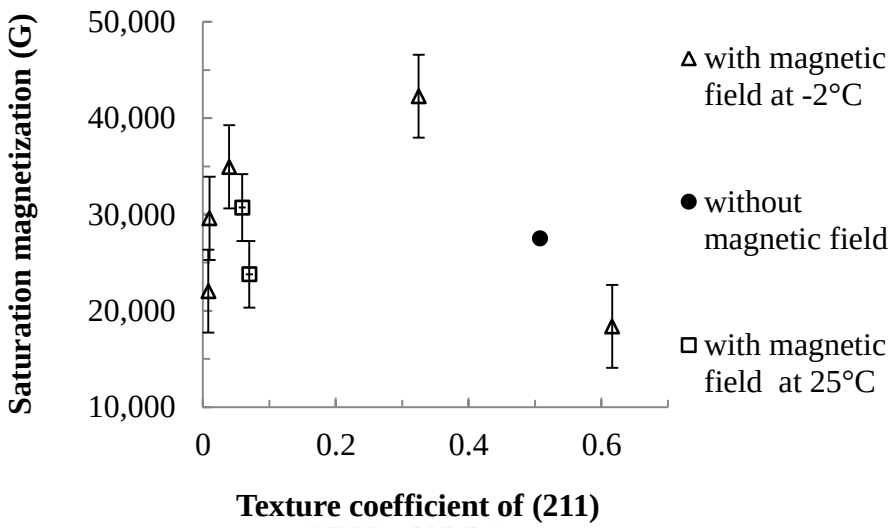

Fig. 5.22 The relation between saturation magnetization and texture coefficient of (a) (110), (b) (200) and (c) (211).

The Fig. 5.23 exhibits the distinct close relation between the saturation magnetization and the uniaxial anisotropy constant in the magnetic field plated films. This means that the increasing in like-atom pair orientation caused by directional induced anisotropy from magnetic field contributes to the increment of saturation magnetization of the films. Moreover, low temperature can significantly improve directional induced anisotropy from the applied magnetic field; because thermal vibration of dipole moment is suppressed in the condition and then the magnetic field easily control the direction of the dipole moments to align in the same direction, which develops the high uniaxial anisotropy and saturation magnetization. Hence, it implies that direction of the moment is also the important characteristic of dipole moment to increase saturation magnetization of the film.

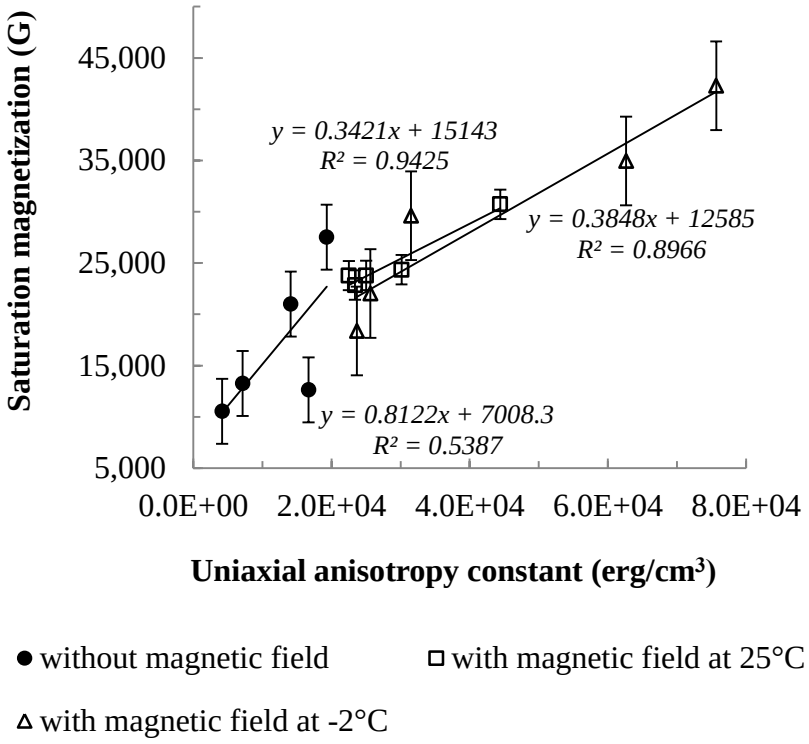

Fig. 5.23 The relation between saturation magnetization and uniaxial anisotropy constant.

5.4 Contribution of Microstructure and Magnetic Domain for Magnetic Properties of CoFe Films

According to the results of the three parts of the research, the influences of the factors' of microstructure and magnetic domain structure on the CoFe films' magnetic properties have been elucidated as the diagram in Fig. 3.1. In summary, the relation of the controlling factors and the magnetic properties can be concluded as follows:

- Chemical composition: chemical composition is mainly controlled by concentration of electrolyte and plating temperature. Fe content in the films can change the soft magnetic properties of the films, which results in:
    - High saturation magnetization, because it increases (110) texture in the films. Whereas, high saturation induced in the magnetized plating films because of high uniaxial anisotropy caused by low Fe content.

  - Low coercivity of the as-deposited films, because of small grain size and low uniaxial anisotropy energy created in the films caused by high Fe content.

- Grain size: grain size is varied with chemical composition, plating duration, annealing and plating temperature of the films. The influence of grain size on coercivity is different as plating conditions. In the as-deposited film, the grain size which smaller and larger than 40 nm tends to decrease in coercivity. For the 200°C annealed films, the larger grain size, the lower coercivity, while larger grain size leads to higher coercivity for the 300°C annealed films. Nevertheless, supported by large grain size tends to generate low coercivity in the magnetic-field plated and -2°C magnetic-field plated films.
- Thickness: thickness is notably governed by plating duration and annealing temperature. Homogeneity of the films definitely depends on the films' thickness. According to defects, pores and other imperfection in the films are suppressed when the films are thick and good soft magnetic properties are achieved.
- Roughness: roughness increases with the increment of thickness. Furthermore, it is able to be altered by annealing and plating temperature. However, the study reveals that roughness has no significant effect on the films' magnetic properties.
- Crystallographic orientation: crystallographic orientation distinctly depends on the films' composition. The (110) texture increment dominates high saturation magnetization. However, for the magnetic field-plating, crystallographic texture is not a key parameter of the films' saturation magnetization, but induced uniaxial anisotropy becomes predominated.
- Domain structure: domain structure is as a function of film's thickness. Stripe-like pattern indicates high coercivity, while bubble-like pattern suggests low coercivity of the films. The larger bubble size, the lower coercivity.

จุฬาลงกรณ์มหาวิทยาลัย
Chulalongkorn University

- Anisotropy: the anisotropy in this research is measured in term of uniaxial anisotropy. It can be controlled by chemical composition, thickness, magnetic field and plating temperature. The influence of uniaxial anisotropy can govern in both saturation magnetization and coercivity of the films. It is clearly presented that saturation magnetization increases with uniaxial anisotropy for the magnetic-field plated films in room and low (-2°C) temperatures. In addition, coercivity also closely relates to uniaxial anisotropy that:
    - Coercivity depends on uniaxial anisotropy for the as-deposited films.
    - Annealing activates high uniaxial anisotropy leading to high coercivity for the annealed films.
    - Magnetic field during plating process generates directional induced anisotropy with in-plane direction or easy axis which is the same direction of VSM measurement. This causes easy switching magnetization of dipole moments in the films, leading to low coercivity.
- Internal stress: the films' porosity causes compressive stress especially in high Fe-content films, while tensile stress is naturally developed in the films. In this study, the films' stress is deviated by annealing. The results reveal that stress is not a key parameter, because other factors, namely uniaxial anisotropy and grain size, prevail over stress affecting coercivity.
- To achieve a high saturation magnetization, a CoFe film should own adequate thickness for its homogeneity and contains Fe content lower than 65 wt.%. To enhance high directional induced anisotropy, magnetic-field plating at low temperature can be applied.
- To achieve low coercivity, post annealing at 200°C should follow the magnetic-field plating process at low temperature for controlling an appropriate grain size and hence coercivity. However, as described in the section 5.2.1, annealing can alter induced anisotropy because of

thermal vibration. Hence, magnetic-field post annealing should be considered for this purpose.

5.5 Comparison of CoFe Alloyed Films' Soft Magnetic Properties

To compare the outstanding results of CoFe films from this research to the results of CoFe alloyed films from previous study of other researchers as shown in Fig. 5.24. The results exhibit that this research is able to invent the maximum saturation magnetization of CoFe film of around 42 kG from the plating with magnetic field at -2°C, but the coercivity of the film is still high (about 17.1 Oe). The minimum coercivity produced in this research also still high around 10.2 Oe, while the minimum coercivity of CoFe alloyed film ($Co_{19}Fe_{52}Ni_{29}$) from previous researches is only 1 Oe [25].

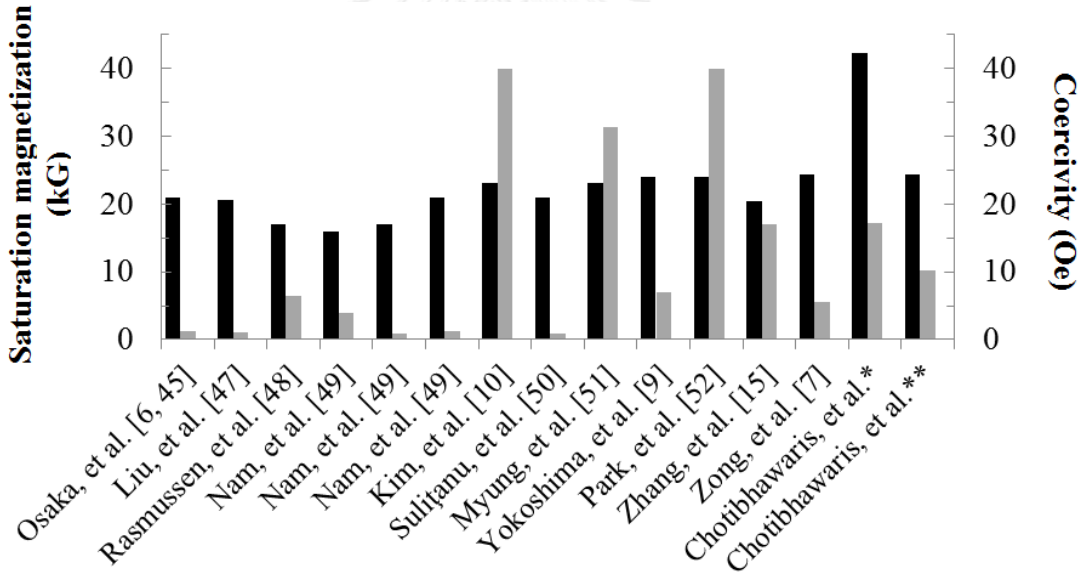

*The maximum saturation magnetization result from magnetic-field plating at -2°C in this thesis.

**The minimum coercivity result from magnetic-field plating at room temperature in this thesis.

Fig. 5.24 The soft magnetic properties of CoFe alloyed films from previous researches compared to the results of this thesis.

CHAPTER VI
CONCLUSION

The research in this thesis dissertation focuses on the mechanism of the CoFe alloys' soft magnetic properties, coercivity and saturation magnetization, that the films are fabricated by electrodeposition method with various chemical compositions and fabrication techniques – with/without annealing and induced magnetic-field plating. The results of the films' soft magnetic properties are measured by a vibrating sample magnetometer (VSM). In addition, the investigation mentions the possible factors of the films' structure, which potentially affect the magnetic properties, namely: thickness, surface roughness, grain size, domain pattern and crystallographic orientation. Such thorough study leads to comprehension of the soft magnetic mechanism of the CoFe deposits. The dissertation include the important findings:

- Part I: Defects in thin films lead to high coercivity and low saturation magnetization resulting in poor soft magnetic properties which dispenses stripe-like pattern of domain. Thickness plays a significant role on good soft magnetic properties of CoFe films, because of homogeneity which provides the domain of bubble-like pattern. In addition, large bubble size depicts low coercivity of thick films. Furthermore, grain size and uniaxial anisotropy of thick films obviously found to influence on their coercivity, the minimum value is 18.6 Oe from thick film with the lowest grain size of 28 nm and uniaxial anisotropy of 4.18×10^3 erg/cm^3. Whereas, (110) texture dominates on their saturation magnetization. The maximum saturation magnetization of 25 kG is attained from the film containing the highest (110) texture of 0.63.
- Part II: annealing affects to change in stress, uniaxial anisotropy and grain size of the films.
    - The films' coercivity clearly decreases as grain size increment for 200°C annealed films, but depends on grain size for 300°C annealed films. The minimum coercivity of 12.9 Oe is

achieved with the lowest grain size of 47.6 nm of 200°C annealed film

- Annealing gives the films' relaxation and results in magnetoelastic anisotropy decrement, but uniaxial anisotropy substantially increases and prevails over magnetoelastic anisotropy that it is clearly seen for 300°C annealed films. Hence, uniaxial anisotropy is a considerable factor which increases the coercivity of 300°C annealed films.
- Stress changed by annealing has very slight effect on (110) texture and then saturation magnetization is almost the same.

- Part III: directional induced anisotropy is generated by magnetic field and low temperature resulting in high uniaxial anisotropy and then increment of the films' saturation magnetization which reaches the maximum value of 42.3 kG with uniaxial anisotropy of 7.6×10^4 erg/cm^3 from magnetic-field plating at -2°C. In addition, the directional induced anisotropy reduces coercivity because of easy magnetization in in-plane direction or easy axis. The films' coercivity also tends to decrease as increasing of grain size. The minimum coercivity reaches 10.2 Oe of the film from magnetic-field plating at room temperature.

Finally, from the experiments conducted in this dissertation, the improvements of CoFe soft magnetic properties and their magnetic mechanism including by (i) proper chemical composition, (ii) high thickness and (iii) magnetic-field plating at low temperature were examined. The understanding achieved here may be generalized to some other soft magnetic alloy deposits. Moreover, the methodological and analytical procedure developed and performed in this thesis could be applied for an investigation of other soft magnetic materials.

จุฬาลงกรณ์มหาวิทยาลัย
Chulalongkorn University

REFERENCES

1. Osaka, T., Yokoshima, T., Shiga, D., Imai, K. and Takashima, K., *A high moment CoFe soft magnetic thin film prepared by electrodeposition.* Electrochemical and Solid-State Letters, 2003. **6**(4): p. C53-C55.
2. Spaldin, N.A., *Magnetic materials : fundamentals and applications*. 2nd ed. 2011, Cambridge: Cambridge Unversitiy Press. 274.
3. Osaka, T., *Recent development of magnetic recording head core materials by plating method.* Electrochemica Acta, 1999. **44**: p. 3885-3890.
4. Qin, X.Y., Kim. J. G. and Lee, J. S., *Synthesis and magnetic properties of nanostructured Ni-Fe Alloys.* NanoStructured Materials, 1999. **11**(2): p. 259–270.
5. Osaka, T., Asahi, T., Yokoshima, K. and Tokihiko, J., *Development of high-performance magnetic thin film for high-density magnetic recording.* Electrochimica Acta, 2005. **50**(23): p. 4576-4585.
6. Osaka, T., *Electrodeposition of highly functional thin films for magnetic recording devices of the next century.* Electrochimica Acta, 2000. **45**: p. 3311–3321.
7. Zong, B., Han, G., Qiu, J., Guo, Z., Wang, L., Yeo, W. K. and Liu, B., *Ultrasoft and high magnetic moment CoFe films directly electrodeposited from a B-reducer contained solution.* Research Letters in Physical Chemistry, 2008. **2008**: p. 1-4.
8. Miyake, Y., and Kato, M., *Soft magnetic thin film and magnetic recording head*, Kawasaki, Editor. 2008, Fujitsu Limited: Japan. p. 1-5.
9. Yokoshima, T., Imai, K., Hiraiwa, T. and Osaka, T., *Preparation of high-Bs Co–Fe soft magnetic thin films by electrodeposition.* IEEE Transactions on Magnetics, 2004. **40**(4).
10. Kim, D., Park, D. Y., Yoo, B. Y., Sumodjo, P. T. A. and Myung, N. V., *Magnetic properties of nanocrystalline iron group thin film alloys electrodeposited from sulfate and chloride baths.* Electrochimica Acta, 2003. **48**: p. 819-830.
11. Kumari, T.P., Raja, M., Kumara, M. A., Srinath, S. and Kamata, S. V., *Effect of thickness on structure, microstructure, residual stress and soft magnetic properties of DC sputtered Fe65Co35 soft magnetic thin film.* Journal of Magnetism and Magnetic Materials, 2014. **365** p. 93–99.
12. Kockar, H., Alper, M., Kuru, H. and Meydan, T., *Magnetic anisotropy and its thickness dependence for NiFe alloy films electrodeposited on polycrystalline Cu substrates.* Magnetism and Magnetic Materials, 2006. **304**: p. e736-e738.
13. Kraus, L., Chayka, O., Frait, Z. and Vázquez, M., *Influence of Thickness on Magnetic Properties of Electrolytic Ni-Fe Films Deposited on Cu Wires.* IEEE TRANSACTIONS ON MAGNETICS, 2012. **48**: p. 1348-1351.
14. Ohta, M., and Yoshizawa, Y., *Improvement of soft magnetic properties in (Fe0.85B0.15)100-xCux melt-spun alloys.* Materials Transactions, 2007. **48**(9): p. 2378-2380.
15. Luo, Q.a.J., A. H., *High-precision determination of residual stress of polycrystalline coatings using optimised XRD-sin2ψ technique.* Surface and Coatings Technology, 2010. **205**(5): p. 1403-1408.

16. Sabharwal, S., Palit, S., Tokas, R. B., Poswal, A. K. and Sangeeta, *Electroless deposition, post annealing and characterization of nickel films on silicon.* Bulletin of Materials Science, 2008. **31**(5): p. 729–736.
17. Lowenheim, F.A., *Modern Electroplating*. 1968, New York: John Wiley & Sons. 769.
18. Zhang, Y.a.I., D. G., *Characterization of Co–Fe and Co–Fe–Ni soft magnetic films electrodeposited from citrate-stabilized sulfate baths.* Materials Science and Engineering: B, 2007. **140**(1-2): p. 15-22.
19. Brankovic, S.R., *Saccharin effect on properties of 2.4T CoFe films.* Electrochimica Acta 2012. **84**: p. 139– 144.
20. Bozorth, R.M., *Ferromagnetism*. 1978, The United States of America: American Telephone and Telegraph Company. 968.
21. Chen, Y.T.a.C., C. C., *Effect of grain size on magnetic and nanomechanical properties of Co60Fe20B20 thin films.* Journal of Alloys and Compounds, 2010. **498**(2): p. 113-117.
22. Chen, Y.T., Jen, S. U., Yao, Y. D., Wu, J. M., Hwang, G. H., Tsai, T. L., Chang, Y. C. and Sun, A. C., *Magnetic, structural and electrical properties of ordered and disordered Co50Fe50 films.* Journal of Magnetism and Magnetic Materials, 2006. **304**(1): p. e71-e74.
23. Gautard, D., Couderchon, G. and Coutu, L., *50-50 CoFe alloys-magnetic and mechanical properties.* Journal of Magnetism and Magnetic Materials, 1996. **160**: p. 359-360.
24. Nakajima, T., Takeuchi, T., Yuito, I., Kato, K., Saito, M., Abe, K., Sasaki, T., Sekiguchi, T., and Yamaura, S., *Effect of annealing on magnetostrictive properties of Fe-Co alloy thin films.* Materials Transactions, 2014. **55**(3): p. 556-560.
25. Liu, X., Evans, P. and Zangari, G., *Electrodeposited Co-Fe and Co-Fe-Ni alloy films for magnetic recording write heads.* IEEE Transactions on Magnetics, 2000. **36**(5): p. 3479-3481.
26. Du, J., Li, G., Wang, Q., Ma, Y., Cao, Y., and He, J., *Microstructural evolution and magnetic properties of nanocrystalline Fe films prepared in a high magnetic field.* Vacuum, 2015. **121**: p. 88-95.
27. Cullity, B.D.a.G., C. D., *Introduction to magnetic materials*. 2 ed. 2009: A John Wiley & Sons. 308.
28. Monzon, L.M.A., and Coey, J. M. D. , *Magnetic fields in electrochemistry: The Lorentz force. A mini-review.* Electrochemistry Communications, 2014. **42**: p. 38–41.
29. Zieliński, M., *Influence of constant magnetic field on the electrodeposition of cobalt and cobalt alloys.* International Journal of Electrochemical Science, 2013. **8**: p. 12192 - 12204.
30. Matsushima, H., Fukunaka, Y., Kikuchi, S., Ispas, A., and Andreas Bund4, *Iron electrodeposition in a magnetic field.* International Journal of Electrochemical Science, 2012. **7**: p. 9345 - 9353.
31. Yundan, Y., Wei, L., Junwei, L., Hongliang, G., Lixia, S., Li, J., and Guoying, W., *Effect of magnetic fields on pulse plating of cobalt films.* Rare Metals, 2012. **31**: p. 125-129.

32. Koza, J.A., Uhlemann, M., Mickel, C., Gebert, A., and Schultz, L., *The effect of magnetic field on the electrodeposition of CoFe alloys.* Journal of Magnetism and Magnetic Materials, 2009. **321**: p. 2265–2268.
33. Tang, D.D.a.L., Y.-J., *Magnetic memory fundamentals and technology*. 2010, New York: Cambridge University Press. 1-70.
34. Jiles, D., *Introduction to magnetism and magnetic materials*. 2 ed. 1998, New York: Talor and Francis. 536.
35. Herzer, G., *Nanocrystalline soft magnetic materials.* Journal of Magnetism and Magnetic Materials, 1996. **157/158**: p. 133-136.
36. McHenry, M.E.a.L., D. E., *Nano-scale materials development for future magnetic applications.* Acta Materialia, 2000. **48**: p. 223-238.
37. O'Handley, R.C., *Modern magnetic materials, principle and applications*. 2000, Canada: John Wiley & Sons. 740.
38. McHenry, M.E., Willard, M. A., Iwanabe, H., Sutton, R. A., Turgut, Z., Hsiao, A. and Laughlin, D. E., *Nanocrystalline materials for high temperature soft magnetic applications: A current prospectus.* Bull. Mater. Sci., 1999. **22**(3): p. 495-501.
39. Herzer, G., *Grain size dependence of coercivity and permeability in nanocrystalline ferromagnet.* IEEE Transactions on Magnetics, 1990. **26**(5): p. 1397-1402.
40. Herzer, G., *Soft magnetic nanocrystalline materials.* Scripta Metallurgica et Materialia, 1995. **33**(10/11): p. 1741-1756.
41. Vopsaroiu, M., Georgieva, M., Grundy, P. J., Fernandez, G. V., Manzoor, S., Thwaites, M. J. and O'Grady, K., *Preparation of high moment CoFe films with controlled grain size and coercivity.* Journal of Applied Physics, 2005. **97**(10): p. 10N303-10N303-3.
42. Sun, N.X., Xiao, Q. F. and York, B., *Stress, microstructure, and magnetic softness of high saturation magnetization (B[sub s]) FeCoN films.* Journal of Applied Physics, 2005. **97**(10): p. 10F906-10F906-3.
43. Coey, J.M.D., *Magnetism and magnetic materials*. 2009, Cambridge: Cambridge university press.
44. Yu, W., *Optimization of stress in sputtered high magnetization FeCo for magnetic recording heads*, in *Electrical and Computer Engineering*. 2001, Carnegie Mellon University: Pittsburgh, Pennsylvania. p. 54.
45. Ispas, A., *Electrochemical phase formation of Ni and Ni-Fe alloys in a magnetic field*, in *Mathematics and Natural Sciences*. 2007, Dresden University of Technology: Dresden, Germany. p. 137.
46. Luborsky, F.E., *Magnetic anneal anisotropy in amorphous alloys.* IEEE Transactions on Magnetics, 1977. **MAG-13**(2): p. 953-956.
47. Ispas, A., Matsushima, H.,Plieth, W., and Bund, A., *Influence of a magnetic field on the electrodeposition of nickel–iron alloys.* Electrochimica Acta, 2007. **52**: p. 2785–2795.
48. Mearian, L. *Want a 100TB disk drive? You'll have to wait 'til 2025*. 2014 [cited 2015 2015 Oct 02]; Available from: http://www.computerworld.com/article/2852233/want-a-100tb-disk-drive-youll-have-to-wait-til-2025.html.

49. Spaldin, N.A., *Magnetic Materials, Fundamentals and Applications*. 2 ed. 2011, New York: Cambridge University Press. 135-184.
50. Osaka, T., *Introduction of electrochemical microsystem technologies from ultra high density magnetic recording.* Electrochimica Acta, 2001. **47**: p. 23–28.
51. McHenry, M.E., Willard, M. A., and Laughlin, D. E., *Amorphous and nanocrystalline materials for applications as soft magnets.* Progress in Materials Science, 1999. **44**: p. 291-433.
52. Paunovic, M.a.S., M., *Fundamentals of electrochemical deposition*. 2006. 373.
53. Rasmussen, F.E., Ravnkilde, J. T., Tang, P. T., Hansen, O., and Bouwstra, S., *Electroplating and characterization of cobalt-nickle-iron and nickel-iron for magnetic microsystems applications.* Sensors and Actuators A, 2001. **92**: p. 242-248.
54. Nam, H.-S., Yokoshima, T., Nakanishi, T., Osaka, T., Yamazaki, Y., and Lee, D. N., *Microstructure of electroplated soft magnetic CoNiFe thin films.* Thin Solid Films, 2001. **384**: p. 288293.
55. Suliţanu, N.a.B.n., F., *Excellent soft magnetic two-phase nanocrystalline films for various magnetic devices.* Sensors and Actuators A: Physical, 2003. **106**(1-3): p. 212-216.
56. Myung, N.V., Park, D. Y., Urgiles, D. E. and George, T., *Electroformed iron and FeCo alloy.* Electrochimica Acta, 2004. **49**(25): p. 4397-4404.
57. Park, D.Y., Yoo, B. Y., Kelcher, S. and Myung, N. V., *Electrodeposition of low-stress high magnetic moment Fe-rich FeCoNi thin films.* Electrochimica Acta, 2006. **51**(12): p. 2523-2530.
58. Lallemand, F., Ricq, L., Wery, M., Berc¸ot, P. and Pagetti, J., *Kinetic and morphological investigation of CoFe alloy electrodeposition in the presence of organic additives.* Surface and Coatings Technology, 2004. **179**: p. 314–323.
59. Brankovic, S.R., Kagajwala, B., George, J., Majkic, G., Stafford, G. and Ruchhoeft, P., *Stress control in electrodeposited CoFe films—Experimental study and analytical model.* Electrochimica Acta, 2012. **83**: p. 387-393.
60. Koza, J.A., Uhlemann, M., Gebert, A., and Schultz, L., *The effect of a magnetic field on the pH value in front of the electrode surface during the electrodeposition of Co, Fe and CoFe alloys.* Journal of Electroanalytical Chemistry, 2008. **617**: p. 194–202.
61. Qiang, C., Xu, J., Xiao, S., Jiao, Y., Zhang, Z., Liu, Y., Tian, L. and Zhou, Z., *The influence of pH and bath composition on the properties of Fe–Co alloy film electrodeposition.* Applied Surface Science, 2010. **257**(5): p. 1371-1376.
62. Yi, J.B., Li, X. P., Ding, J. and Seet, H. L., *Study of the grain size, particle size and roughness of substrate in relation to the magnetic properties of electroplated permalloy.* Journal of Alloys and Compounds, 2007. **428**(1-2): p. 230-236.
63. Lu, W., Huang, P., He, C. and Yan, B., *Compositional and structural analysis of FeCo films electrodeposited at eifferent temperatures.* International Journal of Electrochemical Science, 2012. **7**: p. 12262 - 12269.

64. Lu, W., Huang, P., Li, K., Yan, P., Wang, Y. and Yan, B., *Effect of bath temperature on the microstructural properties of electrodeposited nanocrystalline FeCo films.* International Journal of Electrochemical Science, 2013. **8**: p. 2354-2364.
65. Krause, A., Koza, A., Ispas, A., Uhlemann, M., Gebert, A., and Bund, A., *Magnetic field induced micro-convective phenomena inside the diffusion layer during the electrodeposition of Co, Ni and Cu.* Electrochimica Acta, 2007. **52**: p. 6338–6345.
66. Koza, J.A., Uhlemann, M., Mickel, C., Gebert, A., and Schultz, L., *The effect of magnetic fields on the electrodeposition of CoFe alloys.* Electrochimica Acta, 2008. **53**: p. 5344–5353.
67. Schuh, C.A., Nieh, T. G. and Iwasaki, H., *The effect of solid solution W additions on the mechanical properties of nanocrystalline Ni.* Acta Materialia 2003. **51**: p. 431–443.
68. Thaiwatthana, S., Jantaping, N. and Limthongkul, P., *Residual stress measurement of low temperature plasma surface alloyed layer using X-ray diffraction techniques.* Surface Engineering, 2012. **28**(4): p. 273-276.
69. Sam, Z.a.A., N., *Nanocomposite Thin Films and Coatings*. 2007: Imperial College Press. 615.
70. Kodama, R.H., *Magnetic nanoparticles.* Magnetism and Magnetic Materials, 1999. **200**.
71. Zhao, Y.-P., Gamache, R. M., Wang, G.-C. , Lu, T.-M., Palasantzas, G. and De Hosson, J. Th. M. , *Effect of surface roughness on magnetic domain wall thickness, domain size and coercivity.* Journal of Applied Physics, 2001. **89**(2): p. 1325-1330.
72. Yu, R.H., Basu, S., Zhang, Y., Parvizi, A. Parvizi-Majidi, and Xiao, J. Q., *Pinning effect of the grain boundaries on magnetic domain wall in FeCo based magnetic alloys.* Journal of Applied Physics, 1999. **85**(9): p. 6655-6659.
73. Rhen, F.M.F.a.R., S., *Dependence of magnetic properties on micro- to nanostructure of CoNiFe films.* Applied Physics, 2008. **103**: p. 1-4.
74. Rizal, C.S.a.Y.U., Y., *Magnetoresistance and Magnetic Anisotropy Properties of Strain-Induced Co/Ag Multilayer Films.* IEEE TRANSACTIONS ON MAGNETICS, 2009. **45**(6): p. 2399-2402.
75. Osaka, T., et al., *A High Moment CoFe Soft Magnetic Thin Film Prepared by Electrodeposition.* Electrochemical and Solid-State Letters, 2003. **6**(4): p. C53.
76. *Magnetism fundamentals*. 2005: Springer. 507.
77. Gamburg, Y.D.a.Z., G., *Theory and practice of metal electrodeposition*. 2011: Springer. 378.
78. Ohring, M., *The materials science of thin films*. 1992: Academic Press.
79. Miguel, C., Zhukov, A., del Val, J. J., and Gonza´ lez, J., *Coercivity and induced magnetic anisotropy by stress and/or field annealing in Fe- and Co-based.* Journal of Magnetism and Magnetic Materials, 2005. **294**: p. 245–251.
80. Smallman, R.E., and Bishop, R. J., *Metals and materials science, processes, application*. 1995, Oxford: Buttterworth-Heinemann. 431.

81. Grachev, S.Y., Tichelaar, F. D. and Janssen, G. C. A. M., *Stress in sputter-deposited Cr films: Influence of Ar pressure.* Journal of applied physics, 2005. **97**(073508): p. 073508-1-073508-4.
82. Chotibhawaris, T., Luangvaranunt, T., Jantaratana, P. and Boonyongmaneerat, Y., *Influence of the electrodeposited Co-Fe alloys' characteristics on their magnetic properties.* Advanced Materials Research, 2014. **1025-1026**: p. 709-716.

APPENDICES

จุฬาลงกรณ์มหาวิทยาลัย
Chulalongkorn University

APPENDIX A

AFM Images of The Surface of The CoFe Deposits

A.1 The CoFe Films of 0.5-hr Plating

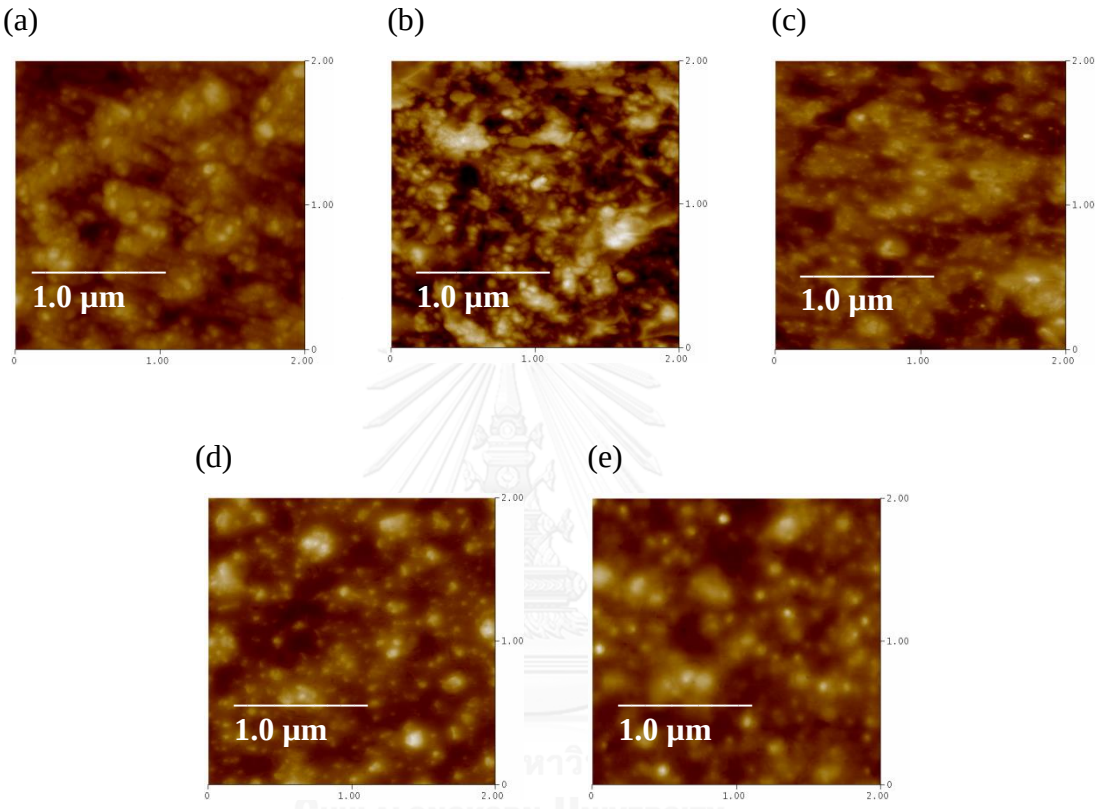

Fig. A.1 The CoFe films with: (a) 55.1, (b) 61.4, (c) 68.7, (d) 74.7, (e) 80.9 wt.%Fe of 0.5-hr plating.

A.2 The CoFe Films of 4-hr Plating

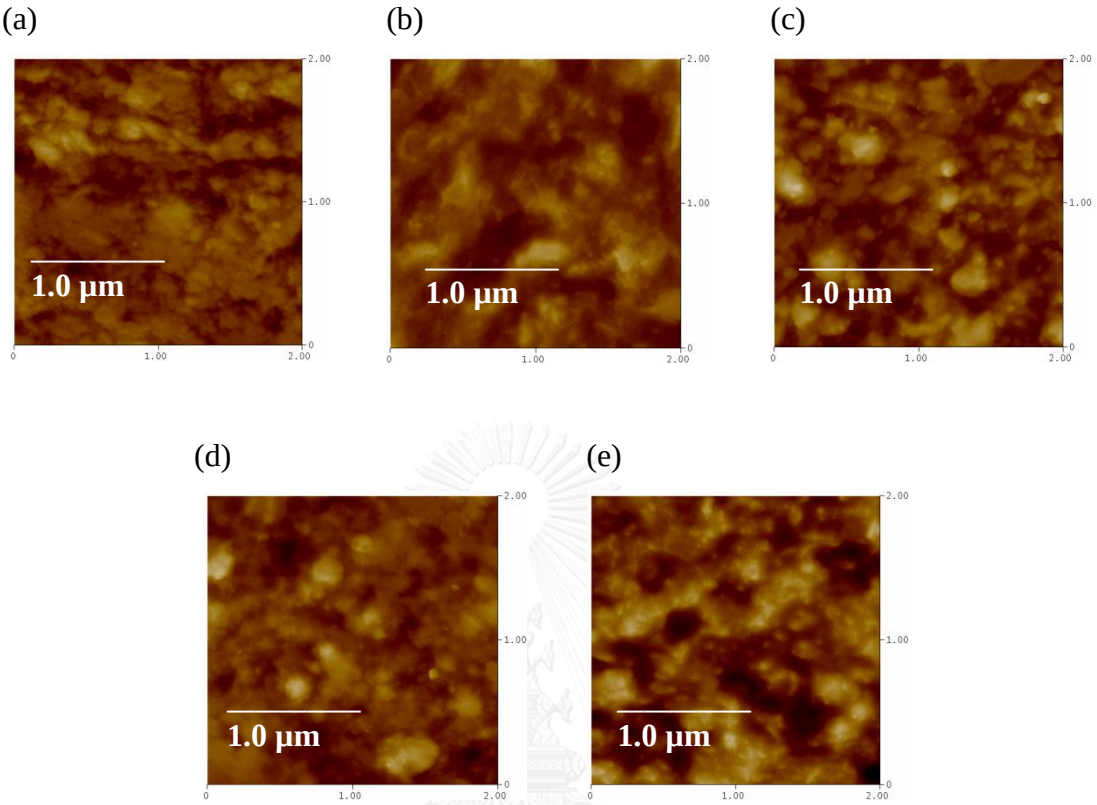

Fig. A.2 The CoFe films with: (a) 57.3, (b) 63.8, (c) 69.3, (d) 74.8, (e) 80.0 wt.%Fe of 4-hr plating.

จุฬาลงกรณ์มหาวิทยาลัย
Chulalongkorn University

A.3 The 4-hr Plated CoFe Films of 200°C Annealing Process

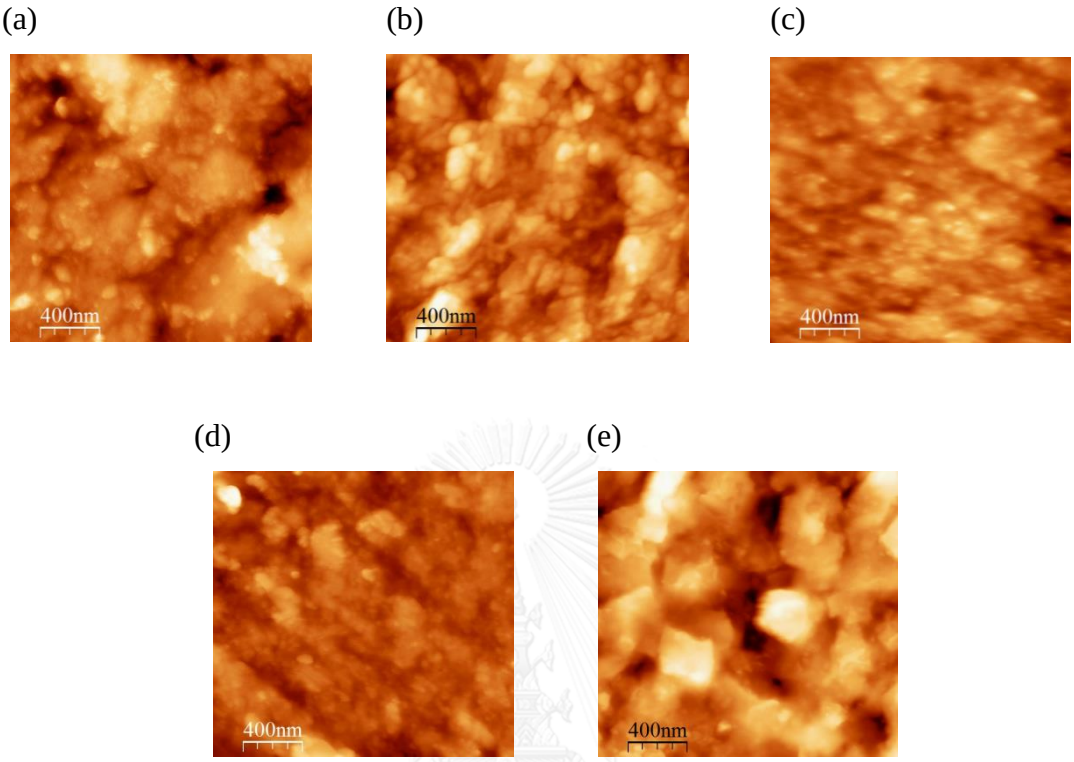

Fig. A.3 The 200°C annealed CoFe films with: (a) 57.3, (b) 63.8, (c) 69.3, (d) 74.8, (e) 80.0 wt.%Fe of 4-hr plating.

จุฬาลงกรณ์มหาวิทยาลัย
Chulalongkorn University

A.4 The 4-hr Plated CoFe Films of 300°C Annealing Process

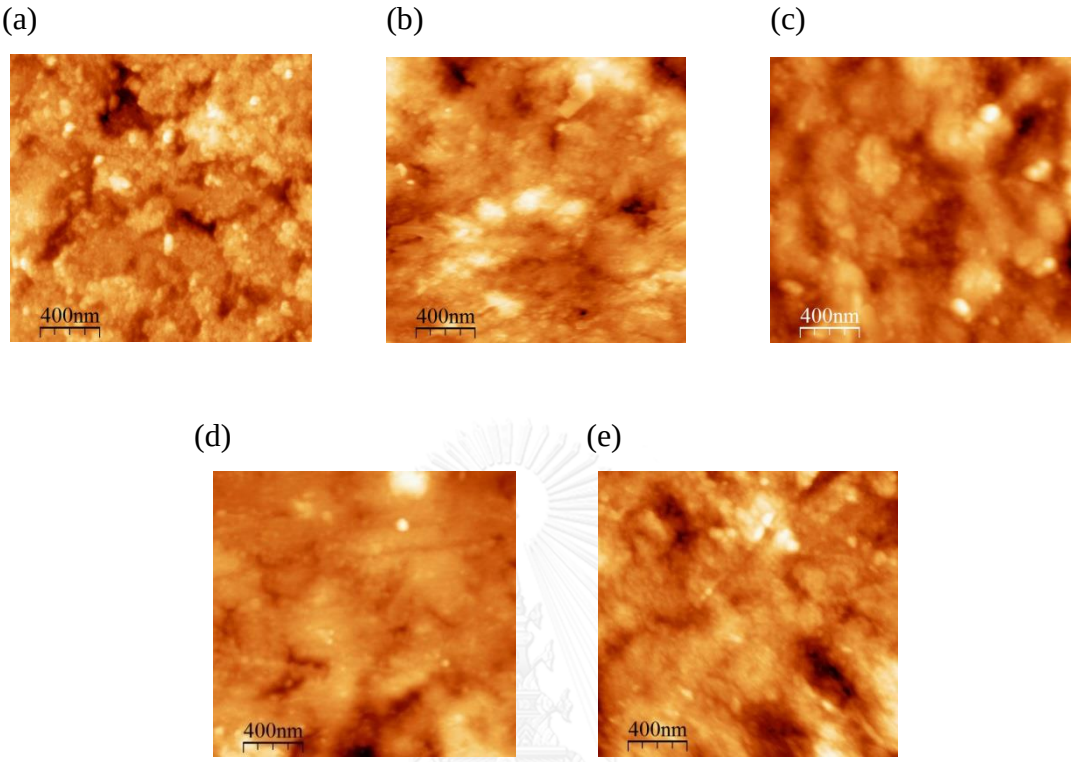

Fig. A.4 The 300°C annealed CoFe films with: (a) 57.3, (b) 63.8, (c) 69.3, (d) 74.8, (e) 80.0 wt.%Fe of 4-hr plating.

จุฬาลงกรณ์มหาวิทยาลัย
Chulalongkorn University

A.5 The CoFe Films of Magnetic-Field Plating at room temperature

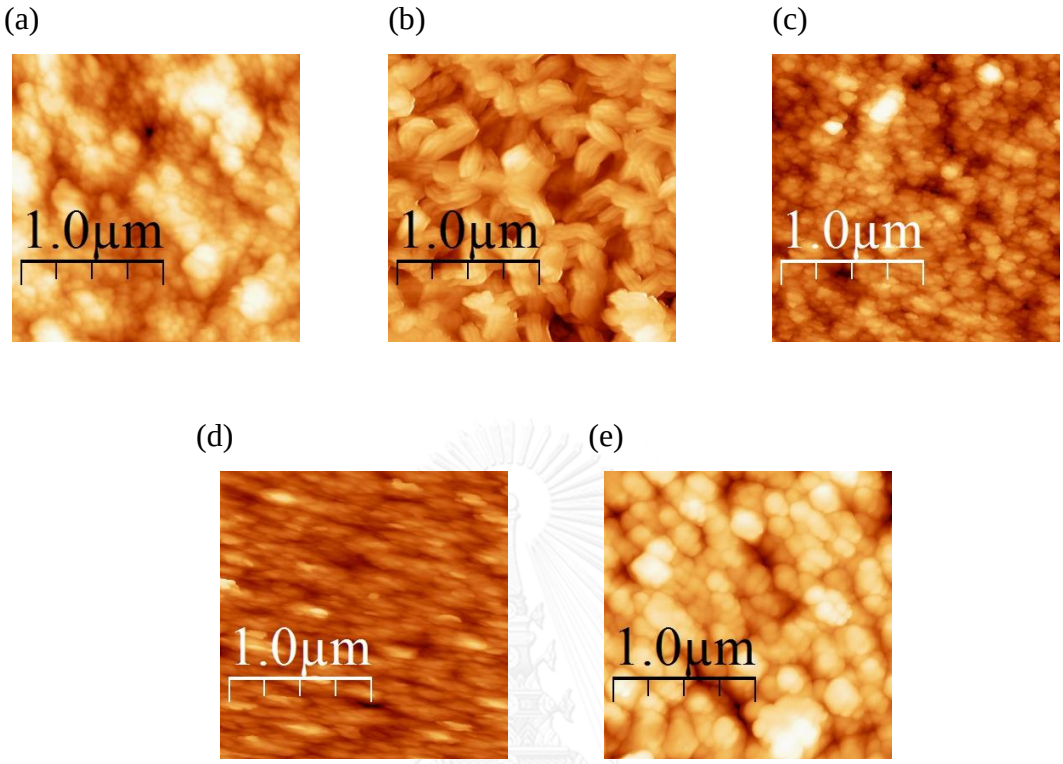

Fig. A.5 The CoFe films with: (a) 57.8, (b) 68.1, (c) 69.3, (d) 75.4, (e) 82.0 wt.%Fe of magnetic-field plating.

จุฬาลงกรณ์มหาวิทยาลัย
Chulalongkorn University

A.6 The CoFe Films of Magnetic-Field Plating at -2°C

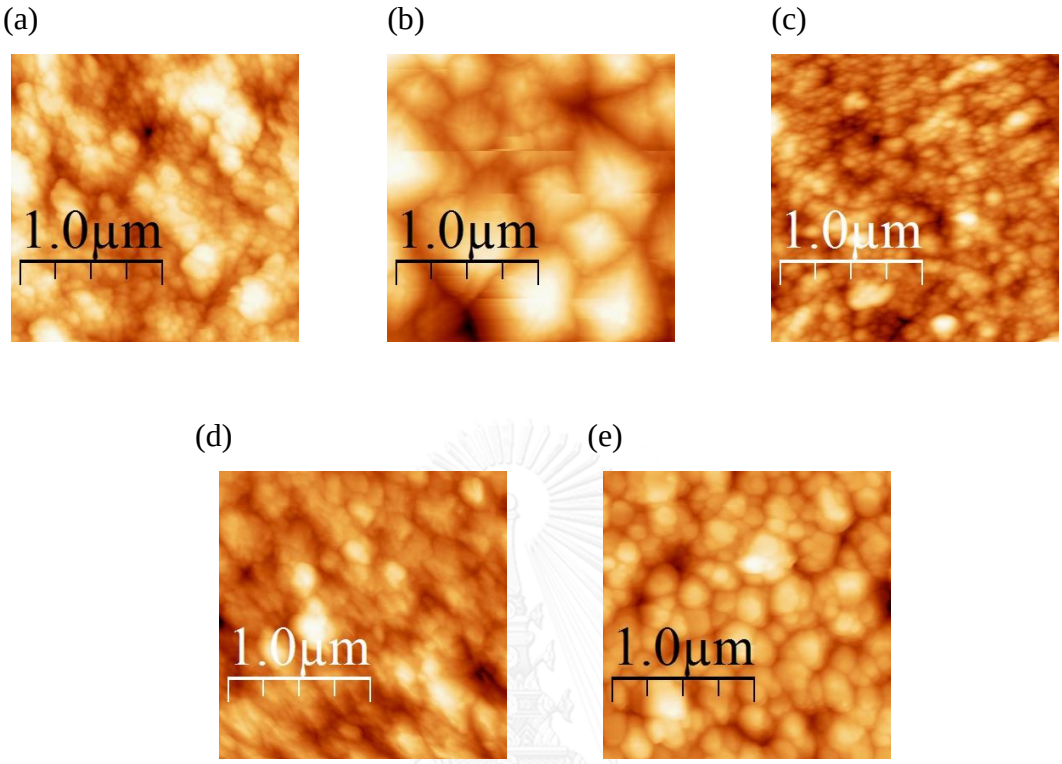

Fig. A.6 The CoFe films with: (a) 64.4, (b) 71.8, (c) 77.8, (d) 81.8, (e) 89.1 wt.%Fe of magnetic-field plating at -2°C.

จุฬาลงกรณ์มหาวิทยาลัย
Chulalongkorn University

APPENDIX B

Crystallographic and Structural Data of The CoFe Deposits

B.1 The CoFe Films of 0.5-hr Plating

Table B.1.1 Roughness and thickness of the CoFe films of 0.5-hr plating

wt.% Fe	Roughness (nm)	Thickness (μm)
80.9	7.285	0.565
74.7	7.529	0.724
68.7	7.668	0.686
61.4	13.348	0.629
55.1	7.893	0.103

Table B.1.2 Crystallographic data of the CoFe films of 0.5-hr plating

wt.% Fe	(110)				
	Crystallite size ($\mathring{A}$)	Lattice spacing ($\mathring{A}$)	2 theta of (110)	Intensity (%)	Texture coefficient
80.9	318	2.035	44.491	100	1
74.7	208	2.033	44.524	100	1
68.7	480	2.029	44.626	100	1
61.4	245	2.035	44.495	100	1
55.1	193	2.025	44.718	100	1

Chulalongkorn University

B.2 The CoFe Films of 4-hr Plating

Table B.2.1 Roughness and thickness of the CoFe films of 4-hr plating

wt.% Fe	Roughness (nm)	Thickness (μm)
80.0	20.03	2.51
74.8	12.9	1.41
69.3	14.64	1.16
63.8	12.91	1.38
57.3	12.32	2.42

Table B.2.2 Crystallographic data of the CoFe films of 4-hr plating

wt.% Fe	(110)				
	Crystallite size ($\mathring{A}$)	Lattice spacing ($\mathring{A}$)	2 theta of (110)	Intensity (%)	Texture coefficient
80.0	239	2.0325	44.541	7.2	0.0200
74.8	718	2.0411	44.344	31.2	0.0837
69.3	573	2.0300	44.598	36.9	0.0982
63.8	533	2.0269	44.671	57.5	0.1490
57.3	611	2.0276	44.654	100	0.6327
wt.% Fe	(200)				
	Crystallite size ($\mathring{A}$)	Lattice spacing ($\mathring{A}$)	2 theta of (110)	Intensity (%)	Texture coefficient
80.0	313	1.4337	64.994	100	1.9802
74.8	374	1.4373	64.814	100	1.9163
69.3	400	1.4306	65.155	100	1.9018
63.8	434	1.4297	65.2	100	1.8510
57.3	261	1.4295	65.211	40.9	1.8484
wt.% Fe	(211)				
	Crystallite size ($\mathring{A}$)	Lattice spacing ($\mathring{A}$)	2 theta of (110)	Intensity (%)	Texture coefficient
80.0					
74.8					
69.3					
63.8					
57.3	304	1.1665	82.65	20.5	0.5188

จุฬาลงกรณ์มหาวิทยาลัย
Chulalongkorn University

B.3 The 4-hr Plated CoFe Films of 200°C Annealing Process

Table B.3.1 Roughness and thickness of the 200°C annealed CoFe films

wt.% Fe	Roughness (nm)	Thickness (μm)
80.0	34.06	1.48
74.8	19.7	1.12
69.3	10.29	0.98
63.8	13.48	1.32
57.3	20.06	2.26

Table B.3.2 Crystallographic data of the 200°C annealed CoFe films

wt.% Fe	(110)				
	Crystallite size (Å)	Lattice spacing (Å)	2 theta of (110)	Intensity (%)	Texture coefficient
80.0	478	2.0267	44.675	8.6	0.0238
74.8	539	2.0237	44.745	18.9	0.0516
69.3	543	2.0237	44.746	18.8	0.0513
63.8	569	2.0225	44.774	37	0.1351
57.3	713	2.0271	44.666	100	0.5136
wt.% Fe	(200)				
	Crystallite size (Å)	Lattice spacing (Å)	2 theta of (110)	Intensity (%)	Texture coefficient
80.0	356	1.4329	65.237	100	1.9762
74.8	400	1.4293	65.221	100	1.9484
69.3	398	1.4293	65.143	100	1.9487
63.8	547	1.4286	65.256	100	2.6091
57.3	385	1.4284	65.267	51.5	1.7226
wt.% Fe	(211)				
	Crystallite size (Å)	Lattice spacing (Å)	2 theta of (110)	Intensity (%)	Texture coefficient
80.0					
74.8					
69.3					
63.8	312	1.1675	82.563	17.5	0.2557
57.3	300	1.1659	82.669	43.2	0.8092

จุฬาลงกรณ์มหาวิทยาลัย
Chulalongkorn University

B.4 The 4-hr Plated CoFe Films of 300°C Annealing Process

Table B.4.1 Roughness and thickness of the 300°C annealed CoFe films

wt.% Fe	Roughness (nm)	Thickness (μm)
80.0	17.77	1.20
74.8	5.25	0.99
69.3	9.12	0.97
63.8	4.28	1.29
57.3	9.35	2.27

Table B.4.2 Crystallographic ata of the 300°C annealed CoFe films

wt.% Fe	(110)				
	Crystallite size (Å)	Lattice spacing (Å)	2 theta of (110)	Intensity (%)	Texture coefficient
80.0	650	2.0311	44.574	10.7	0.0295
74.8	936	2.0285	44.638	56.1	0.1456
69.3	818	2.0292	44.619	84.2	0.2109
63.8	674	2.0253	44.707	56.5	0.1466
57.3	574	2.0276	44.654	100	0.3405
wt.% Fe	(200)				
	Crystallite size (Å)	Lattice spacing (Å)	2 theta of (110)	Intensity (%)	Texture coefficient
80.0	376	1.4348	64.938	100	1.9705
74.8	319	1.432	65.081	100	1.8544
69.3	467	1.4319	65.088	100	1.7891
63.8	390	1.4302	65.092	100	1.8534
57.3	373	1.4291	65.232	73.3	1.7825
wt.% Fe	(211)				
	Crystallite size (Å)	Lattice spacing (Å)	2 theta of (110)	Intensity (%)	Texture coefficient
80.0					
74.8					
69.3					
63.8					
57.3	281	1.1663	82.667	64.4	0.8770

จุฬาลงกรณ์มหาวิทยาลัย
Chulalongkorn University

B.5 The CoFe Films of Magnetic-Field Plating at room temperature

Table B.5.1 Roughness and thickness of the magnetic-field plated CoFe films

wt.% Fe	Roughness (nm)	Thickness (μm)
82.0	23.7	0.92
75.4	24.8	1.13
68.1	15.8	1.12
63.8	31.6	1.64
57.8	18.9	1.85

Table B.5.2 Crystallographic data of the magnetic-field plated CoFe films

wt.% Fe	(110)				
	Crystallite size (Å)	Lattice spacing (Å)	2 theta of (110)	Intensity (%)	Texture coefficient
82.0	553	2.0272	44.665	38.8	0.1030
75.4	826	2.0246	44.723	13.4	0.0368
68.1	671	2.0247	44.721	39.6	0.1539
63.8	510	2.0216	44.795	37.6	0.1000
57.8	613	2.0217	44.792	19.7	0.0789
wt.% Fe	(200)				
	Crystallite size (Å)	Lattice spacing (Å)	2 theta of (110)	Intensity (%)	Texture coefficient
82.0	417	1.4305	65.159	100	1.8970
75.4	539	1.43	65.186	100	1.9632
68.1	561	1.43	65.184	100	2.7761
63.8	524	1.4293	65.219	100	1.9000
57.8	440	1.4288	65.247	100	2.8618
wt.% Fe	(211)				
	Crystallite size (Å)	Lattice spacing (Å)	2 theta of (110)	Intensity (%)	Texture coefficient
82.0					
75.4					
68.1	702	1.1667	82.63	4.5	0.0700
63.8					
57.8	377	1.1655	82.734	3.7	0.0593

จุฬาลงกรณ์มหาวิทยาลัย
Chulalongkorn University

B.6 The CoFe Films of Magnetic-Field Plating at -2°C

Table B.6.1 Roughness and thickness of the -2°C magnetic-field plated CoFe films

wt.% Fe	Roughness (nm)	Thickness (μm)
89.1	26.3	1.48
81.8	20.3	1.77
77.8	15.7	1.49
71.8	16	1.38
64.4	31	1.08

Table B.6.2 Crystallographic data of the -2°C magnetic-field plated CoFe films

wt.% Fe	(110)				
	Crystallite size (Å)	Lattice spacing (Å)	2 theta of (110)	Intensity (%)	Texture coefficient
89.1	641	2.0239	44.741	100	0.8281
81.8	986	2.0254	44.706	8	0.0331
77.8	635	2.0249	44.718	4.8	0.0200
71.8	565	2.0253	44.707	3.3	0.0136
64.4	351	2.0227	44.769	3.9	0.0145
wt.% Fe	(200)				
	Crystallite size (Å)	Lattice spacing (Å)	2 theta of (110)	Intensity (%)	Texture coefficient
89.1	321	1.4335	65.007	26.3	1.5557
81.8	241	1.4313	65.116	100	2.9586
77.8	246	1.43	65.185	100	2.9701
71.8	275	1.4308	65.144	100	2.9468
64.4	250	1.4294	65.216	100	2.6607
wt.% Fe	(211)				
	Crystallite size (Å)	Lattice spacing (Å)	2 theta of (110)	Intensity (%)	Texture coefficient
89.1	387	1.1676	82.555	18.6	0.6161
81.8	256	1.1686	82.471	0.5	0.0083
77.8	834	1.1668	82.627	0.6	0.0100
71.8	972	1.1687	82.465	2.4	0.0396
64.4	397	1.1683	82.492	21.8	0.3248

จุฬาลงกรณ์มหาวิทยาลัย
Chulalongkorn University

B.7 Relation between Lattice Constant and d Spacing of Crystallographic System

Table B.7.1 Relation between lattice parameter and lattice spacing

Crystallographic plane	Lattice constant (a) vs. lattice spacing (d) value
(110)	$a(110) = d\sqrt{2}$
(200)	$a(200) = 2d$
(211)	$a(211) = d\sqrt{6}$

APPENDIX C

Magnetic Data of The CoFe Deposits

C.1 The CoFe Films of 0.5-hr Plating

Table C.1.1 Magnetic data of the CoFe films of 0.5-hr plating

wt.% Fe	B_s (G)	H_c (Oe)	H_k (Oe)	K_u (erg/cm^3)	L_{ex} (nm)
80.9	9,891.5	41.9	26.3	8.81×10^3	26.3
74.7	8,067.7	43.5	25.4	2.24×10^4	25.4
68.7	8,868.8	44.8	27.4	8.20×10^3	27.4
61.4	12,892.3	42.7	22.5	1.07×10^4	22.5
55.1	10,034.4	44.0	24.2	8.18×10^3	24.2

C.2 The CoFe Films of 4-hr Plating

Table C.2.1 Magnetic data of the CoFe films of 4-hr plating

wt.% Fe	B_s (G)	H_c (Oe)	H_k (Oe)	K_u (erg/cm^3)	L_{ex} (nm)
80.0	10,548.4	18.6	11.8	4.18×10^3	219.2
74.8	12,626.6	22.5	21.9	1.67×10^4	109.7
69.3	13,257.4	18.6	15.6	7.14×10^3	167.9
63.8	20,982.5	21.2	18.0	1.41×10^4	119.4
57.3	27,507.7	32.4	19.1	1.93×10^4	102.1

Chulalongkorn University

C.3 The 4-hr Plated CoFe Films of 200°C Annealing Process

Table C.3.1 Magnetic data of the 200°C annealed CoFe films

wt.% Fe	B_s (G)	H_c (Oe)	H_k (Oe)	K_u (erg/cm^3)	L_{ex} (nm)
80.0	13,050.7	21.0	16.0	7.27×10^3	166.3
74.8	14,074.5	17.6	21.1	2.47×10^4	90.2
69.3	14,838.8	16.6	13.7	7.25×10^3	166.6
63.8	20,222.3	12.9	12.4	9.00×10^3	149.6
57.3	24,994.1	18.8	16.5	1.51×10^4	115.4

C.4 The 4-hr Plated CoFe Films of 300°C Annealing Process

Table C.4.1 Magnetic data of the 300°C annealed CoFe films

wt.% Fe	B_s (G)	H_c (Oe)	H_k (Oe)	K_u (erg/cm^3)	L_{ex} (nm)
80.0	11,293.7	38.8	36.9	1.42×10^4	118.9
74.8	12,456.4	40.2	67.4	4.53×10^4	66.6
69.3	12,770.5	42.2	41.3	1.82×10^4	105.1
63.8	19,531.9	38.1	42.5	2.98×10^4	82.1
57.3	26,704.6	37.5	53.5	5.24×10^4	62.0

C.5 The CoFe Films of Magnetic-Field Plating at Room Temperature

Table C.5.1 Magnetic data of the magnetic-field plated CoFe films

wt.% Fe	B_s (G)	H_c (Oe)	H_k (Oe)	K_u (erg/cm^3)	L_{ex} (nm)
82.0	23,780.0	13.0	28.2	2.25×10^4	94.5
75.4	22,846.4	11.5	30.7	2.34×10^4	92.7
68.1	23,783.1	11.4	31.3	2.50×10^4	89.7
63.8	24,349.1	10.2	36.7	3.01×10^4	81.7
57.8	30,725.7	15.3	41.3	4.44×10^4	67.4

C.6 The CoFe Films of Magnetic-Field Plating at -2°C

จุฬาลงกรณ์มหาวิทยาลัย
Chulalongkorn University

Table C.6.1 Magnetic data of the magnetic-field plated CoFe films at -2°C

wt.% Fe	B_s (G)	H_c (Oe)	H_k (Oe)	K_u (erg/cm^3)	L_{ex} (nm)
89.1	18,379.5	19.2	40.2	2.37×10^4	92.1
81.8	22,031.9	16.5	35.1	2.56×10^4	88.6
77.8	29,610.4	13.0	30.6	3.15×10^4	79.9
71.8	34,951.3	17.3	50.4	6.26×10^4	56.7
64.4	42,287.4	17.1	49.3	7.57×10^4	51.6

VITA

Name: Mr.Thanakrit Chotibhawaris

Birthday: December01, 1974

Education :

- Bachelor of Engineering (Industrial Engineering), Department of Industrial Engineering, Faculty of Engineering, Khon Kaen University, 1997

- Master of Engineering (Metallurgical Engineering), Department of Production Engineering, Faculty of Engineering, King Mongkut's University of Technology Thonburi, 2007

Past position :

- Production engineer, Vee Rubber Co., Ltd.

- Maintenance engineer and head of water and steam unit, Union Textile Industry Co., Ltd.

- Plant engineer, IBM Storage Products (Thailand) Co., Ltd.

Current position :

- Instructor of the Department of Industrial and Logistics Engineering, Faculty of Engineering, Mahanakorn University of Technology

จุฬาลงกรณ์มหาวิทยาลัย
Chulalongkorn University